Exploring factors affecting the distribution of *Saccharomyces cerevisiae* tRNA nucleotidyltransferase

Shayesteh Kiani

A Thesis

in

The Department

of

Biology

Presented in Partial Fulfillment of the Requirements for

The Degree of Master of Science (Biology) at

Concordia University

Montreal, Quebec, Canada

December 2019

CONCORDIA UNIVERSITY

School of Graduate Studies

This is to certify that the thesis prepared

By: Shayesteh Kiani

Entitled: Exploring factors affecting the distribution of *Saccharomyces cerevisiae* tRNA nucleotidyltransferase

Submitted in partial fulfillment of the requirements for the degree of

Master of Science (Biology)

Complies with the regulations of the University and meets the accepted standards with respect to originality and quality.

Signed by the final Examining Committee:

Dr. Alisa Piekny	_____	Chair & Examiner
Dr. Isabelle Benoit-Gelber	_____	Examiner
Dr. Ann English	_____	External Examiner
Dr. Paul Joyce	_____	Supervisor

Approved by Dr. Robert Weladji _____ Graduate Program Director

Dr. André Roy _____ Dean of Faculty

Date: December 2019

ABSTRACT

Exploring factors affecting the activity and distribution of *Saccharomyces cerevisiae* tRNA nucleotidyltransferase

Shayesteh Kiani

The enzyme ATP(CTP): tRNA-specific tRNA nucleotidyltransferase (also known as Cca1, the CCA-adding enzyme) adds to all tRNAs the 3'-cytidine, cytidine, and adenosine (CCA) tail required for aminoacylation. A single essential nuclear gene, *CCA1*, in *Saccharomyces cerevisiae* codes for versions of this protein found in the cytosol, nucleus and mitochondrion (Chen *et al.*, 1992). Here, we use mass spectrometry to explore factors involved in the distribution and activity of this enzyme. These factors may be *cis*-acting, *e.g.*, post-translational modifications (PTMs) of Cca1, or *trans*-acting, *e.g.*, accessory proteins involved in Cca1 activity or which serve to direct Cca1 to specific locations in the cell.

Specific PTMs, *i.e.*, phosphorylation and/or acetylation, were identified on amino acids S4, T5, T7, S12, T17, T19, and S21 at the N-terminus of Cca1 and also on K57, K118, K150, K328, T407, and K507. Most of these PTMs are reported for the first time in this study. These PTMs might impact enzyme localization (as the N-terminal cluster of PTMs is near the known mitochondrial targeting signal) or activity as some post-translationally modified amino acids (*e.g.*, K118, K150) are in important functional domains of the protein. Differences between the PTMs detected at specific positions in different cellular fractions, suggest the role of these modifications in Cca1 localization. Moreover, some conserved PTMs (*e.g.*, K150, T407, and K507) across different conditions and fraction might implicate these specific modifications in enzyme activity.

As Cca1 is an essential enzyme present in different parts of the cell (mitochondria, nucleus and cytosol), we identified proteins interacting with it that might mediate its function or localization. Among the proteins identified were the karyopherins Kap95, Kap104 and Kap123, which allowed us to predict a nuclear localization signal in a eukaryotic CCA-adding enzyme for the first time. Additionally, Cca1 was shown to interact with other enzymes required for tRNA maturation and repair.

ACKNOWLEDGMENTS

I would like to thank my supervisor Dr. Paul Joyce for his invaluable support and guidance during my undergraduate and graduate study. I always thank him to open the door of research for me in the second year of my undergraduate study, and later on provide me with a more rewarding graduate research opportunity. I convey my appreciation to Dr. Pamela Hanic-Joyce who generously offered different strains of *Saccharomyces cerevisiae* and always guided me and other students in the lab with her expertise. I learned a lot of valuable lessons from this wonderful couple and I will apply them in the rest of my life and career. I thank Dr. Jiang and the Centre for Biological Aspects of Mass Spectrometry (CBAMS) for providing instruments and assistance for the mass spectrometric analysis. My committee members Dr. Alisa Piekny and Dr. Isabelle Benoit Gelber are acknowledged for giving me their valuable time and helping me to complete my project. I convey my appreciation to Dr. English for providing strains and sharing some lab tools.

Sometimes brave decisions must be taken at the right moments to change a person's life for better. One of the most important milestones in my life was when I decided to come to Canada alone to peruse my university study. Although it was a great opportunity for me to grow, still very challenging and it was not possible to go through that difficult time without support from my loved ones. I would like to give a special thanks to my lovely parents who gave me any supports a person can imagine from emotional and financial support to abandoning their life and career in our home country to live with me in Canada. I thank them very much and never forget their sacrifices. I definitely set this step as one of the steps toward my ultimate goal to make a difference in people's lives. I also like to thank my older siblings for their love and support during my study.

TABLE OF CONTENTS

LIST OF FIGURES

LIST OF TABLES

LIST OF APPENDICES

LIST OF ABBREVIATIONS

APS	Ammonium persulfate
CCA	Cytidine-cytidine-adenosine
CID	Collision-induced dissociation
CTP	Cytidine triphosphate
FDR	False discovery rate
GST	Glutathione S-transferase
IgG	Immunoglobulin G
IPTG	Isopropyl-β-D-thiogalactopyranoside
LOF	Loss-of-function
LC	Liquid chromatography
MS	Mass spectrometry
NLS	Nuclear localization signal
NTP	Nucleoside triphosphate
PAGE	Polyacrylamide gel electrophoresis
PBS	Phosphate-buffered saline
PCR	Polymerase chain reaction
PDB	Protein Data Bank
PTM	Post-translational modification
SC-URA	Synthetic complete medium minus uracil
SDS	Sodium dodecyl sulfate

SIFD	Sideroblastic anemia associated with B-cell Immunodeficiency, periodic Fevers and developmental Delay
TAP tag	Tandem affinity purification tag
TBE	Tris/Borate/EDTA
TEMED	Tetraethylmethlenediamine
TEV protease	Tobacco Etch Virus protease
tRNA-NT	ATP(CTP):tRNA nucleotidyltransferase
ts	Temperature-sensitive
UTP	Uridine triphosphate
YPD	Yeast extract, Peptone, Dextrose
YT	Yeast extract, Tryptone

1. INTRODUCTION

1.1 Transfer RNAs (tRNAs)

Crick's adaptor hypothesis (Crick, 1958) proposed the existence of small molecules that allow the information contained in nucleic acids to be translated into the sequence of amino acids in proteins. This was proven to be the case when transfer RNAs (tRNAs) were identified as these adaptor molecules (Hoagland *et al*., 1958). These small molecules (Fig. 1.1) play an essential role in protein synthesis as they deliver amino acids to the ribosome for translation. Transfer RNAs have well-defined secondary and tertiary structures and end in a 3'-terminal cytidine-cytidine-adenosine (CCA) sequence (Fig. 1.1).

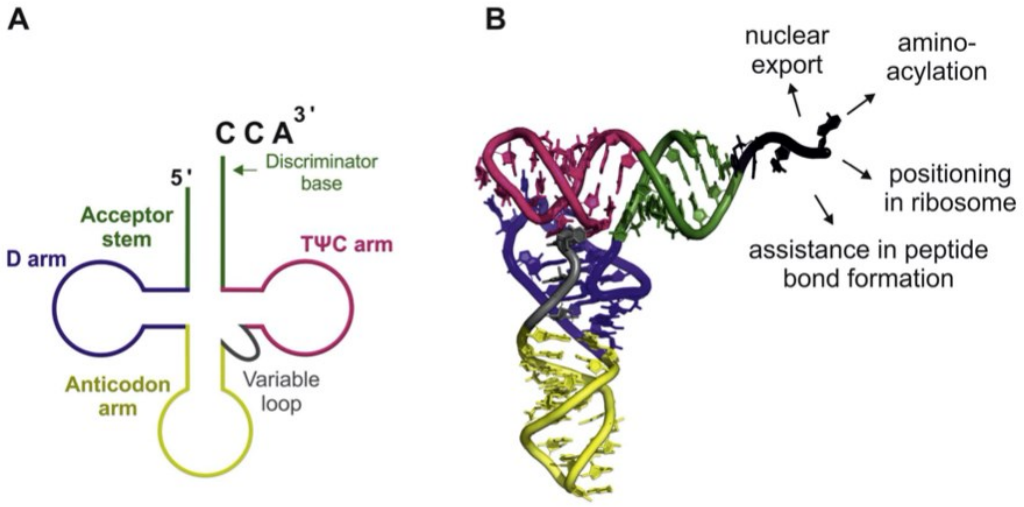

Figure 1.1: Secondary and tertiary structure of tRNA. **(A)** Secondary structure displaying conserved elements of a tRNA including the discriminator base and the CCA sequence. **(B)** Tertiary structure with some of the diverse functions ascribed to the CCA sequence. Shown here is the crystal structure of the cytosolic $tRNA^{Phe}$ from *Saccharomyces cerevisiae* (PDB ID: 1TN1), with an equivalent colour scheme to **(A)** (Wellner *et al*., 2018, reproduced with permission).

The role first recognized for this CCA sequence was as the site of amino acid attachment for delivery to the ribosome in protein synthesis (Sprinzl and Cramer, 1979). However, this CCA sequence plays other roles in protein synthesis too. For example, it is recognized by elongation factor EF-Tu and ensures proper positioning of the amino acid at the ribosomal A-site (Green and Noller 1997, Liu *et al*., 1998). The CCA sequence also assists in the catalysis of peptide bond

formation (Kim and Green, 1999) and helps to coordinate the water molecules required for nucleophilic attack and hydrolysis of the peptidyl-tRNA ester linkage during protein synthesis (Simonovic and Steitz, 2008). In all eukaryotes characterized to date, this CCA sequence is not encoded in any tRNA genes (Juhling *et al*. 2009), so it must be added post-transcriptionally. This post-transcriptional CCA addition typically is carried out by the enzyme ATP(CTP):tRNA-specific tRNA nucleotidyltransferase (the CCA-adding enzyme).

1.2 ATP(CTP):tRNA-specific tRNA nucleotidyltransferase structure

All tRNA nucleotidyltransferases are members of the polβ-type nucleotidyltransferase superfamily (Aravind and Koonin, 1999) and are found in the three domains of life. Based on sequence conservation and available crystal structures, tRNA nucleotidyltransferases have been divided into two classes (Yue *et al*., 1996): Class I (found in the Archaea) and Class II (found in Bacteria and Eukaryota). While Class I tRNA nucleotidyltransferases show little sequence conservation except for a small region tightly associated with the active site (Xiong *et al.*, 2003), Class II enzymes show a much greater degree of sequence conservation particularly in the amino-terminal portion of the protein (Shanmugam *et al*., 1996, Yue *et al*., 1996). Overall, Class II enzymes show a seahorse-shaped higher order structure (Fig. 1.2) with conserved head, neck, body and tail domains (Li *et al.*, 2002, Augustin *et al*., 2003). The catalytic region of the enzyme is found in the head and neck domains (Vörtler and Mörl, 2010) shown by the arrow in Fig. 1.2. This amino-terminal portion of the protein (Fig. 1.3) contains five well-conserved motifs (A-E) to which specific functions have been assigned through extensive structural (Augustin *et al*., 2003; Li *et al.*, 2002; Tomita *et al*., 2004; Tomita *et al*., 2006, Toh *et al*., 2009) and functional (Steitz, 1998; Li *et al.*, 2002; Xiong *et al*., 2006; Cho *et al*., 2007; Lizano *et al*., 2008; Betat *et al*., 2010) analyses.

Motif A (residues 64-84 of the yeast enzyme in Fig. 1.3) contains a conserved GGxVRD sequence (where X is any amino acid) that is part of the consensus fold (five-stranded antiparallel β-sheet flanked by two α-helices) found in all members of the polβ-type nucleotidyltransferase superfamily (Holm and Sander, 1995). In addition, motif A also contains the conserved DxD sequence that coordinates the two magnesium ions required for catalysis and the binding of incoming nucleotide triphosphates (Steitz, 1998; Li *et al.*, 2002; Betat *et al*., 2010).

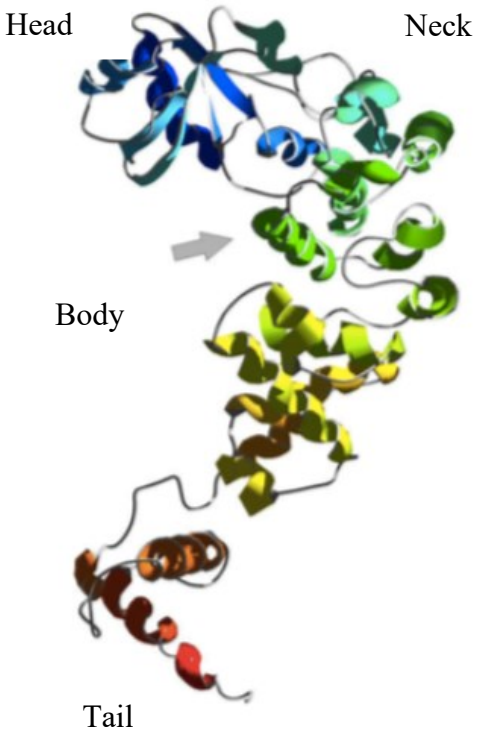

Figure 1.2: Class II tRNA nucleotidyltransferase. The catalytic region of the enzyme is located in the head and neck domains and is indicated by a grey arrow. The structure is colored rainbow from blue (N terminal) to red (C terminal) (Vörtler and Mörl, 2010, reproduced with permission).

Motif B (residues 164-180 of the yeast enzyme in Fig. 1.3) functions in ribose recognition and plays a role in purine-specific base stacking with the incoming ribonucleotide triphosphates (Li *et al.*, 2002). This motif includes the conserved RRD sequence that recognizes the 2′-OH group of the bound NTP and discriminates against deoxynucleotides (Li *et al.*, 2002). Specifically, the guanidinium group of the central arginine residue of these three amino acids hydrogen bonds with the 2′-hydroxyl group of the incoming nucleotide. Deoxyribonucleotides, lacking this 2'-OH group, are unable to form this hydrogen bond and so bind less efficiently. Replacement of this arginine side chain by isoleucine (which cannot form this hydrogen bond) generated an enzyme that added dCdCdA to the tRNA primer (Cho *et al*., 2007). Motifs A and B are connected by a flexible loop that changes its conformation to accommodate the purine (ATP) after the addition of the pyrimidine (CMP) residues (McGann and Deutscher 1980; Zhu *et al*. 1986; Li *et al.*, 2002; Augustin *et al*., 2003; Tomita *et al*., 2004; Neuenfeldt *et al*., 2008; Just *et al.,* 2008; Toh *et al*., 2009; Hoffmeier *et al*., 2010).

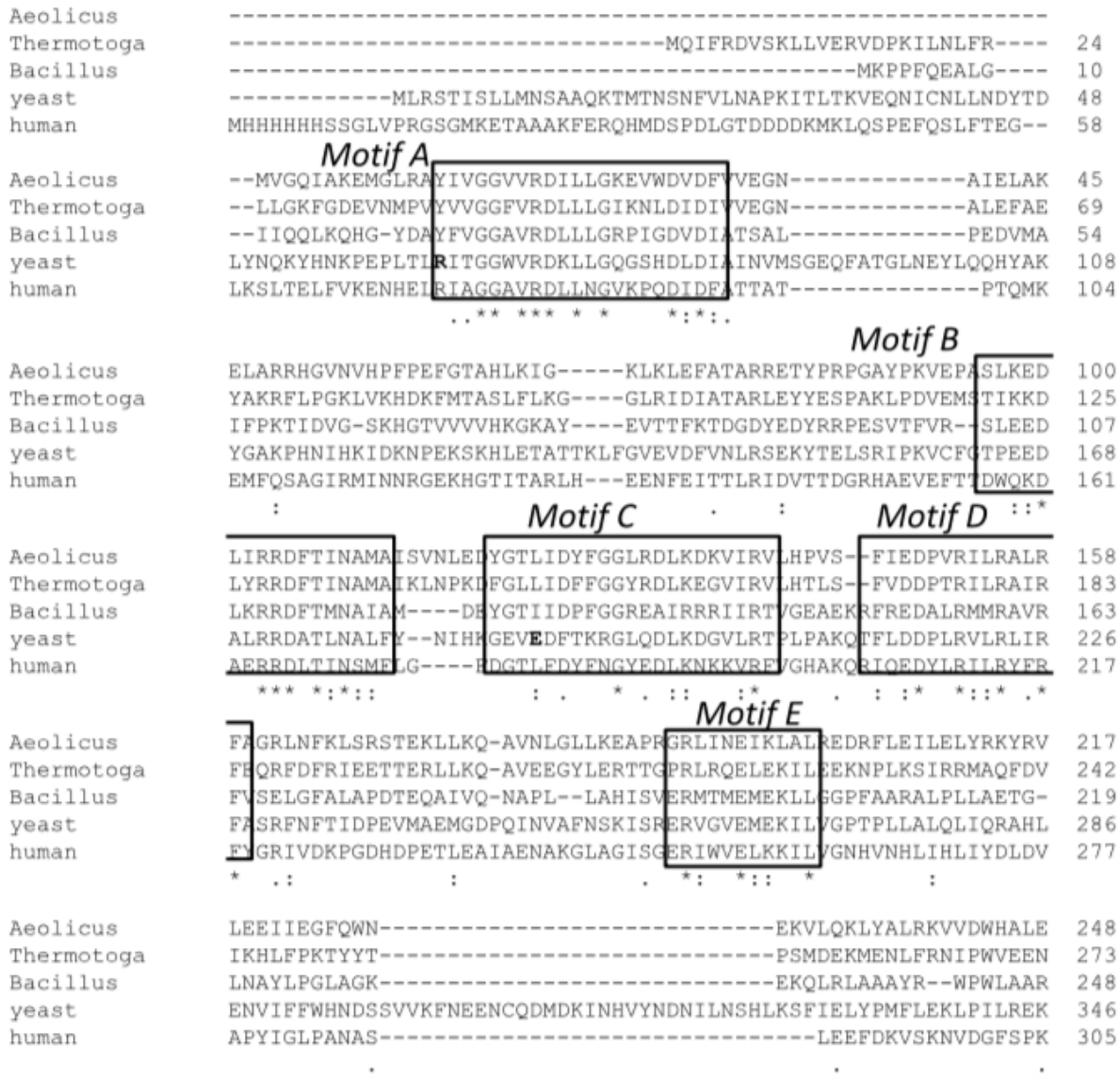

Figure 1.3: Alignment of the head and neck domains of five class II tRNA nucleotidyltransferases. The alignment was performed using Clustal W software (Martin *et al*., 2007). Letters are standard one letter code for the amino acids, numbers represent residue positions in the protein. R64 and E189, involved in suppressing and generating, respectively, a temperature-sensitive phenotype in yeast are shown in bold. Amino acid identity, strongly conserved and weakly conserved residues are indicated by (*), (:), and (.) respectively (Goring *et al*., 2013, reproduced with permission).

Motif C (residues 186- 206 of the yeast enzyme in Fig. 1.3) shows the least sequence conservation and also is thought to alter its organization to accommodate the growing tRNA template for the subsequent cycles of CMP and AMP incorporation (Ernst *et al*., 2015). In particular, we noted that a mutation that converts the glutamic acid at position 189 (bold in Fig.

1.3) to phenylalanine (E189F) in yeast tRNA nucleotidyltransferase results in a temperature-sensitive (*ts*) phenotype (Shan *et al*., 2008) and an approximately 100-fold decrease in turnover number (Rahman, 2017). Moreover, the conversion of the adjacent aspartic acid to alanine (D190A) also resulted in a *ts* phenotype and a 275-fold reduction in activity (Rahman, 2017). In both cases these mutations effected catalysis more dramatically than substrate binding. This also was reported for the human enzyme where conversion of the aspartic acid at the corresponding position to alanine (D139A) resulted in a similar reduction in catalytic rate and a limited change in substrate binding (Ernst *et al*., 2015). These authors further revealed, using EPR spectroscopy, that the D139A substitution interferes with interdomain movements within the protein. Our analysis revealed that the R64W yeast variant (bold at the beginning of motif A in Fig. 1.3) could suppress the temperature-sensitive (*ts*) phenotype (Goring *et al*., 2013) and increase the catalytic activity of the E189F or D190A variant by approximately five fold (Rahman, 2017) suggesting that the arrangement in space of motifs A and C is important for enzyme activity.

Motif D (residues 213-228 in the yeast enzyme in Fig. 1.3) with its conserved EDxxR sequence acts as an amino-acid based template for CCA addition. Specifically, Watson-Crick-like hydrogen bonds are formed between the conserved glutamic acid, aspartic acid and arginine residues of the protein and the base moieties of the bound nucleotides (Li *et al*., 2002). This generates a nucleotide binding pocket for each incoming CTP or ATP, but discriminates against GTP and UTP, which would require a different arrangement of hydrogen bonds (Li *et al*., 2002, Cho *et al*., 2007). After the incorporation of the two CMP residues the structure of the active site and the arrangement of the E, D and R residues are reorganized to accept ATP instead of CTP, *i.e*., the binding pocket gets larger and the potential for hydrogen bonding changes (Li *et al*., 2002).

Motif E (residues 259-269 in the yeast enzyme in Fig. 1.3) has two proposed functions: 1) as a stabilizer of the helix-turn structure in motif D and/or 2) as a site of interaction of the enzyme with the growing 3′ end of the tRNA substrate (Li *et al*., 2002). When we converted the conserved arginine in motif E in the *Candida glabrata* CCA-adding enzyme to alanine, lysine or methionine the enzyme was not able to add the CCA sequence to a tRNA template lacking this sequence (Arthur, 2009). These results suggest that this conserved arginine (R260) plays a role in binding and orienting the tRNA substrate appropriately for catalysis supporting the second proposed function.

In contrast to the conservation of the amino-terminal portions of tRNA nucleotidyltransferase defining the catalytic core (as seen in Fig. 1.3), the carboxy-terminal portion of the protein containing the body and tail domains shows remarkable sequence variability. The C-terminal portion of the protein is predicted to be involved in RNA substrate selection (Tomita *et al*., 2004). Specifically, the body and tail domains contain multiple α-helices that recognize the acceptor and TψC helices (Fig. 1.1, A) of the tRNA (Tomita and Yamashita, 2014). We have shown that the single point mutation resulting in the conversion of isoleucine at position 326 to threonine (I326T) in the body domain of human tRNA nucleotidyltransferase resulted in an approximately 20-fold increase in the dissociation constant for tRNA consistent with reduced binding of the tRNA substrate (Leibovitch *et al*., 2019).

1.3 Functions of tRNA nucleotidyltransferase

In eukaryotes, where tRNA primary transcripts lack the 3'-terminal CCA sequence (Juhling *et al*. 2009), tRNA nucleotidyltransferase (the CCA-adding enzyme) is required for CCA addition during tRNA maturation (Deutscher, 1992). Given the central role that the CCA tag plays in aminoacylation and protein synthesis (Section 1.1), the CCA-adding enzyme was predicted to be required for cell viability. The essential nature of the CCA-adding enzyme was shown first almost 30 years ago when a *ts* mutation was identified in the *Saccharomyces cerevisiae CCA1* gene encoding tRNA nucleotidyltransferase (Aebi *et al*., 1990). In this *ts* strain, after the shift to the restrictive temperature (37℃) , tRNAs with an incomplete CCA tag accumulate (Aebi *et al*., 1990) and protein synthesis rapidly ceases (Peltz *et al*., 1992). More recently, partial loss-of-function (LOF) mutations were identified in the *TRNT1* gene encoding the human CCA-adding enzyme (Aksentijevich *et al.* 2014; Chakraborty *et al.*, 2014; Sasarman *et al.,* 2015; DeLuca *et al.,* 2016; Hull *et al.,* 2016; Wedatilake *et al*., 2016; Frans *et al*., 2017; Lougaris *et al*., 2018; Giannelou *et al*., 2018; Bader-Meunier *et al*., 2018; Gorodetsky *et al*., 2018; Kumaki *et al*., 2019; Jfri *et al*., 2019). Patients carrying these mutations present a wide range of clinical severities ranging from sideroblastic anemia, B-cell immunodeficiency, periodic fevers and developmental delay in congenital SIFD (Chakraborty *et al.*, 2014) to sensorineural hearing loss, cardiomyopathy and central nervous system abnormalities (Wiseman *et al*., 2013). The disease phenotypes may manifest in specific tissues or locations, *e.g.*, retinitis pigmentosum due to degeneration of cells of the retina (Sharma and Rando, 2017) or more systemically, as in SIFD (Chakraborty *et al.*, 2014).

In vitro characterization of the SIFD variants (Chakraborty *et al.*, 2014) showed that all variants (T154I, M158V, L166I, R190I, I223T, I326T) had reduced thermal stability while a subset of them (M158V, R190I, I223T, and I326T) also reduced the catalytic efficiency of the enzyme (Leibovitch *et al.*, 2018, Leibovitch *et al*., 2019). Given the central role of the CCA-adding enzyme in tRNA maturation it is not surprising that mutations that effect the activity of this enzyme can lead to disease phenotypes. However, the diverse set of phenotypes associated with its variants suggests that the CCA-adding enzyme may have roles other than CCA addition during tRNA maturation.

1.3.1 Requirement during nuclear export of tRNAs

As described previously, the CCA sequence is not encoded in eukaryotic tRNA genes it so must be added post-transcriptionally by the CCA-adding enzyme (Juhling *et al*. 2009). This step in tRNA biogenesis has been shown to occur in the nucleus in organisms as diverse as Xenopus (Melton *et al.,* 1980; Lund and Dahlberg, 1998) and yeast (Wolfe *et al.,* 1996), and it has been shown that CCA addition is required for efficient tRNA nuclear export in vertebrate cells (Arts *et al*.,1998; Lipowsky *et al*., 1999) and for the export of some, but not all, tRNAs in yeast (Sarkar *et al*., 1999) (Fig. 1.4). Crystallographic data demonstrate interactions between the 3'-CCA overhang of tRNAs and residues of the exportin Los1/Xpot component of the nuclear tRNA export machinery (Cook *et al*., 2009). In fact, CCA addition and subsequent aminoacylation have been proposed to serve as quality control steps required for tRNA export from the nucleus (Lund and Dahlberg, 1998; Steiner-Mosonyi and Mangroo, 2004). This ensures that only functional tRNAs are released from the nucleus to function in cytoplasmic protein synthesis. Therefore, the CCA-adding enzyme must function in the nucleus.

1.3.2 Repair of damaged 3'-termini

The CCA-adding enzyme also functions in the cytosol. In *Saccharomyces cerevisiae* the terminal AMP residue of tRNAs was shown to be turned over in exponentially growing cells (Rosset and Monier, 1965). This suggests a role for the CCA-adding enzyme in the repair of tRNAs damaged by exonuclease activity (Rosset and Monier, 1965). In *Escherichia coli* all tRNA genes encode the CCA sequence and all tRNAs are transcribed with a complete CCA tag such that the CCA-adding enzyme is not required for tRNA maturation. Nonetheless, disrupting the gene

encoding tRNA nucleotidyltransferase in *E. coli* resulted in up to 15% of the tRNA population lacking a complete CCA 3'-terminus and a slow-growth phenotype (Zhu and Deutscher, 1987). These results show that tRNA 3'-ends can be damaged and that one additional function of the CCA-adding enzyme is to repair tRNAs damaged at their 3'-ends. Given the long half-lives of tRNAs ranging from hours to days (Nwagwu and Nana, 1980; Kanerva and Maenpaa, 1981, Karnahl and Wasternack, 1992) it is important to maintain an intact 3'-terminus for aminoacylation.

1.3.3 Quality control

While repairing damaged 3'-termini may be one way to ensure that tRNAs remain functional, the CCA-adding activity has additional roles in tRNA quality control (Fig. 1.4). For example, tRNA nucleotidyltransferase plays a role in ensuring that damaged tRNAs are not aminoacylated and delivered to the ribosome where they could deleteriously effect translation. In *E. coli* a break in the nucleic acid backbone of the tRNA even far from the aminoacyl stem prevents efficient CCA addition with a k_{app} value ~ 1000-fold lower than that of the intact tRNA (Dupasquier *et al*., 2008). Without the CCA sequence, the damaged tRNA cannot be aminoacylated and can be a target for further degradation.

In addition to targeting some tRNAs for degradation by not adding the CCA terminus, the CCA-adding enzyme can direct other tRNAs for degradation by adding not one but two CCA sequences to the tRNA 3'-end (Wilusz *et al*., 2011, Kuhn *et al*., 2015). This extended polymerization occurs in all three domains of life and is in response to hypomodification and/or aberrant tertiary structures (Wilusz *et al*., 2011). CCACCA-containing tRNAs are targeted for degradation by the rapid tRNA decay (RTD) pathway (Wilusz *et al*., 2011) as the features that lead to CCACCA addition are common to those that target tRNAs for degradation (Alexandrov *et al*., 2006, Chernyakov *et al*., 2008, Kotelawala *et al*., 2008, Whipple *et al*., 2011). CCACCA addition prevents aminoacylation and marks damaged tRNAs for degradation to prevent possible errors in translation from occurring with these incorrectly formed tRNAs (Wilusz *et al*., 2011). The RTD pathway is mediated by 5'-3' exonucleases Rat1 and Xrn1 and indirectly regulated by Met22 (Dichtl *et al*., 1997).

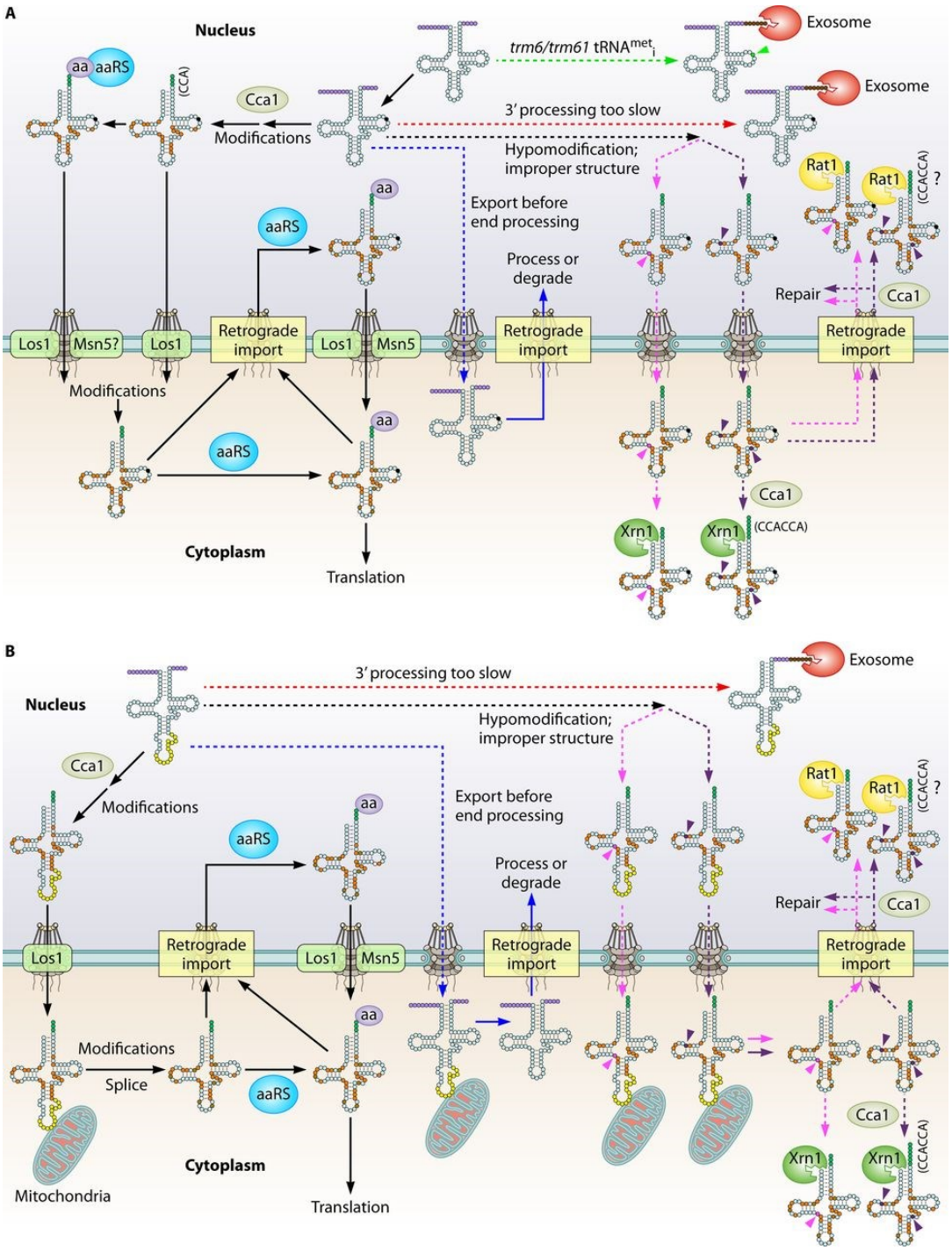

Figure 1.4: tRNA quality control pathways. **(A)** For tRNAs lacking introns **(B)** For tRNAs containing introns. Cloverleaf structures are tRNAs with colour coded circles. Purple circles demonstrate transcribed leader and trailer sequences at the 5'and 3' termini, respectively. The mature exons and introns are shown by blue and yellow circles respectively. Green circles indicate the post-transcriptionally added CCA nucleotides. A black circle depicts a modification known to occur on initial pre-tRNA transcripts. Orange, brown, and open circles show different post-transcriptional modifications (Hopper and Huang, 2015, reproduced with permission).

1.3.4 Response to cellular stress

When vertebrate cells undergo oxidative stress, angiogenin removes the 3'-terminal adenosine residue from tRNAs by an endonucleolytic cleavage such that aminoacylation is blocked and translation is repressed (Czech *et al.,* 2013). Upon removal of the environmental stress, the CCA-adding enzyme can restore the CCA sequence to the tRNAs to allow translation to occur efficiently again. This dynamic removal/readdition process allows cells to repress and reactivate protein synthesis with a low metabolic cost (Czech *et al.,* 2013). It also has been reported that under temperature or oxidative stress, or nutrient limitation (Shaheen e*t al.,* 2007; Hurto *et al*., 2007; Whitney *et al*., 2007; Kramer and Hopper 2013; Watanabe *et al*., 2013; Chen *et al.,* 2016; Schwenzer *et al*., 2019) tRNAs may move from the cytosol to the nucleus through a retrograde import pathway (Fig. 1.4) as another way to repress translation. Upon removal of the stress the tRNAs then return to the cytoplasm (Shaheen and Hopper, 2005; Shaheen e*t al.,* 2007; Takano *et al*., 2005; Whitney *et al*., 2007). The re-export of some of these tRNAs from the nucleus will require a complete CCA terminus so that the CCA-adding enzyme also plays a role in this re-export pathway that allows translation to increase with removal of the stress or nutrient limitation (Czech *et al.,* 2013).

Taken together, all of this suggests that the CCA-adding enzyme may play multiple roles in the cell in addition to tRNA maturation. Also, its levels in the cytosol or the nucleus may change as the conditions in the cell change. As tRNAs move from the nucleus to the cytosol and back to the nucleus and again to the cytosol perhaps the CCA-adding enzyme also needs to be distributed at different levels throughout the cell. Moreover, in yeast under conditions of anaerobic and aerobic respiration different amounts of the CCA-adding enzyme may be required in the cytosol and mitochondrion.

1.4 Localization of tRNA nucleotidyltransferase

As described above, the CCA-adding enzyme functions in the nucleus and in the cytosol in the synthesis, repair and quality control of tRNAs. In addition, both mitochondria and plastids encode their own tRNA genes lacking the 3'-terminal CCA sequence (Juhling *et al*. 2009) such that tRNA nucleotidyltransferase also is required in those organelles for tRNA biosynthesis and repair. So, in eukaryotic cells the CCA-adding enzyme may be required in up to four distinct sub-cellular

compartments (nucleus, mitochondrion, plastid and cytosol). Interestingly, a single gene typically codes for the CCA-adding enzyme that functions in all of these locations. Specifically, analysis of the complete sequences of 163 eukaryotic genomes revealed only nine genomes with more than one gene showing conserved sequences characteristic of tRNA nucleotidyltransferases (Leibovitch *et al*., 2013). This suggests that in multiple different eukaryotes a single nuclear gene is responsible for generating the CCA-adding enzyme that functions in multiple intracellular destinations. This was shown to be the case in yeast (Chen *et al.,* 1990), humans (Chakraborty *et al.*, 2014) and Arabidopsis (Leibovitch *et al*., 2013). In fact, the Arabidopsis CCA-adding enzyme was the first protein identified with "quadral" localization, *i.e*., it functions in the nucleus, cytosol, mitochondrion and plastid (Leibovitch *et al*., 2013). Proteins which are the products of single genes but function in multiple different destinations in the cell are known as "sorting isozymes" (Martin and Hopper, 1994) and the yeast CCA-adding enzyme was one of the first sorting isozymes identified (Chen *et al.*, 1992). So, after translation on cytoplasmic ribosomes some of the CCA-adding enzyme must be retained in the cytosol for tRNA repair while some of it is targeted to the nucleus or mitochondrion, or plastid (in plants), to carry out its functions in those subcellular locations. Questions remain as to how this protein is transported at the appropriate times and in the correct amounts to carry out the activities required in each of these destinations.

1.4.1 Targeting of the CCA-adding enzyme

Protein localization of sorting isozymes can be regulated at the level of transcription or translation (Martin and Hopper, 1994) or through post-translational modifications (Bannister *et al*., 2000; Ventura *et al*., 2010; Kumar *et al.*, 2017). Different isoforms of a protein can be produced from a single gene using alternative transcription or translation initiation sites, alternative splicing of intron-containing genes, coding frameshifts, alternative translation termination sites or through post-translational modifications (Danpure, 1995; Yogev *et al*., 2011). For example, different transcription initiation sites in the yeast *CCA1* gene result in transcripts of varying lengths such that translation of the longest transcripts generates a protein with 17 additional N-terminal residues, not found in protein generated from the shorter transcripts (Wolfe *et al*., 1994). These 17 extra amino acids form a classical mitochondrial targeting signal (Hansen and Herrmann, 2019) and have been shown to be necessary (Chen *et al.*, 1992) and sufficient (Wolfe *et al*., 1994) for mitochondrial targeting in yeast. Similarly, for the gene encoding the Arabidopsis CCA-adding

enzyme, we showed multiple transcription start sites such that proteins with or without an amino-terminal extension of 68 residues could be generated, depending on which transcript was used (Schmidt von Braun *et al*., 2007). Proteins with the amino-terminal extension were targeted to mitochondria and plastids while those lacking this sequence were found in the cytosol or nucleus (Schmidt von Braun *et al*., 2007). Together these data all support the presence of classical N-terminal mitochondrial (or plastid) targeting signals playing a role in the localization of the CCA-adding enzyme in eukaryotes.

In contrast to the evidence from multiple organisms of classical N-terminal mitochondrial or plastid targeting signals in the CCA-adding enzyme (Chen *et al.*, 1992; Shanmugam *et al*., 1996, Deng *et al*., 2000; Reichert *et al*., 2001, Nagaike *et al*., 2001, Hanic-Joyce and Joyce, 2002, Schmidt von Braun *et al*., 2007), no nuclear localization signal (NLS) has been demonstrated in any CCA-adding enzyme. A computational analysis of the Arabidopsis CCA-adding enzyme revealed two potential nuclear localization signals (Schmidt von Braun *et al*., 2007). The first of these, KAKRQRIE, was found at the carboxy-terminus of the protein (E is the last residue in the polypeptide) in a region predicted to be surface exposed. This sequence contains the signature motif (underlined) of a classical monopartite nuclear localization signal (NLS), K-K/R-X-K/R (Kalderon *et al*., 1984, Lanford and Butel, 1984; Soniat and Chook, 2015). When this sequence was converted to *E*A*EE*Q*E*IE (changed residues in italics) which should also be hydrophilic and surface exposed, since positively charged residues are replaced by negatively charged residues, we did note an altered distribution of the protein. Unexpectedly, we saw a 3-fold increase in cells showing nuclear, plastid, or cytosolic localization with a concomitant decrease in cells showing mitochondrial localization (Leibovitch *et al.*, 2013). So, if the KAKRQRIE sequence plays a role in the nuclear localization of this protein it does not do so in isolation.

We also targeted a second region of the Arabidopsis CCA-adding enzyme for mutagenesis. This sequence KDTKGKSIPVVNHIFKFSMKRK showed some features of a classical bipartite NLS (underlined in the motif), This motif (K/R)(K/R)$X_{10–12}$(K/R)$_{3/5}$, where X is any residue and (K/R)$_{3/5}$ represents three lysine or arginine residues out of five consecutive residues, is found in multiple proteins and in many different organisms (Soniat and Chook, 2015). Again, we converted lysines to glutamates (and in this case the single arginine residue to methionine) to generate the sequence *E*DT*E*G*E*SIPVVNHIFEFSM*EME* (changed residues in italics). As with the previous

mutations, this region of the protein is predicted to be surface exposed and should remain so as we replaced the positively charged lysine residues with negatively charged glutamate residues. Once again, these amino acid substitutions did not provide the anticipated results. The number of cells showing nuclear, plastid and cytosolic protein increased while the cells showing mitochondrial localization decreased (Leibovitch *et al.*, 2013). Again, if this region of the protein contains a nuclear localization signal then it does not act in isolation. Taken together these data suggest that the distribution of the CCA-adding enzyme is a complicated process.

1.4.2 Protein targeting

A minimum of two things are needed for a protein to be targeted to a specific location: 1) intrinsic signals that govern that protein's transport and localization in the cell and 2) something to recognize these signals.

The cargo protein contains the targeting information which is recognized by the nuclear transport receptor, Imp (importin), which interacts with the protein and escorts it into the nucleus (Görlich and Kutay, 1999). Once in the nucleus, the cargo is released and the receptor returns to the cytoplasm (Görlich and Kutay, 1999). A similar process, but in reverse, allows certain proteins to be exported from the nucleus by exportins (Görlich and Kutay, 1999). Therefore, to define any targeting pathway one must identify both *cis*- and *trans*-acting elements. The *cis*-elements are the intrinsic signals contained on the protein of interest and the *trans*-acting elements are the proteins that recognize these signals (Görlich and Kutay, 1999).

With sorting isozymes there is an additional level of complexity as multiple different targeting signals can be present on a single protein to interact with multiple different receptors. Moreover, there may be regulation as to which signals are used. For example, we showed that *Candida glabrata* cells grown on a non-fermentable carbon source generate more of a longer transcript potentially coding for the CCA-adding enzyme with its mitochondrial targeting signal than when grown on glucose when they do not need the mitochondrial targeting signal for mitochondrial protein synthesis (Hanic-Joyce and Joyce 2002). So, while this regulation is at the level of transcription there are examples among other sorting isozymes where the regulation is at the level of post-translational modification.

Swi5, a transcription factor, is synthesized during the S, G2 and M phases of the cell cycle but remains in the cytosol to be translocated to the nucleus when cells enter G1 (Nasmyth *et al*., 1990). Cytosolic Swi5 has phosphorylated serine residues near its nuclear localization signal that inactivate or mask the NLS function. On the switch from M phase to G1, these residues are dephosphorylated and the protein can enter the nucleus to activate transcription of its target genes (Moll *et al*., 1991). A similar mode of regulation is seen with other proteins with regulated entry to the nucleus, *e.g*., lamin B2, and SV40 T-antigen (Hennekes *et al*., 1993, Rihs *et al*., 1991, Jans *et al*., 1991). In fact, reversible phosphorylation is one of the best characterized mechanisms for regulating nuclear import and export. While phosphorylation can down-regulate nuclear import as discussed previously, it also can up-regulate nuclear import (Nardozzi *et al*., 2010). Although it is relatively easy to appreciate that phosphorylation and the introduction of negatively charged phosphate groups near a positively charged NLS would disrupt potential interactions with a receptor protein, it is less obvious why phosphorylation could enhance binding to the receptor. In the case of STAT1, a member of the Signal Transducers and Activators of Transcription family of transcription factors, which typically resides in the cytosol, stimulation of extracellular receptors leads to phosphorylation at a tyrosine residue such that dimerization of STAT1 is induced. Once the dimer is formed, structural rearrangement takes place to expose a dimer-specific NLS and the protein can be imported into the nucleus (Shuai *et al*., 1994, Wenta *et al.,* 2008).

Phosphorylation and dephosphorylation also regulate protein targeting to destinations other than the nucleus. For example, protein targeting to chloroplasts can be mediated by targeting signal phosphorylation and dephosphorylation. A number of chloroplast proteins, *e.g*., ferredoxin (preFd), the small subunit of ribulose-bisphosphate-carboxylase (preSSU), the thylakoid localized light-harvesting chlorophyll a/b-binding protein (preLHCP), and the thylakoid lumen-localized proteins of the oxygen-evolving complex of 23 kDa (preOE23) and 33 kDa (preOE33) were shown to possess phosphorylated serine and threonine residues in their targeting signals, which must be removed to obtain complete import (Waegemann and Soll, 1996). Further, it has been proposed that post-translational modifications of chloroplast transit peptides regulate chloroplast biogenesis allowing the plant to react dynamically in response to environmental changes (Lamberti *et al*., 2011). Phosphorylation and dephosphorylation also may mediate mitochondrial targeting. For

example, mitochondrial import of Tom22 was shown to be regulated by phosphorylation (Schmidt *et al*., 2010; Schmidt *et al.,* 2011).

Other studies have demonstrated the role of post-translational acetylation of many proteins. Acetylation has been identified in proteins involved in nuclear import. For example, acetylation of a single lysine residue in human importin-alpha increases its ability to bind to importin-beta (Bannister *et al*., 2000). In yeast, tyrosyl-tRNA synthetase has its classical aminoacylation function in the cytosol, but when cells are exposed to oxidative stress it translocates to the nucleus where it has a role in protecting DNA from oxidative damage. This shift in location is mediated primarily by acetylation of residue K244 near the NLS, which activates nuclear localization (Cao *et al*., 2017) to alter protein distribution. Acetylation also mediated nuclear localization of transcriptional corepressor CtBP2 (Zhao *et al*., 2006). Acetylation of lysine residues in glyceraldehyde-3-phosphate dehydrogenase resulted in nuclear localization of this protein within a human cell (Ventura *et al*., 2010). Finally, acetylation of signaling adaptor p66Sch promotes S36 phosphorylation and its localization to the mitochondrion (Kumar *et al.*, 2017).

In eukaryotes, post-translational modification of proteins is widespread. These modifications can affect not only protein localization, but also its structure, solubility, and/or function inside the cell (activation/inactivation). In this study, I will concentrate primarily on how these PTMs may be related to protein targeting.

1.5 *Saccharomyces cerevisiae* as a model organism

Saccharomyces cerevisiae, commonly known as baker's yeast, is used as the model organism in this study because of its unique physiology (Johnson and Echavarri-Erasun, 2011). While it has some features of prokaryotes such as a short doubling time (Brewer *et al*., 1984), it shares many features with multicellular eukaryotes including humans (Kachroo *et al*., 2015). Moreover, it has been studied since the time of Pasteur (Pasteur, 1879) and is well-characterized metabolically (Curto, 1994), genetically (Mortimer and Schild, 1980), and at the level of its genome (Goffeau *et al*., 1996) and proteome (Garrels *et al*., 1997). Also, as a eukaryote, it has the cellular machinery required to modify proteins post-translationally (Johnson and Echavarri-Erasun, 2011). Although fermentation (anaerobic respiration) is the major pathway for energy production in *S. cerevisiae* (even in the presence of oxygen), it can shift to aerobic respiration (requiring oxidative

phosphorylation and the electron transport chain in the mitochondrion) when glucose is limiting (Gasmi *et al*., 2014). This change in metabolism provides us with different cellular conditions to use to compare the localization of the CCA-adding enzyme. For example, during fermentation its role in the mitochondrion is small, as functional mitochondrial tRNAs are not needed for translation of the mitochondrially-encoded components of the electron-transport chain. However, when glucose is limiting, mitochondrial protein synthesis is required for aerobic respiration so the CCA-adding enzyme is needed in mitochondria. Taken together, all of these features make *Saccharomyces cerevisiae* an excellent model organism to study factors that may influence the structure, function or localization of the CCA-adding enzyme.

1.6 Label-free LC-MS/MS proteomics

Mass spectrometry is a powerful technique that has been used for protein identification and proteomics analyses for more than 25 years (Henzel *et al*., 1993; Mann *et al*., 1993; Pappin *et al*., 1993; James *et al*., 1993). The high sensitivity (femtomole level of detection) and accuracy (1% false discovery rate) of this method make it an ideal alternative to traditional amino acid sequencing techniques (Larsen and Roepstorff, 2000). Mass spectrometry can be used to process a small amount of a purified protein as well as complex protein mixtures with high mass accuracy and sensitivity (Larsen and Roepstorff, 2000). Liquid chromatography (LC) coupled to tandem mass spectrometry (LC-MS/MS) allows for proteins of interest to be separated first by LC and then to be separated by molecular weight by one mass spectrometer before being fragmented and subsequently identified based on the sizes of their fragments by a second mass spectrometer (Fig. 1.5). Linking LC-MS/MS to computational analysis and defined protein data bases allows data-dependent analysis (DDA) to be used to identify and quantify proteins and their post-translational modifications. The following steps to identify and quantify peptides in MS-based proteomics (Domon and Aebersold, 2010) are generally followed after initial sample preparation involving proteolytic digestion of all proteins into peptides and separation of these peptides using reversed phase liquid chromatography. First, the pool of peptides is vaporized and changed to the gas phase by heating. Then, this vapour is exposed to an electron beam which converts the vapors to ions (either positively charged or negatively charged). As mass spectrometry only identifies charged species these ions will be identified while any uncharged species will not be seen (Fig. 1.5, step 1). Second, these ions are sorted according to their masses. This is done in two steps. First through

acceleration (where lighter molecules move more quickly toward a charged plate than do heavier molecules) and second through deflection (where molecules are deflected in a magnetic field again based on their mass). Because of this, molecules of different masses travel through the spectrometer at different speeds and reach the detector in order of increasing mass. The relative amounts of each molecule are then determined based on their mass to charge ratio (m/z) which is reasonably straightforward as most molecules have a charge of one (Fig. 1.5, step 2). A more informative form of MS (tandem MS) then allows for selected precursor ions in the gas phase to be further fragmented through collision-activated dissociation (CAD). In this approach, again an electric field is used to accelerate the charged particles but, in this case, not in a vacuum but into a neutral gas such as helium (Fig. 1.5, step 3). The charged molecules can then collide with the gas molecules several times converting kinetic energy to internal energy, eventually breaking the weakest covalent chemical bonds in the molecules of interest (Fig. 1.5, step 4). The resulting fragment ions are extracted from the collision chamber and injected again into a mass analyzer such that fragment-ion masses and product-ion spectra can be generated. In proteomic analyses this allows peptide sequence to be determined from the ensemble of fragment-ion masses (Fig. 1.5, step 5). These steps are followed by post-acquisition data processing and analysis (Domon and Aebersold, 2010).

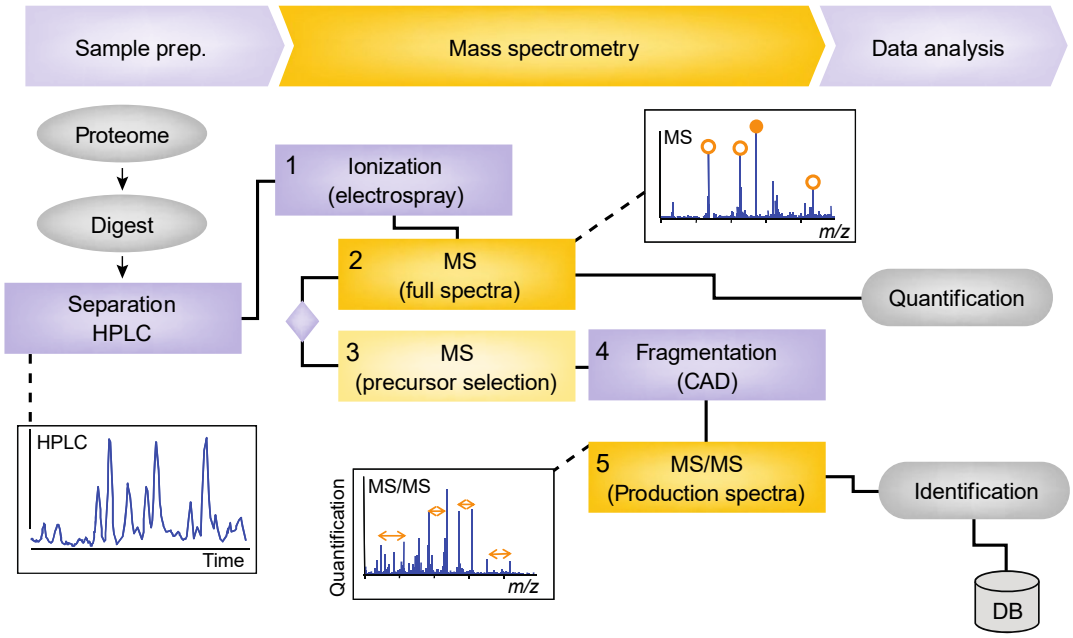

Figure 1.5: A typical mass spectrometry experimental procedure to identify proteins and their post-translational modifications (Domon and Aebersold, 2010, reproduced with permission).

Analyzing a protein at the level of its peptides allows the identification of post-translational modifications. Stable modifications such as acetylations that cause small mass shifts can be readily identified from the MS/MS spectrum. On the other hand, unstable modifications like phosphorylation are more challenging to identify due to the loss of the mass adduct during the ionization process or CAD. Phosphoserine and phosphothreonine often undergo loss of HPO_3 (80 Da) and/or H_3P0_4 (98 Da), thus further steps are required for a successful PTM identification (Parker *et al*., 2010). A method known as Data Dependent™ Neutral Loss MS^3 ($DDNLMS^3$) detects and isolates a neutral loss ion fragment from an MS/MS experiment and subjects it to more fragmentation steps. So, fragments that lacked a charge and would not be seen by MS are further fragmented and ionized to generate an MS3 scan (Thermo scientific, PSB 122_62576). The majority of proteomic studies to date have used mass spectrometry approaches to identify proteins and their PTMs and there are many examples in the literature (*e.g*., Tatara, *et al*., 2010; Li *et al*., 2012; Moore *et al*., 2013; Martinez-Gil *et al*., 2017).

1.7 Project objectives

Given the role of the CCA-adding enzyme in tRNA maturation and repair, protection and degradation and its varied functions in different locations in the cells, the objective of my project was to identify *cis*- or *trans*-acting factors that affect the localization or activity of the CCA-adding enzyme in *Saccharomyces cerevisiae.* To explore the *cis*-acting factors, tandem mass spectrometry (MS/MS) was used to identify post-translational modifications of the enzyme in yeast cells at different growth stages (early, middle and late log phase) and in different carbon sources (glucose and glycerol) to see if there were differences in the PTMs when cells were growing fermentatively (not requiring mitochondrial respiration) or aerobically (requiring mitochondrial respiration) suggesting that these PTMs may play a role in determining the localization of this enzyme. To explore *trans*-acting factors, *i.e*., accessory proteins that interact with Cca1 and which may vary depending on the localization or activity of Cca1, we used TAP and GST pulldown assays, followed by MS/MS to identify partner proteins interacting with Cca1 from yeast grown under different conditions. The primary focus of this study was in the OD_{600} range of 1.0, which is post-diauxic shift in *S. cerevisiae* (Lavova *et al*., 2014). This is near the point where any glucose in the medium has been used and the cells shift from fermentation to aerobic respiration (Lavova *et al*., 2014). We anticipated that this change in respiration pattern would affect the localization of Cca1

such that we could explore factors affecting the distribution of this enzyme under these different conditions. Similarly growing cells on a non-fermentable carbon source such as glycerol would force the cells to carry out aerobic respiration with the concomitant stresses associated with that (Vasylkovska *et al*., 2015; Babazadeh *et al.*, 2017) such that again we may see differences in factors affecting Cca1 localization under these different conditions.

2. MATERIALS AND METHODS

2.1 Strains, growth media and solutions

Saccharomyces cerevisiae and *Escherichia coli* strains and plasmids used in this study are indicated in Table 2.1.

Table 2.1: *Saccharomyces cerevisiae* and *Escherichia coli* strains and plasmids used in this study.

Strains/Plasmids	Relevant information	Genetic Background
W303-1B	Yeast genetic background for transformations and gene expression	MATα *ade2-1 his3-11,15 leu2-3,112 trp1-1 ura3- 1 can1-100*
XL2-Blue	*E. coli* strain for plasmid propagation (Stratagene)	*endA1 supE44 thi-1 hsdR17recA1 gyrA96 relA1 lac [F′proAB lacIqZΔM15 Tn10 (Tetr)* Amy Cam^r]
BL21(DE3)	*E. coli* strain for protein expression (New England BioLabs)	*E. coli* str. B F$^-$ *ompT gal dcm lon hsdS$_B$*($r_B^-m_B^-$) λ(DE3 [*lacI lacUV5-T7p07 ind1 sam7 nin5*]) [*malB*$^+$]$_{K-12}$(λ^S)
p426-CCA1/TAP	*CCA1*-TAP amplified from strain YSC1178 (Harju *et al*., 2004) and cloned into p426-GPD (Mumberg *et al.*, 1995) for overexpression in yeast (Guan, 2018)	
pTAP	TAP tag from p426-CCA1/TAP cloned into p426-GPD (Mumberg *et al*., 1995) for overexpression in yeast (this work)	
pGEX-2T-Scr9-1	Yeast *CCA1* open reading frame cloned in frame to the 3' terminus of GST in pGEX-2T (GE Healthcare) for expression in *E. coli* (Goring *et al*., 2013)	
pGEX-2T	GST in pGEX-2T for expression in *E. coli* (GE Healthcare)	
ScSK-CCA1-TAP	Strain W303-1B carrying plasmid p426-CCA1/TAP with *URA3* marker	MATα *ade2-1 his3-11,15 leu2-3,112 trp1-1 ura3- 1 can1-100*+ p426-CCA1/TAP (*URA3*)
ScSK-TAP	Strain W303-1B carrying plasmid p426-TAP with *URA3* marker	MATα *ade2-1 his3-11,15 leu2-3,112 trp1-1 ura3- 1 can1-100*+ p426-TAP (*URA3*)

Growth media, solutions, buffers and their required ingredients are listed in Table 2.2.

Table 2.2: Recipes for buffers, solutions and growth media

Buffers/Solutions/Media	Recipe
100X T-mix (Guthrie and Fink, 1991)	0.2% tryptophan, 0.3% tyrosine, 2% threonine, adjusted to pH 10 with NaOH, filter sterilized
30% Acrylamide Solution (29 :1) (Sambrook *et al.*, 1989)	29 g acrylamide, 1 g *bis*-acrylamide; in a final volume of 100 mL in dH_2O
5X SDS Loading Dye (Modified from Walker, 2002)	45 mM Tris-HCl (pH 6.8), 10% SDS (w/v), 50% glycerol (v/v), 25% β-mercaptoethanol (v/v), 0.25% bromophenol blue (w/v)
5X SDS Running Buffer (Modified from Sambrook *et al.*, 1989)	72 g (1 M) glycine, 15 g (1 M) Tris-HCl, 5 g (17 mM) SDS, dH_2O to one litre
5X TBE (1 L) (Modified from Sambrook *et al.*, 1989)	30 g (250 mM) Tris, 15.5 g (25 mM) boric acid, 10 mL 0.5 M EDTA (5 mM, pH 8.0), dH_2O to one liter
GST Elution Buffer (Modified from Lin, 2008)	50 mM Tris-HCL pH 8.0, 10 mM reduced glutathione, 20 mM DTT
Yeast Lysis Buffer (Modified from Ghaemmaghami *et al*., 2003)	50 mM Tris-HCl (pH 8.0),150 mM NaCl, 0.2% NP-40, 10% glycerol, containing one tablet of cOmplete, EDTA free protease inhibitor cocktail (MilliporeSigma) per 10 ml, 1 mM PMSF and 1mM DTT (add just before using)
Bacterial lysis buffer (modified from Shan *et al*., 2008)	50 mM Tris-HCl pH 7.6, 0.1 mM EDTA, 100 mM NaCl, 100 µg/ml lysozyme,0.1 mM PMSF, and 1X EDTA free protease inhibitor cocktail (MilliporeSigma) /10 ml
PBS (1X) (pH 7.45) (Sambrook *et al.*, 1989)	8 g (137 mM) NaCl, 0.2 g (2.7 mM) KCl, 2.68 (10 mM) Na_2HPO_4, 0.25 g (1.8 mM) KH_2PO_4; fill to 1 litre with dH_2O and store at 4 °C, adjusted pH with HCl
PLAG	15% glycerol, 40% Polyethylene glycol MW 3350, 10% 1.0 M lithium acetate, 1% 1.0 M Tris-HCl pH 7.5-8.0, 0.2% ml 0.5 M EDTA pH 8, plus 10 µl herring sperm DNA and stored at -80ºC
SC (-URA) (Guthrie and Fink, 1991)	0.67% yeast nitrogen base without amino acids, 2% glucose, 20 mg/l: adenine, L-histidine-HCl, L-arginine-HCl, L-methionine, 30 mg/l: L-leucine, L-isoleucine, L-lysine-HCl, 50 mg/l: phenylalanine. Autoclave. when cool, add 10 ml/l 100X T-mix (plates: 1.5 % agar)
SDS Destaining Solution B (Wong *et al*., 2000)	10% isopropanol, 10% acetic acid, 0.005% Coomassie Brilliant Blue
SDS Destaining Solution D (Wong *et al*., 2000)	10% isopropanol, 10% acetic acid
SDS Staining Solution A (Wong *et al*., 2000)	25% isopropanol, 10% acetic acid, 0.05% Coomassie Brilliant Blue

YPD (Guthrie and Fink, 1991)	2% peptone, 2% glucose, 1% yeast extract (plates:1.5% agar)
YT (Sambrook *et al*., 1989)	0.5% yeast extract, 0.8% tryptone, 0.5% NaCl
Binding buffer for phosphorylation enrichment (GE Healthcare, Instruction 28-9537-65 AB, TiO2 Mag Sepharose™)	1 M glycolic acid in 80% acetonitrile, 5% trifluoroacetic acid
Wash buffer for phosphorylation enrichment (GE Healthcare, Instruction 28-9537-65 AB, TiO2 Mag Sepharose™)	8% acetonitrile, 1% trifluoroacetic acid
Elution buffer for phosphorylation enrichment (GE Healthcare, Instruction 28-9537-65 AB, TiO2 Mag Sepharose™)	5% ammonium hydroxide, pH 12
SDS-PAGE 13% resolving gel (10 ml) (Modified from Sambrook *et al*., 1989)	4.3 ml 30% acrylamide, 3.0 ml dH_2O, 2.5 ml Tris (1.5 M, pH8.8), 100 µl APS (10%), 100 µl SDS (10%), 10 µl TEMED
SDS-PAGE 10% stacking gel (10 ml) (Modified from Sambrook *et al*., 1989)	1.4 ml 30% acrylamide, 6.0 ml dH_2O, 2.5 ml Tris (0.5 M, pH 6.8), 100 µl APS (10%), 100 µl SDS (10%), 10 µl TEMED

2.2 Construction of pTAP

2.2.1 Polymerase chain reaction (PCR)

The DNA region encoding the Tandem Affinity Purification (TAP) tag in plasmid p426-CCA1/TAP was amplified by the polymerase chain reaction (PCR) using primers TAPF and TAPR (Table 2.3). Each reaction contained 10-30 ng of template, 10 pmol of forward and reverse primers, 10 µl 5X HF buffer (NEB), 1 unit of NEB Phusion high fidelity DNA polymerase (2 000 U/ml), and 200 µM dNTPs in a final volume of 50 µl (adjusted using dH_2O). Control reactions excluded one or both primers. Reactions were performed in a BIO RAD T100™ thermal cycler as follows: initial denaturation at 98℃ for 3 min, followed by 34 cycles of 30 s denaturation at 98℃, 30 s annealing at 46℃, 5 min extension at 72℃, with a final extension at 72℃ for 10 min before storing

at 4ºC overnight or at -20ºC for longer storage. A 10-µl aliquot of the PCR product was loaded on a 1% agarose/1X TBE gel with electrophoresis at 1 h at 100V to confirm the success of the PCR.

Table 2.3: Primer sequences used to amplify the TAP tag to be cloned into p426-GPD vector.

Primers Name	Sequence (5'→ 3') Locations of restriction sites underlined	Restriction site Added
TAPF	GGAGGGACTAGTATGGAACGACGGA TCCCCGGG	*Spe*I site: ACTAGT
TAPR	TATATTGTCGACCCTCACTGATGATT CGCGTCTAC	*Sal*I site: GTCGAC

2.2.2 Phenol extraction and ethanol precipitation (Ausubel *et al.*, 1989)

Once the success of the PCR reaction had been confirmed by viewing the gel, an equal volume of phenol was added to the remaining sample with vortexing for several min followed by centrifugation at 12 000 xg at 4℃ for 3 min. The aqueous phase was collected and one tenth volume of 3 M sodium acetate and two volumes of 99% ethanol were added with vortexing followed by incubation at -80℃ for a minimum of 30 min or at -20℃ overnight. This was followed by centrifugation for 20-30 min at 12 000 xg to pellet the DNA and the supernatant was discarded. The DNA pellet remaining was washed with 300-500 of µl 80% ethanol with centrifugation at 12 000 xg for 5 min at 4℃. The ethanol was removed and the DNA was dried in a desiccator for at least 20 min. The dried DNA was resuspended in 10 µl sterile dH_2O.

2.2.3 Restriction digestions

An appropriate amount of purified PCR product or p426 plasmid was diluted to a final volume of 40 µl to which was added 4 µl of 10×Cutsmart buffer, 2 µl of *Spe*I-HF (20 000 U/ml) and 2 µl of *Sal*I-HF (20 000 U/ml). After gentle mixing, the samples were placed in a 37°C water bath for 1 h. The digested samples were separated by agarose gel electrophoresis (Section 2.2.1) and the desired fragments were excised from the gel (Section 2.2.4).

2.2.4 Isolation of DNA fragments from agarose gels (modified from Breitkreutz *et al*., 2010)

After restriction digestion, DNA samples were electrophoresed as above (Section 2.2.1 and 2.2.3) and visualized on a Foto/Prep®I transilluminator using preparative light setting. A blunt metal spatula was used to excise DNA fragments, which were placed in a microfuge tube containing 300 µl of phenol saturated with 0.1 M Tris-HCl pH 8 for vigorous vortexing for 10 min, followed by storage at -80℃ for a minimum of 30 min. After that, the microfuge tubes were placed in a 37℃ water bath for 10 min and the phenol freeze-thaw cycle was repeated one more time. After the second freeze-thaw cycle, 150 µl of dH_2O and 40 µl of 3 M sodium acetate pH 5.2 were added and after 30 s vortexing the sample was centrifuged for 5 min at 12 000 xg. The aqueous phase was transferred to a new microfuge tube and the sodium acetate concentration was adjusted to at least 0.3 M. An equal volume of phenol was added to the aqueous phase with vortexing for 1 min and centrifugation at 12 000 xg for 3 min at 4℃. The extraction step was repeated twice with equal volumes of water saturated ether. All three extraction steps were performed under a fume hood.

2.2.5 Ligation reactions

Appropriate amounts of vector (typically ~50 ng of DNA) and insert (typically ~150 ng of DNA) were mixed in a sterile microfuge tube with 2 µl of 10X ligation buffer (NEB), 0.4 µl of T4 DNA ligase (NEB, 400 U/µl) and sterile dH_2O to a final volume of 20 µl by stirring with the pipette tip and incubated overnight at 4ºC.

2.2.6 *E. coli* transformation (Ausubel *et al*., 1989)

E. coli XL2-Blue or BL-21(DE3) competent cells were prepared according to the procedure of Capage and Hill (1979) and incubated overnight at 4℃ before storage at -80℃ for at least one day (Dagert and Ehrlich, 1979). A 50-µl aliquot of these frozen cells was thawed on ice and added to a prechilled sterile microfuge tube on ice. Subsequently, 5 µl of a ligation mix or 10-50 ng of purified intact plasmid was added with stirring by pipette tip to the tube which was kept on ice for at least 20 min. This was followed by a 45 s heat shock at 42℃ and 1 min chilling on ice. Then, 500 µl YT or LB medium without antibiotic was added to the microfuge tube with gentle mixing and incubation at 37℃ for 1 h. After centrifugation at 12 000 xg for 1 min to pellet the cells, 400

µl of the medium was removed and the cells were resuspended in the remaining medium and plated on YT or LB plates containing ampicillin.

2.3 Expression and purification of Cca1-TAP from *S. cerevisiae* W303-1B

2.3.1 *S. cerevisiae* transformation (Dohmen *et al*., 1991)

Competent W303-1B cells (a patch of W303-1B cells mixed with 1 ml of sterile PLAG containing 15% glycerol, 40% Polyethylene glycol MW 3350, 10% 1.0 M lithium acetate, 1% 1.0 M Tris-HCl pH 7.5-8.0, 0.2% ml 0.5 M EDTA pH 8, plus 10 µl of herring sperm DNA and stored at -80ºC) were thawed on ice and 75 µl aliquots were dispensed into sterile microfuge tubes. Then, 1.5-2.5 ng of sterile plasmid (p426-CCA1/TAP or pTAP or controls) was added with gentle mixing and incubation at 42℃ for 2 h. The cells were spread on SC-URA plates and incubated at 30℃ for one to three days. Colonies were selected from the plate, inoculated into 10 ml SC-URA liquid medium and grown overnight at room temperature with shaking at 225 rpm. A freezer stock for storage at -80ºC was made using 700 µl of culture plus 300 µl 50% glycerol.

2.3.2 Protein expression and whole-cell lysis (modified from Breitkreutz *et al*., 2010)

A single colony of W303-1B cells, transformed with the appropriate plasmid (Section 2.3.1), was inoculated into 10 ml of SC-URA and grown overnight at 30℃ with 225 rpm shaking. The next day this starter culture was added to 1 l of SC-URA medium with incubation as above to reach an appropriate OD_{600}. Cells were harvested at different times to reflect different stages of the growth phase. Growth in rich medium was for 9 h (early log phase, OD_{600} of 0.3), or 60 h (late log phase, OD_{600} of 3.5). In contrast, growth in synthetic complete medium lacking uracil (SC-URA) with glucose as the carbon source was for 16 h (post-diauxic shift, OD_{600} of 1.0). The incubation was increased to 21 h when cells were grown on SC-URA medium containing glycerol as the carbon source to reach an OD_{600} of 1.0. The culture was transferred to 500 ml centrifuge bottles and the cells were harvested by centrifugation at 3 000 xg for 20 min. The supernatant was discarded and the cell pellets (typically with a volume of ~1-2 ml) were resuspended by pipetting gently in 5-10 volumes of ice cold 20 mM HEPES (pH 7.5) containing 10 mM EDTA, transferred to 15 ml tubes and centrifuged at 3 000 xg for 5 min. The supernatant was pipetted away and the volume of the remaining pellet was measured and an equal volume of lysis buffer containing cOmplete™, EDTA-free protease inhibitor cocktail (MilliporeSigma) and 1% Triton X-100 was

added to the cells with gentle mixing with the pipette tip. Then, 1 ml aliquots of the cell suspension were distributed into 1.5 ml microfuge tubes and ~500 µl of acid washed (Kohrer and Domdey, 1991) glass beads (MilliporeSigma, diameter 425-600 µm) were added to the tube. Samples were vortexed at maximum speed for 4 cycles of 5 min at 4℃ with a 5 min on ice between each cycle. The beads and debris were pelleted by centrifuging at 12 000 xg for 10 min and the supernatants were transferred to a fresh 15-ml tube. An aliquot of the whole-cell lysate before protein purification was saved to be analyzed by SDS PAGE.

2.3.3 Yeast subcellular fractionation (Gregg *et al*., 2009)

After cell lysis (Section 2.3.2), unbroken cells, large debris and nuclei were harvested by centrifugation at 1 500 xg at 4℃ for 5 min. The resulting supernatant was transferred to a new tube and centrifuged for another 5 min at 3 000 xg at 4℃. The cell pellets that remained were stored at 4℃ while the supernatant was transferred to a new tube and centrifuged for 15 min at 14 000 xg at 4℃. The supernatant after this centrifugation was collected as the cytosolic fraction and the cell pellet stored at 4℃. The 3 000 xg and 14 000 xg cell pellets were resuspended in an appropriate amount of 1% Triton X-100 in 1X PBS and incubated at 4℃ for 20-30 min to lyse the organellar membranes (Gurtubay *et al*., 1980), then the samples were centrifuged at 12 000 xg for 10 min and the supernatant transferred to a fresh microfuge tube. The proteins released from the 3 000 xg pellet define the nuclear fraction and those released from the 12 000 xg fraction define the mitochondrial fraction (Gregg *et al*., 2009).

2.3.4 Affinity purification of recombinant Cca1-TAP or TAP (modified from Breitkreutz *et al*., 2010)

The TAP-tagged fusion protein was purified in two steps. The whole-cell extract was transferred to a 2 ml microfuge or 15 ml Falcon™ conical tube (depending on the lysate volume) containing 100-200 µl of pre-washed Sepharose GST beads (BIOGOLD) with incubation at 4℃ for 1 h with an end-over-end rotation to account for non-specific binding. The beads were pelleted by centrifugation at 1 500 xg for 1-2 min at 4℃ and the supernatant gently removed without disturbing the pelleted beads. Then, the pre-cleared lysate was added to 100 µl of IgG Sepharose™ 6 Fast Flow beads (GE Healthcare), which had been prewashed 3X with lysis buffer. The supernatant liquid and the beads were mixed by end-over-end rotation at 4℃ overnight. The next

day, the sample were centrifuged at 1 500 xg for 1-2 min and the supernatant was transferred to a new tube for further analysis by SDS-PAGE. The IgG beads were washed 3X for 1h at 4ºC with end-over-end rotation with 1 ml of lysis buffer without protease inhibitors, followed by centrifugation and removal of the supernatant as described above. Then, 250 µl of 1X SDS loading buffer (50 µl 5X SDS loading buffer + 200 µl lysis buffer) was added to the IgG beads with incubation for 1 h at 37℃. After that, the beads and associate proteins were boiled for 5 min and beads were pelleted by centrifugation at 1 500 xg for 1-2 min before analysis of a small aliquot of the supernatant fluid by SDS-PAGE. The remaining supernatant was placed at -80℃ after addition of glycerol to 10% for storage.

2.3.5 Sodium dodecyl sulfate polyacrylamide gel electrophoresis (SDS-PAGE) (modified from Sambrook *et al*., 1989)

Proteins in a specific fraction were separated using 13% resolving and 10% stacking gels with 4 cm by 10 cm gel plates separated by 0.75 mm spacers. Approximately 20 µl of Cca1-TAP or TAP purified protein (as prepared in Section 2.3.4) was analyzed by SDS-PAGE. The eluted Cca1-GST or GST pulldown samples (as prepared in Section 2.4.3) were mixed with an appropriate amount of 5X SDS loading dye and boiled for 5 min before loading the gel. The samples were loaded into the wells, immersed in 1x SDS-PAGE running buffer (Table 2.2) and electrophoresis was carried out at 200 V for 1 h on the bench top. The gel was stained based on the modified version of the protocol of Wong *et al*. (2000). The gel was immersed in staining solution A, microwaved in 1000 KW Microwave oven (Whirlpool) on maximum for 20 s and incubated in a ROSI 1000^{TM} reciprocating/Orbital Shaking incubator (Thermolyne) for 5 min to stain. Staining solution A was discarded and the procedure repeated with staining solution B. Solution B was discarded and destaining solution was added. After 20 s in the microwave as above, the gel was detained for 30 min in the ROSI 1000^{TM} reciprocating/orbital shaking incubator (Thermolyne). Finally, the gel was washed with multiple volumes of dH_2O and scanned on a SNAPSCAN 1212 scanner (AGFA).

2.3.6 *In vivo* pulldown assay

After protein expression in yeast (Section 2.3.2) and affinity purification of recombinant protein (Section 2.3.4), 20 µl of the affinity purified proteins were loaded on a 13% resolving gel

to separate the proteins based on their sizes. This allowed the protein representing Cca1-TAP (~84 kDa) to be identified and extracted from the gel to be analyzed by MS/MS to identify post-translational modifications. The same amount of proteins were concentrated in a 10% stacking gel for proteomics study such that after electrophoresis at 200 V for 30 min, all of the proteins in the sample were concentrated in the stacking gel and could be isolated for MS/MS analysis. The gels were stained as in Section 2.3.5 and desired bands excised from the gels for MS/MS analysis. The same procedure was followed for the TAP tag alone as a negative control to detect the proteins that bind non-specifically to the TAP tag and these proteins were subtracted from the proteomics sample leaving only potential protein partners of *S. cerevisiae* Cca1. In one of the biological replicates grown on glucose to OD_{600} of 1.0, the cells were divided into two aliquots with one aliquot treated with a final concentration of 30 ng RNAseA/ml of protein solution (70-120 Kunitz units/mg, protein, BioShop Canada Inc. Burlington, ON) (Leibovitch, 2016) during the cell lysis and purification to increase the specificity of Cca1-interacting proteins by reducing those that may interact with RNA associated with Cca1. Previous UV-Vis analysis (A_{280}/A_{260}) showed that this concentration of RNAseA was sufficient to remove RNA from *E. coli* extracts containing heterologously expressed Cca1 (Chung, 2019).

2.3.7 Phosphorylation enrichment using TiO_2 Mag Sepharose™ beads

The protocol provided by the manufacturer was used for enrichment of phosphopeptides (GE Healthcare, Instruction 28-9537-65 AB). An appropriate amount of purified proteins (typically 30-60 µg) was used for phosphorylation enrichment. The magnetic particles were collected by placing 50 µl of TiO_2 Mag Sepharose™ 20% medium slurry (GE Healthcare) in a 1.5 ml microfuge tube in contact with the DynaMag™-2 magnetic particle concentrator (Invitrogen) such that the storage solution could be pipetted away. The beads then were washed in 500 µl of binding solution by manual inversion and the binding solution was removed after the beads were pelleted using the DynaMag™-2 magnetic particle concentrator as above. Peptides in 20-30 µl of reconstitution solution (97% W6-4 Water Optima® LC/MS, 2% acetonitrile, 1% formic acid) and 4 volumes of binding buffer were added to the breads with incubation at room temperature for 30 min with end-over-end rotation. Then, the samples were placed in a DynaMag™-2 magnetic particle concentrator (Invitrogen) and the binding buffer with non-phosphorylated peptides removed. The magnetic beads were washed with 500 µl of wash buffer as above. This step was repeated twice to

reduce non-specific binding and 50 µl of elution buffer was added to the beads with incubation for 5 min with end-over-end rotation at room temperature to elute the peptides of interest. The eluate was transferred to a 1.5-ml microfuge tube and the elution step was repeated one more time with all of the eluted peptides collected in one tube. The samples were dried in a SpeedVac at 40℃ and stored at – 20℃.

2.4 Expression and purification of yeast tRNA nucleotidyltransferase recombinant protein (GST-Cca1) in *E. coli* BL21(DE3)

2.4.1 Heterologous tRNA nucleotidyltransferase protein expression and whole-cell lysis

(modified from Shan *et al*., 2008)

A 10 ml starter culture of *E. coli* BL-21(DE3) cells carrying the plasmid of interest was grown overnight in LB medium with 100 µg/ml ampicillin at 37℃ with shaking (225 rpm) in an Innova™ 4330 refrigerated incubator shaker (New Brunswick Scientific). The next day, 700 µl of the overnight culture was mixed with 300 µl of sterile 50% glycerol in a sterile microfuge tube with gentle mixing for storage at -80°C as a freezer stock. The remaining overnight culture was added to 1 l of LB medium containing 100 µg/ml of ampicillin with incubation as above until the samples reached an appropriate OD_{600} (about 2-3 h incubation gave an OD_{600} of 0.4 to 0.6). Recombinant protein production was induced by adding D-lactose and IPTG to final concentrations of 0.02% and 0.5 mM, respectively, and the cultures were incubated at 19℃ and 225 rpm for 16-20 h. The cells were harvested by centrifugation at 4℃ for 15 min at 4 000 xg and the cell pellets (after recording the wet weight) were stored at -80℃ for at least 1 h before cell lysis. Frozen cell pellets were thawed on ice and resuspended in 2 ml of bacterial lysis buffer per gram of cell pellet by 10 cycles of 30 s vortexing with 30 s chilling on ice between cycles. The cell suspension was passed through a Thermospectonic French Pressure Cell for 4 cycles at 1 000 psi and the whole- cell lysate was centrifuged at 14 000 xg for 30 min at 4℃. After transferring the supernatant into a new tube, centrifugation was repeated to remove all cell debris and the resulting clear supernatant was passed through the GST column.

2.4.2 GST-fusion affinity chromatography (Harper and Speicher, 2011)

About 2-3 ml of Glutathione Agarose Resin (BIOGOLD) was packed in a 10 cm × 1.5 cm Bio-Rad column and used to purify the GST-fusion tRNA-NT protein. The column was equilibrated by passing about 10 bed volumes of 1X PBS (pH 7.45) through it. The resin was regenerated at the end of the purification by washing with 5 ml of 6 M guanidine-HCl, 50 ml of dH_2O and 50 ml of 70% ethanol and stored in 20% ethanol at 4℃.

2.4.3 GST purification and dialysis (modified from Shan *et al*., 2008)

The whole-cell lysate (Section 2.4.1) was passed through a Glutathione Fast Flow 4B column overnight at 4℃. A pump (VWR) was used to cycle the lysate through the column at flow rate of 1 ml/min. The next day, the flow-through was collected and the column was washed with 300-500 ml of 1X PBS to eliminate proteins that bound to the column non-specifically. Then, GST alone or the Cca1-GST fusion protein was eluted from the column using 10 ml of GST elution buffer and collected in 1 ml fractions in 1.5 ml microfuge tubes. The eluted fractions were analyzed by SDS-PAGE and the fractions containing the desired protein were pooled, transferred to a dialysis bag (Spectra/Por^R 7 Dialysis Membrane Pre-treated RC Tubing MWCO 50 kDa), and dialyzed overnight against 5 l of 1X PBS at 4℃, with buffer changes after 2 h and 4 h. The following day, the samples were analyzed by SDS-PAGE to check the purity of the protein of interest. The protein concentration was determined using the Bradford assay with BSA as the standard (Bradford, 1976; Bio-Rad Laboratories 2018) or by comparison to known concentrations of BSA on an SDS-PAGE gel to estimate the concentration of the protein of interest by ImageJ software (Schindelin *et al*., 2012). A final concentration of 10% (v/v) glycerol was added to the aliquots of the purified protein for storage at -80℃.

2.4.4 *In vitro* pulldown assay

Equimolar amounts of heterologously expressed and purified Cca1-GST or GST were used for the *in vitro* pulldown assays. Three conditions (1:10, 1:20 and 1:100 ratios of bait to prey) were tested. Appropriate amounts of Cca1-GST or GST diluted with 100 µl of 1X PBS containing 1X protease inhibitor cocktail were mixed with prewashed 20 µl of Glutathione High Capacity Magnetic Agarose beads (Sigma-Aldrich) in a microfuge tube and incubated with end-over-end rotation for 1 h at 4℃. The yeast whole-cell lysate (prepared as described in Section 2.3.2, with

the exception that W303-1B cells were grown in YPD rather than SC-URA) was added and incubation continued for 2 h at 4℃. The next day, the beads were pelleted by centrifugation at 1 500 xg for 1-2 min and washed 3X for 15 min with 10 volumes of 1X PBS with end-over-end rotation at 4℃. Then, Cca1-GST with other associated proteins was eluted from the beads using 50 µl of GST elution buffer and an aliquot was analyzed by SDS-PAGE. Finally, the concentrated band containing the desired protein and any interacting proteins was extracted from the gel using a clean sharp blade and transferred to a microfuge tube and stored at -80℃ freezer for analysis by MS/MS (Section 2.5). In addition, the beads alone were incubated with the whole-cell lysate to identify and remove proteins that bound non-specifically to the beads.

2.5 Mass spectrometric analysis to identify tRNA nucleotidyltransferase PTMs and interacting partners (All protocols provided by the Center for Biological Application of Mass Spectrometry of Concordia University)

2.5.1 Sample preparation for mass spectrometry

All procedures were performed at room temperature and all solutions containing NH_4HCO_3 were freshly prepared each day. The appropriate gel slices (typically about 1 x 1 x 0.5 mm pieces), were excised from SDS-PAGE gels (as described in Section 2.4.4), and transferred to 1.5-ml microfuge tubes. Each gel slice first was incubated in 200-300 µl of 50 mM NH_4HCO_3 containing 10 mM DL-dithiothreitol (DTT) followed by vortexing for 30 s and centrifugation for about 30 s at 2 000 xg. The supernatant was discarded and the gel slice was incubated in the dark for 30 min in 200-300 µl of a 50 mM NH_4HCO_3 solution containing 50 mM iodoacetamide followed by centrifugation and removal of the solution as described above. The gel pieces then were incubated for 15 min sequentially in 200-300 µl of 50 mM NH_4HCO_3, 25 mM NH_4HCO_3 with 5% acetonitrile (ACN), and 50% ACN. This final step was repeated once more, followed by a 10-min incubation of the gel pieces in 100% ACN. After incubation in 100% ACN, the gel slices were dried in a SpeedVac at 40℃ (typically for 10 min). The gels were rehydrated in 25 mM NH_4HCO_3 containing 0.01 µg/ µl trypsin and incubated at 30℃ overnight. The next day, three extraction steps using extraction solution (60% ACN containing 0.5% formic acid) at 4X the volume of the digestion solution were done and the samples were dried in a speed vac at 40℃ and stored at – 20℃ for MS analysis. For MS analysis, an appropriate amount of reconstitution solution (97% W6-4 Water

Optima^{R} LC/MS, 2% acetonitrile, 1% formic acid) was added to the peptides to allow for the injection of about 50-200 ng of peptides for MS analysis.

2.5.2 Mass spectrometric analysis method and procedure

The Thermo EASY nanoLC^{TM} II system coupled to a Thermo LTQ Orbitrap Velos mass spectrometer equipped with a nano-spray ion source was used to perform the mass spectrometric analyses. Typically, 2 µl of sample, or 5 µl of pull-down or phosphorylation-enriched sample (50-200 ng) were injected onto a 10 cm × 100 µm column in-house packed with Michrom Bioresources Inc. Magic C18 stationary phase (5 µm particle diameter and 300Å pore size). A 20-70 min linear gradient (20 min for BSA, 45 min for purified protein, 70 min for protein complexes) with a flow rate of 400 nl/min was used to elute peptides with declining amounts of mobile phase A (96.9% water, 3% acetonitrile, 0.1% formic acid) and increasing amounts of mobile phase B (97% acetonitrile, 2.9% water, 0.1% formic acid).

A full MS spectrum with an m/z range of 400-1400 was recorded on the Orbitrap at a resolution of 60 000 and the ten most abundant multiple charged ions were selected for MS/MS sequencing in the linear trap with the option of dynamic exclusion. A normalized collision energy of 35% with an activation time of 10 ms was used to perform collision-activated dissociation (CAD) of the peptides. In the case of the phosphorylation-enriched samples using TiO_2, if a phosphate neutral loss of 80 or 98 from the precursor ion was detected, further fragmentation of the neutral loss ion for MS^3 sequencing using CAD with multistage activation was enabled.

2.5.3 *Saccharomyces cerevisiae* database search

Thermo Proteome Discoverer software (v2.2) was used to analyze the MS data with the SEQUEST search engine. The search was against the *S. cerevisiae* proteome database from UniProt. The proteolytic enzyme trypsin (full) and the maximum missed cleavage sites were set at two to define the peptide database search. Mass tolerances of the fragment ion and precursor ion were set at 0.6 Da and 10 ppm, respectively. Only peptides and proteins with the false discovery rate (FDR) of less than 1% (high confidence) were reported.

3. RESULTS

3.1 Post-translational modification (PTM) of the Cca1 protein

Cells were harvested at different cell densities after growth on fermentable or non-fermentable carbon sources. Cells were lysed and the lysate from the appropriate fraction loaded onto an IgG column to retain the Cca1-TAP tagged fusion protein. The protein retained on the column was subsequently eluted and subjected to mass spectrometric analyses to identify post-translational modifications (PTMs). Although tryptic peptides two (STISLLMNSAAQK) and three (TMTNSNFVLNAPK) showed multiple positions which could show PTMs, no peptide was detected containing more than one site that had been phosphorylated and/or acetylated.

For two conditions, glucose growth to OD_{600} of 1.0 and OD_{600} of 2.5, phosphorylation enrichment of tryptic peptides using TiO_2 magnetic beads was performed. This additional step was to ensure capture of all phosphorylated positions since due to the dynamic nature of this type of modification (reversible) the abundance of peptides containing this modification tended to be low.

The PTMs detected in this study have been identified through MS^2, Data Dependent™ Neutral Loss MS^3 (phosphorylated positions) or with the Proteome Discoverer application (v2.2) feature for label-free quantification. Using this feature, LC/MS peaks in individual raw data files are detected and mapped to identified peptide spectrum matches (PSMs) by an algorithm to create unique features from peaks. Then, the program takes all of the LC/MS peaks within a small retention-time range and searches for peaks that build isotope patterns across all files (Thermo Proteome Discoverer User Guide Software Version 2.2_XCALI-97808, 2017). The percentage of modified peptides was calculated by taking the ratio of modified peptides over the total number of identified peptides multiplied by 100%.

The phosphorylations or acetylations found in the proteins under these various conditions are shown in Tables 3.1 to 3.8 and summarized in Tables 3.9 (acetylation) and 3.10 (phosphorylation). The positions modified are shown on the primary sequence of Cca1 in Fig. 3.1.

Table 3.1: Post-translational modifications identified on Cca1 from yeast cells grown on glucose to OD_{600} of 0.3.

Amino acid	T	K	K
Position	19	150	507
Phosphorylation			
Acetylation	+	+	+

Table 3.2: Post-translational modifications identified on Cca1 from yeast cells grown on glucose to OD_{600} of 1.0.

Amino acid	S	T	S	S	T	T	S	K	K	K	S	T	K
Position	4	5	7	12	17	19	21	57	118	150	328	407	507
Phosphorylation	+	+	+	+		+	+						
Acetylation	+	+	+		+	+	+	+	+	+	+	+	+

Table 3.3: Post-translational modifications identified on Cca1 from yeast cells grown on glucose to OD_{600} of 2.5.

Amino acid	S	T	S	T	T	S	K	K	S	K	T	T
Position	4	5	7	17	19	21	150	312	328	398	407	507
Phosphorylation	+	+	+		+	+						
Acetylation	+	+	+	+	+	+	+	+	+	+	+	+

Table 3.4: Post-translational modifications identified on Cca1 from yeast cells grown on glucose to OD_{600} of 3.5.

Amino acid	S	T	S	K
Position	4	5	7	150
Phosphorylation				
Acetylation	+	+	+	+

Table 3.5: Post-translational modifications identified on Cca1 from yeast cells grown on glycerol to OD_{600} of 1.0.

Amino acid	S	T	S	S	T	K	K	K	K	T	K	T	T
Position	4	5	7	12	17	57	118	150	312	407	507	528	530
Phosphorylation	+	+	+	+									
Acetylation	+	+	+		+	+	+	+	+	+	+	+	+

Table 3.6: Post-translational modifications identified on Cca1 in the mitochondrial fraction from yeast cells grown on glucose to OD_{600} of 1.0.

Amino acid	S	T	S	S	T	S	K	K	K	K	S	T
Position	4	5	7	12	19	21	57	118	150	185	328	407
Phosphorylation	+	+	+	+	+	+						
Acetylation	+	+	+		+	+	+	+	+	+	+	+

Table 3.7: Post-translational modifications identified on Cca1 in the nuclear fraction from yeast cells grown on glucose to OD_{600} of 1.0.

Amino acid	S	T	S	S	T	S	T	K	K	K	S	T	K
Position	4	5	7	12	19	21	17	57	118	150	328	407	507
Phosphorylation	+	+	+	+	+	+							
Acetylation							+	+	+	+	+	+	+

Table 3.8: Post-translational modifications identified on Cca1 in the cytosolic fraction from yeast cells grown in glucose to OD_{600} of 1.0.

Amino acid	S	T	S	S	T	S	K	K	K	K	S	T	K
Position	4	5	7	12	19	21	57	118	150	185	328	407	507
Phosphorylation	+	+	+	+	+	+							
Acetylation	+	+	+				+	+	+	+	+	+	+

Figure 3.1: Amino acid sequence of yeast Cca1 showing positions post-translationally modified to contain phosphoryl and/or acetyl groups. Amino acids showing phosphorylation, acetylation, or phosphorylation and acetylation are highlighted in cyan, yellow and green, respectively.

MLRSTISLLMNSAAQKTMTNSNFVLNAPKITLTKVEQNICNLLNDYTDLYNQKYHNKPEPLTLR
ITGGWVRDKLLGQGSHDLDIAINVMSGEQFATGLNEYLQQHYAKYGAKPHNIHKIDKNPEKSKH
LETATTKLFGVEVDFVNLRSEKYTELSRIPKVCFGTPEEDALRRDATLNALFYNIHKGEVEDFT
KRGLQDLKDGVLRTPLPAKQTFLDDPLRVLRLIRFASRFNFTIDPEVMAEMGDPQINVAFNSKI
SRERVGVEMEKILVGPTPLLALQLIQRAHLENVIFFWHNDSSVVKFNEENCQDMDKINHVYNDN
ILNSHLKSFIELYPMFLEKLPILREKIGRSPGFQQNFILSAILSPMANLQIIGNPKKKINNLVS
VTESIVKEGLKLSKNDAAVIAKTVDSICSYEEILAKFADRSQLKKSEIGIFLRNFNGEWETAHF
ASLSDAFLKIPKLETKKIELLFQNYNEFYSYIFDNNLNNCHELKPIVDGKQMAKLLQMKPGPWL
GKINNEAIRWQFDNPTGTDQELITHLKAILPKYL

Table 3.9: Summary of all acetylated sites found on Cca1 at different conditions. (Only data from experiments for which three biological replicates have been performed are presented).

Condition / Acetylation	Glucose (OD_{600} of 1)	Mitochondria l fraction (OD_{600} of 1)	Nuclear fraction (OD_{600} of 1)	Cytosolic Fraction (OD_{600} of 1)	Glycerol (OD_{600} of 1)
S4-T5-S7 (1X)	+++	+		+++	++
T19-S21 (1X)	++		+++	++	
T17	+++		++	++	+++
K57	+++	+	++	++	+
K118	+++	+	++	++	++
K150	+++	+++	+++	+++	+++
K185	+	+		++	
K312	+	+			
S328	++	++	++	++	
T407	++	++	++	++	+++
K507	++	+	+++	++	+++
T528-T530 (2X)	+	+			+

+ PTM produced only in 1 replicate out of 3
++ PTM reproduced in 2 replicates out of 3
+++ PTM reproduced in all 3 replicates
1X: In each peptide only one of these positions showed acetylation
2X: Both positions showed acetylation in a single peptide

Table 3.10: Summary of all phosphorylated sites found on Cca1 at different conditions. (Only data from experiments for which three biological replicates have been performed are presented).

Condition / Phosphorylation	Glucose (OD_{600} of 1)	Mitochondrial fraction (OD_{600} of 1)	Nuclear fraction (OD_{600} of 1)	Cytosolic fraction (OD_{600} of 1)	Glycerol (OD_{600} of 1)
S4-T5-S7-S12 (1X)	+	+	+++	++	++
T19-S21 (1X)	++	+	+	++	

+ PTM produced only in 1 replicate out of 3
++ PTM reproduced in 2 replicates out of 3
+++ PTM reproduced in all 3 replicates
1X: In each peptide only one of these positions showed acetylation

3.2 Identification of proteins interacting with Cca1

Proteins showing interactions with Cca1 were identified using Cca1-TAP-tagged (*in vivo,* gel picture shown in Appendix 1, panel A) or Cca1-GST-tagged (*in vitro,* gel picture shown in Appendix 1, panels B and C) fusion proteins. The *in vivo* approach allowed for the proteins to interact with the Cca1-TAP-tagged fusion protein in the native environment but may have excluded proteins with low levels of expression. In contrast, the *in vitro* approach, although not in the native environment allowed for the amount of proteins which may be interactors to be varied in an attempt to increase the number of interactions observed. Proteins detected in the *in vitro* and *in vivo* assays were categorized based on their gene ontologies (molecular functions and biological processes) defined at UniProt (https://www.uniprot.org/). The false discovery rate and score threshold were determined by Thermo Proteome Discoverer Software Version 2.2 using the superior validation algorithm and Decoy PSM (peptide-spectrum match) to calculate the score threshold and achieve the target FDR. The strict FDR was set to 0.01 and only peptides and proteins with 99% confidence have been reported in this study.

3.2.1 *In vitro* assays

This assay was performed once each with three different bait:prey protein ratios (1:10, 1:20 and 1:100 with 10 µg of bait, and 100 µg, 200 µg or 1000 µg of prey, respectively) to see if increasing this ratio altered the profile of proteins seen as interactors. The total number of interacting proteins identified for experiments with the 1:10 and 1:20 bait:prey ratios were 53 and

59, respectively. When the bait:prey ratio was changed to 1:100 an approximate 6-fold increase in proteins retained (328 proteins) was observed. It seems likely that much of this increase in potential interacting proteins reflects non-specific interactions as when the proteins which interacted with beads alone or with GST bound to the beads were removed, the number of potential interactors went down to 12, 14 and 26, respectively. All proteins detected in different bait:prey ratios are presented in Fig. 3.2 with their numbers of unique peptides and sequence coverage are presented in Appendix 2.

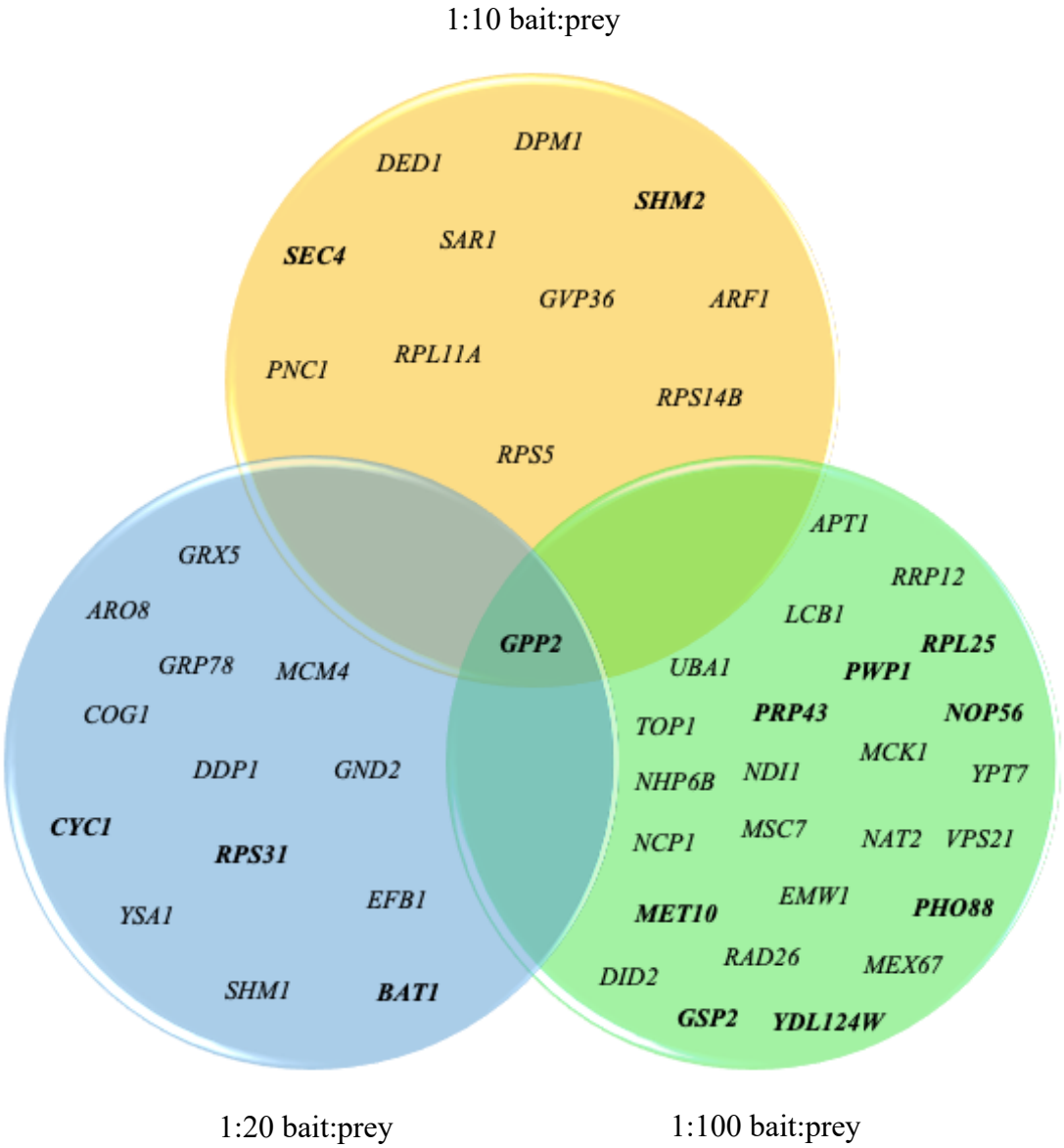

Figure 3.2: All proteins detected in different bait:prey ratios of the *in vitro* assay.

3.2.2 *In vivo* assays

Three biological replicates of the *in vivo* assays were tested from yeast whole-cell lysates grown in glycerol or glucose to OD_{600} of 1. In addition, single replicates were tested from subcellular fractions of cells grown in glucose or glycerol to OD_{600} of 1 followed by MS analysis.

3.2.2.1 Proteins identified in whole-cell lysates from cells grown in glucose to OD_{600} of 1.0

The total number of proteins (259, 228 and 149) identified in each replicate of the whole-cell lysate from cells grown in glucose to OD_{600} of 1 were similar. After removing proteins identified as binding to the TAP-tag alone, the numbers decreased to 88, 86 and 62, respectively. In total, 19 proteins were common to all three replicates, and 29 proteins were found in at least two of the three replicates. All of the proteins detected in different replicates are presented in Fig. 3.3 and proteins identified in two or more replicates are categorized in Appendix 3 with their numbers of unique peptides and sequence coverage.

3.2.2.2 Effects of RNaseA treatment

One of the biological replicates grown in glucose was divided into two aliquots such that half could be treated with RNaseA during the cell lysis and purification to increase the specificity of Cca1-interacting proteins by reducing those that may interact with tRNA associated with Cca1. In the samples with and without RNaseA treatment, 115 and 141 proteins were detected, respectively. This number decreased to 65 and 61, when proteins interacting with the TAP tag alone were eliminated. Of the remaining proteins, 36 were common to both samples. All of the proteins detected in both samples are presented in Fig. 3.4 and the names, sequence coverage and the number of unique peptides of the proteins common to both samples are listed in Appendix 4.

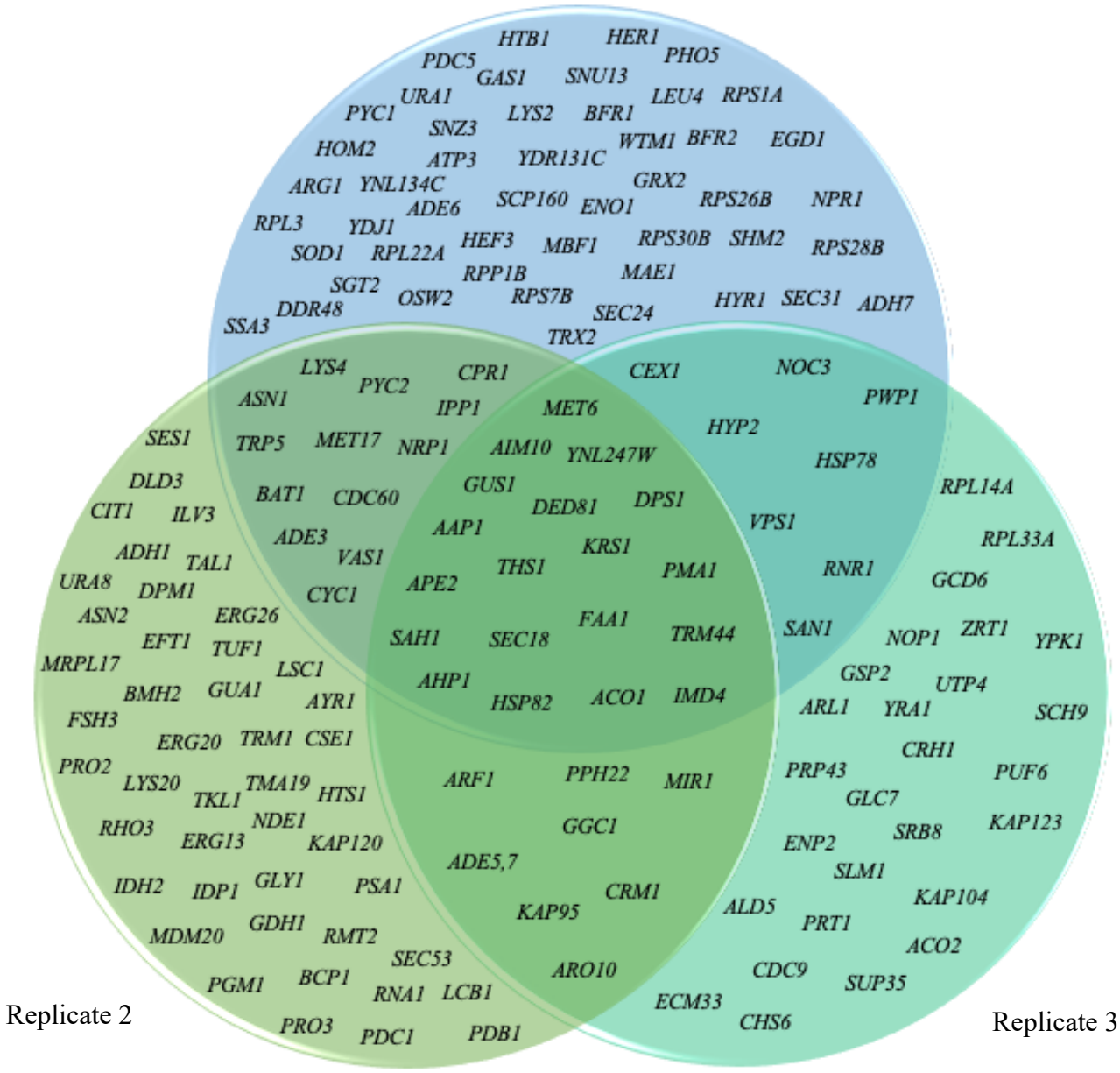

Figure 3.3: Proteins interacting with Cca1 detected in the *in vivo* study of yeast cells grown on glucose to OD_{600} of 1.0.

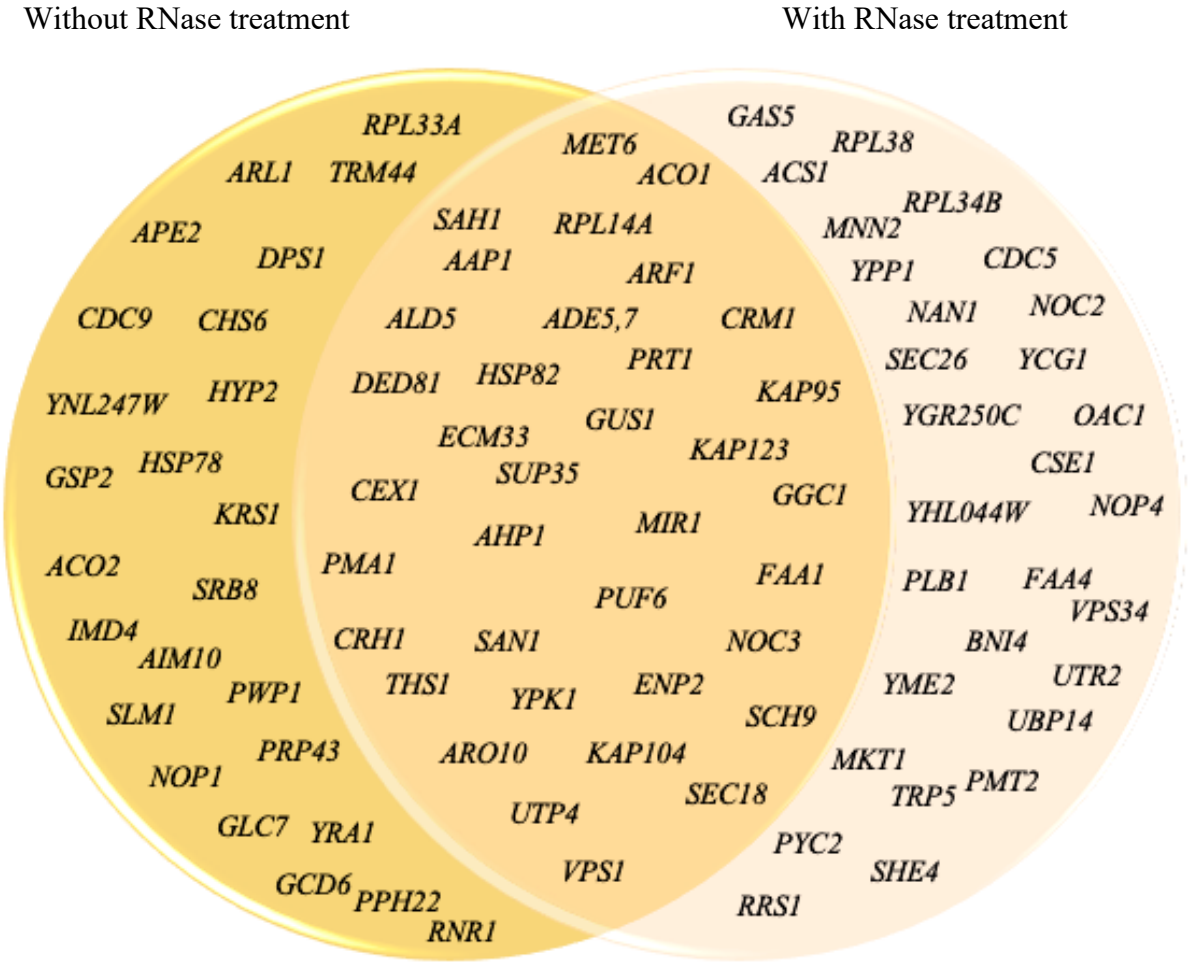

Figure 3.4: Comparison of proteins from whole-cell lysates of yeast cells grown on glucose to OD_{600} of 1.0 identified as interacting with Cca1 with or without pretreatment with RNaseA.

3.2.2.3 Proteins identified in whole-cell lysates from cells grown in glycerol to OD_{600} of 1.0

Three biological replicates have been tested for yeast cells grown on glycerol to OD_{600} of 1.0. The total number of proteins isolated in each replicate was 464, 429 and 442, respectively showing good reproducibility in the number of proteins isolated. After removing proteins that also bound to the TAP tag alone, the numbers decreased to 249, 217 and 216, respectively again showing good reproducibility. Of these, 166 proteins were common to all three replicates. All of the proteins detected in the different replicates are presented in Fig. 3.5 and proteins common to all biological replicates are categorized in Appendix 5.

Replicate 1

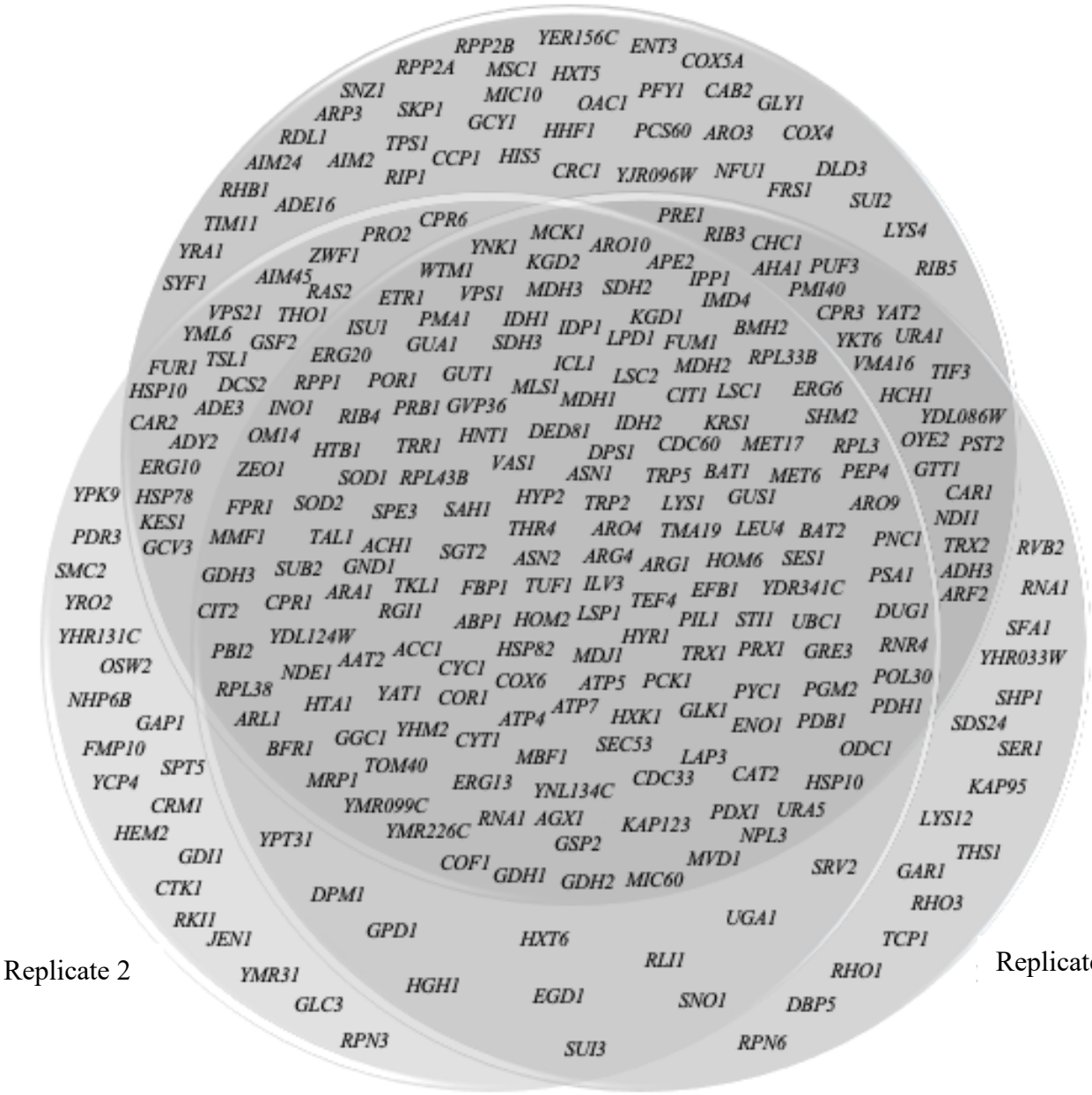

Replicate 2

Replicate 3

Figure 3.5: Proteins interacting with Cca1 detected in the *in vivo* study of yeast cells grown on glycerol to OD_{600} of 1.0.

3.2.2.4 Subcellular fractionation from growth on glucose to OD_{600} of 1.0

Cells were grown on glucose to an OD_{600} of 1.0 and mitochondrial, cytosolic and nuclear fractions were collected.

3.2.2.4.1 Mitochondrial fraction

From the mitochondrial fraction of cells grown on glucose to an OD_{600} of 1.0, 120 proteins were detected. This number was reduced to 23 when the proteins that also bound to the TAP tag alone were removed. These 23 proteins with the numbers of unique peptides and sequence coverage are presented in Appendix 6.

3.2.2.4.2 Nuclear fraction

From the nuclear fraction of cells grown on glucose to an OD_{600} of 1.0, 224 proteins were detected. This number was reduced to 45 when the proteins that bound to TAP alone were removed. These proteins with their number of unique peptides and sequence coverage are presented in Appendix 7.

3.2.2.4.3 Cytosolic fraction

From the cytosolic fraction of cells grown on glucose to an OD_{600} of 1.0, 245 proteins were identified. This number was decreased to 54 by removing those proteins that bound to the TAP tag alone. The proteins remaining are categorized in Appendix 8.

3.2.2.5 Subcellular fractionation from growth on glycerol to OD_{600} of 1.0

A single aliquot of cells was grown on glycerol to an OD_{600} of 1.0 and mitochondrial, cytosolic and nuclear fractions were collected.

3.2.2.5.1 Mitochondrial fraction

The mitochondrial fraction yielded 265 proteins associated with Cca1-TAP. This number was

reduced to 98 when proteins which also bound to the TAP tag alone were removed. These 98 proteins with their number of unique peptides and sequence coverage are listed in Appendix 9.

3.2.2.5.2 Nuclear fraction

The nuclear fraction yielded 615 proteins associated with Cca1-TAP. This number was reduced to 108 when proteins which also bound to the TAP tag alone were removed. These 108 proteins are categorized in Appendix 10.

3.2.2.5.3 Cytosolic fraction

The cytosolic fraction yielded 107 proteins associated with Cca1-TAP. This number was reduced to 18 when proteins which also bound to the TAP tag alone were removed. These 18 proteins with their number of unique peptides and sequence coverage are listed in Appendix 11.

3.3 Protein comparison tables

Comparator tables of proteins identified from different conditions are tabulated in the Appendices (Appenidces 12-15). These data represent the same proteins as described above, but represented for comparator experiments, *e.g.*, glucose versus glycerol.

4. DISCUSSION

In yeast a single gene (*CCA1*) encodes tRNA nucleotidyltransferase (Chen *et al.,* 1990). This protein, Cca1, ensures that functional tRNAs end in the 3'-terminal cytidine-cytidine-adenosine (CCA) tag required for aminoacylation. As tRNA genes do not encode this sequence in yeast, Cca1 plays a role in the maturation of all tRNAs. It also plays another role in repairing damaged 3'-termini which have lost one or more of these nucleotides (Rosset and Monier, 1965). Finally, Cca1 also plays a role in tRNA quality control by ensuring that damaged tRNAs are not used in protein synthesis, either by not adding the 3'-terminal CCA to damaged tRNAs (Wilusz *et al*., 2011, Kuhn *et al*., 2015) or by adding two CCA sequences such that these damaged tRNAs are targeted for degradation (Wilusz *et al*., 2011). In addition, Cca1 is a sorting isozyme in that the single *CCA1* gene encodes the tRNA nucleotidyltransferase that functions in the mitochondrion (for maturation, repair, and quality control), nucleus (for maturation and quality control) and cytosol (for repair and quality control). These characteristics make tRNA nucleotidyltransferase an interesting enzyme for study. With this in mind, I set out to explore *cis*- and *trans*-acting factors that may play a role in the activity or localization of tRNA nucleotidyltransferase in yeast.

4.1 Post-translational modifications (PTMs) of Cca1

PTMs are covalent modifications of proteins translated within a cell. These modifications can impact the activity (Hurt *et al*., 2012), structure (Xin and Radivojac, 2012), function (Kessler and Edelmann, 2011), and/or localization (Cao *et al*., 2017) of proteins and even dictate protein-protein interactions (Drazic *et al*., 2016; Narita *et al*., 2019). Some PTMs, such as phosphorylation, acetylation, glycosylation, or ubiquitination, can be reversible (Leach and Brown, 2012) while others, such as proteolytic cleavages involved in the activation of many proteolytic enzymes (Rogers and Overall, 2013) may be irreversible. As there is only one known proteolytic processing event in Cca1, removal of the 16 amino-terminal amino acids after import into the mitochondrion (Chen *et al.*, 1992), and as high-throughput proteomics approaches have revealed a small number of reversible covalent modifications of Cca1, such as phosphorylations (Albuquerque *et al*., 2008; Soufi *el at*., 2009; Helbig *et al*., 2010) and acetylations (Henriksen *et al*., 2012), these reversible covalent modifications were the primary interest of this study. Here I compared the modifications in the proteins isolated from yeast grown under different conditions and by using two different

approaches. I hoped that by doing this I might see differences that could be related to changes in Cca1 localization (mitochondrial, nuclear or cytosolic) or activity (tRNA maturation, repair, or quality control).

By comparing different conditions and the PTMs seen in each of these conditions there are two general outcomes that could result. In the first case, specific modifications would be found under all conditions tested. This would suggest that these post-translational modifications are always needed for enzyme activity and localization and they may suggest important amino acids required for these. The second possibility is that some PTMs would be seen only under specific experimental conditions. In these cases, the PTMs may offer information on specific characteristics of tRNA nucleotidyltransferase required for growth under the defined experimental conditions. Here I will address both of these situations and what information these PTMs may provide on protein function and localization.

4.1.1 Conserved PTMs across all conditions and fractions

4.1.1.1 Acetylation of K150

Among the 18 positions that I identified as showing post-translational modifications as acetylations or phosphorylations, only position K150 contained the same PTM under all conditions and fractions tested. Acetylation of K150 of Cca1 was reported previously through high throughput studies, but only in one out of four biological replicates (Henriksen *et al*., 2012). In my study, expression of the *CCA1* gene producing this enzyme was under the control of the GPD promoter, which is 1000-fold stronger than its native *CCA1* promoter (Mumberg *et al*., 1995). Overexpression was used to overcome the low endogenous level of Cca1 <0.01% of total yeast cellular proteins (Chen *et al.,* 1990), reported as 4481+/-1161 molecules per cell (SGD available at https://www.yeastgenome.org/locus/S000000970), to allow for clear identification of modification at this position in different conditions. The enzyme showed acetylation at K150 in all conditions and carbon sources tested, making it the most reproducible modification among all PTMs identified in this study. This conserved modification is found in the flexible loop between conserved motifs A and B (Fig. 4.1). Changes in the conformation of this loop are thought to play a role in the switch from CMP incorporation to AMP incorporation into the tRNA substrate and

loss through evolution of this loop in some bacterial species had been linked to the loss of A-adding activity thus generating a CC-adding enzyme (Neuenfeldt *et al*., 2008).

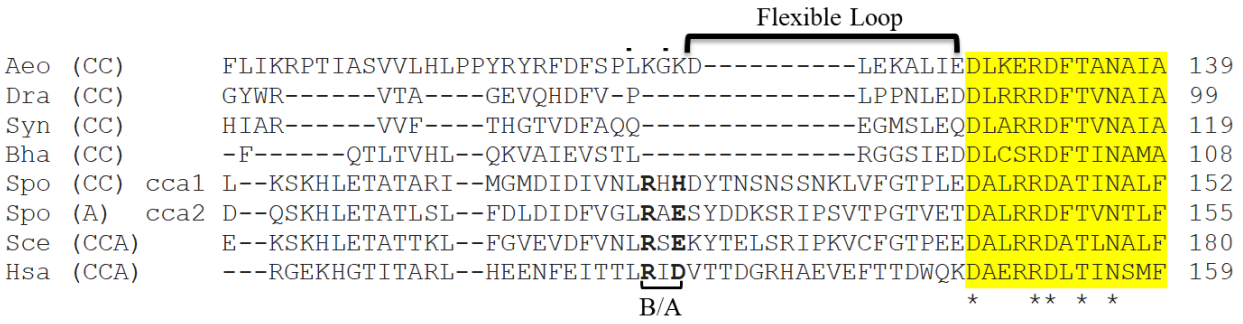

Figure 4.1: Alignment of conserved Motif B (labelled and shaded) and the region upstream of it that defines a flexible loop and the B/A element (when present) in example tRNA nucleotidyltransferases. Sequences represent Spo, *Schizosaccharomyces pombe cca*1 and *cca*2, Aeo, *Aquifex aeolicus*, Bha, *Bacillus halodurans*, Dra, *Deinoccus radiodurans*, Syn, *Synecthococcus* species, Sce *Saccharomyces cerevisiae*, and Hsa, *Homo sapiens* tRNA-NTs. In brackets are the A-, CC- or CCA- adding abilities of these enzymes. Standard one-letter abbreviations for amino acids are used. (*) indicates a position that is perfectly conserved. (-) indicates a gap introduced to optimize alignments. Numbers indicate position in each protein sequence. The B/A element and flexible loop region identified in CCA- and A-adding enzymes (Neuenfeldt *et al*., 2008) are labelled (Reid *et al*., 2019, reproduced with permission).

It is interesting that K150 in the *S. cerevisiae* protein is adjacent to the conserved B/A sequence (where B is a basic amino acid and A is an acidic amino acid) that is thought to position the tRNA-NCC intermediate for terminal AMP incorporation (Neuenfeldt *et al*., 2008, Tomita and Weiner, 2001). If a negatively charged residue is required at this position for interaction with the tRNA substrate it might be deleterious to have a positively charged amino acid such as K150 adjacent to the B/A motif. Acetylating K150 would remove this positive charge. In fact, an alignment of eukaryotic CCA-adding enzymes reveals that only the *S. cerevisiae* enzyme has a positively charged amino acid at this position (Fig. 4.2). Perhaps acetylation at this position is important for optimizing or regulating the activity of Cca1 in *S. cerevisiae*.

When cells were grown on glucose medium the percentage of Cca1 showing acetylated K150 increased from 50% to 83% as the cell density increased from an OD_{600} of 1 to 2.5. Moreover, when the cells grown on glucose to an OD_{600} of 1 were fractionated, the percentage of acetylated K150 in the nuclear fraction was about twice (69%) that seen in the cytosolic fraction (29%). These results may suggest that acetylation at position 150 is more important as cell density increases and, in the nucleus, more than in the cytosol. Determining why this might be the case will require

additional experiments. Structural modeling of the Cca1 protein (Fig. 4.3) shows that this lysine residue is predicted to be on the surface of the enzyme such that it may play a role in interactions with additional proteins perhaps involved in protein localization given that the nuclear form of the enzyme shows increased acetylation.

```
H.sapiens       HEENFEITTLRIDVTTDGRHAEVE-FTTDWQKDAERRDLTINSMF  159
A.thaliana      YDQWIDFVNLRSEEYTENSRIPTMKFGTA-KDDAFRRDLTINSLF  228
C.albicans      FGVDIDFVNLRSEEYTHDSRVPSIEFGTP-EQDAVRRDATLNALF  154
K.lactis        FDVPVDFVNLRSEEYTMESRIPKVEFGTP-YDDAMRRDATLNAMF  154
C.glabrata      FDVEVDFVNLRSEEYTEDSRIPTTQFGTP-EEDALRRDATLNALF  164
S.cerevisiae    FGVEVDFVNLRSEKYTELSRIPKVCFGTP-EEDALRRDATLNALF  180
                    :::  ** :  *   :.    * *   .**:***.*:*::*
```

Figure 4.2: Alignment of conserved Motif B (in italics) and the region upstream of it that defines a flexible loop and the B/A element (in bold) from the eukaryotes *Saccharomyces cerevisiae*, *Homo sapiens*, *Arabidopsis thaliana, Candida albicans, Kluyveromyces lactis*, and *Candida glabrata*. K150 highlighted. Standard one-letter abbreviations for amino acids are used. (*) indicates a position that is perfectly conserved, (:) indicates highly conserved and (.) indicates lower conservation. (-) indicates a gap introduced to optimize alignments. Numbers indicate position in each protein sequence. The alignment was performed using Clustal Omega (Madeira *et al*., 2019).

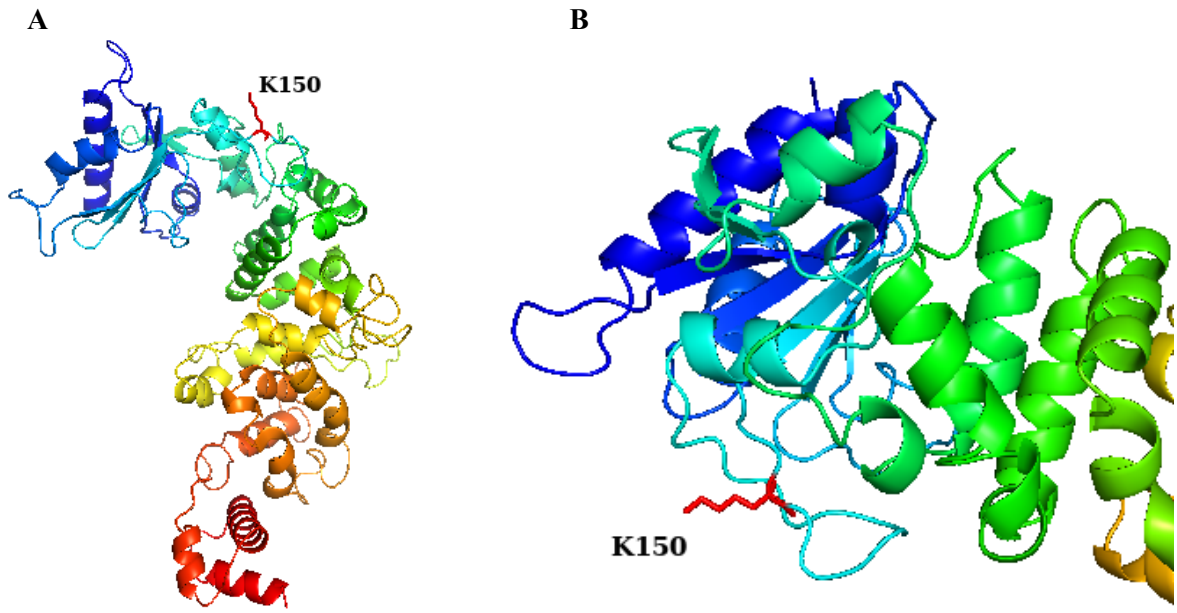

Figure 4.3: Model of *Saccharomyces cerevisiae* Cca1, presented in rainbow colour (N-terminus is blue and C-terminus is red), showing position of K150 (red stick) located in a large flexible loop between Motifs A and B. A) Whole protein. B) Close up of head and neck domains. This model was made based on the crystal structure of the *Thermotoga maritima* CCA-adding enzyme using SWISS-MODEL (Waterhouse *et al*., 2018) and viewed by PyMol (v2.3.2) (Schrödinger).

4.1.1.2 Acetylation of K507

Acetylation at K507 was reproduced in all conditions and fractions tested except for the cells grown to OD_{600} of 3.5 and in two of the mitochondrial replicates. However, the lack of this modification in those samples likely reflects the low overall yield of proteins rather than the absence of the modification. This suggests again that as for acetylation of K150, this modification is generally found in Cca1. The ratio of modified peptide to the total abundance of peptide containing this position increased from 8% in the cytosolic fraction to 16% in the nuclear fraction. Lysine 507 is only 39 amino acids from the C-terminus of the protein, far from the conserved active site motifs in the head and neck region of the protein. Based on modelling of Cca1, it is predicted to be in a loop region connecting two α-helices (Fig. 4.4).

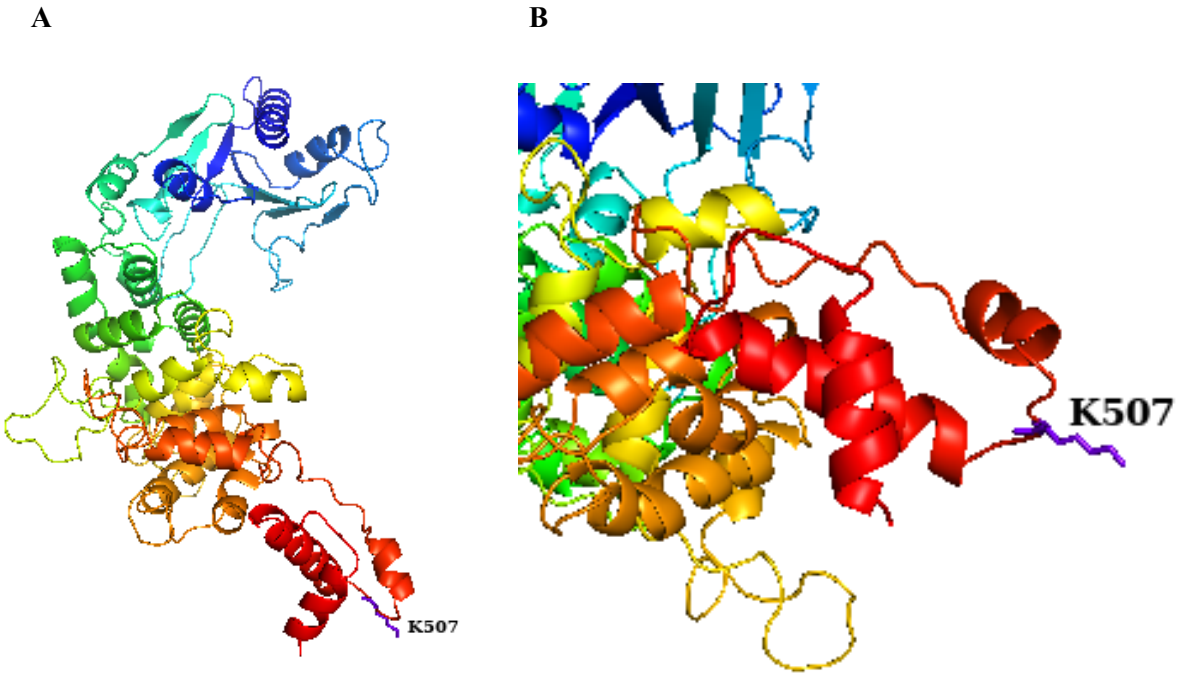

Figure 4.4: Model of *Saccharomyces cerevisiae* Cca1, presented in rainbow colour (N-terminus is blue and C-terminus is red), showing position of K507 (purple stick) near the C-terminus of the enzyme. A) Whole protein. B) Close up of C-terminal region. This model was made based on the crystal structure of *Thermotoga maritima* using SWISS-MODEL (Waterhouse *et al*., 2018) and visualized by PyMol (v2.3.2) (Schrödinger).

In contrast with K150, which is not conserved across species, alignment of Cca1 with tRNA nucleotidyltransferases from bacteria: *Bacillus stearothermophilus*, *Aquifex aeolicus* (Fig. 4.5), or

eukaryotes: *Arabidopsis thaliana, Candida albicans, Kluyveromyces lactis*, *Candida glabrata* (Fig. 4.6) reveals conservation of K507 followed immediately by a conserved helix-breaking amino acid (either glycine or proline). The conservation of this position in both bacteria and eukaryotes suggests that modification at this position is not linked to enzyme targeting, but may play a role in enzyme activity. The C-terminal region of tRNA nucleotidyltransferases has proven to play a role in tRNA binding (Cook *et al*., 2009) and so perhaps acetylation of this residue in eukaryotes is an evolutionary adaptation with some role in regulating tRNA binding.

```
B.stearothermophilus VNGKDVIEWVG-KPAGPWV----KEALDA-IWRAVVNG  380
A.aeolicus           LNGDEIMEILGIKP-GKIVGILKKALLEAQI-DGKVET  492
S.cerevisiae         VDGKQMAKLLQMKP-GPWL---GKINNEA-I-RWQFDN  527
                     ::*:.:.: :  ** *  :    *   :* * :  :.
```

Figure 4.5: Alignment of amino acids near the C-terminus of the *Bacillus stearothermophilus*, *Aquifex aeolicus* and *Saccharomyces cerevisiae* tRNA nucleotidyltransferases. K507 highlighted. Standard one-letter abbreviations for amino acids are used. (*) indicates a position that is perfectly conserved, (:) indicates highly conserved and (.) indicates lower conservation. (-) indicates a gap introduced to optimize alignments. Numbers indicate position in each protein sequence. The alignment was performed using Clustal Omega (Madeira *et al*., 2019).

```
A.thaliana   LGLDKIWDAKPLVNGREIMQIAELKGGSRLIREWQQKLLTWQLAY   587
C.albicans   WDLTNVHLVKPLIDGTTLSKSLGMKPGPWL-RPTIEEILVWQLDN   511
K.lactis     CKLDDVYTLKHIINGKELAKLLDRKPGIWMGETLD-RILIWQLDN   470
C.glabrata   QNLQDSDKMVPIIDGKRMVKILETKPGPWLGKIND-EVILWQFDH   510
S.cerevisiae NNLNNCHELKPIVDGKQMAKLLQMKPGPWLGKINN-EAIRWQFDN   526
               *     .   :::*   :  : .   * *   : :    .::  **:
```

Figure 4.6: Alignment of amino acids near the C-terminus of the *Arabidopsis thaliana, Candida albicans, Kluyveromyces lactis*, *Candida glabrata* and *Saccharomyces cerevisiae* CCA-adding enzymes. K507 is highlighted in bold. Standard one-letter abbreviations for amino acids are used. (*) indicates a position that is perfectly conserved, (:) indicates highly conserved and (.) indicates lower conservation. (-) indicates a gap introduced to optimize alignments. Numbers indicate position in each protein sequence. The alignment was performed using Clustal Omega (Madeira *et al*., 2019).

4.1.1.3 Acetylation of T407

Again, this position was shown to be acetylated under all conditions tested (except when protein abundances were low at OD_{600} of 0.3 and 3.5), suggesting that acetylation of this position also is important in protein function. The primary sequence of this region of the protein was not conserved among the inspected eukaryotic CCA-adding enzymes from *S. cerevisiae, H. sapiens*, *A.*

thaliana, C. albicans, K. lactis, and *C. glabrata* (Fig. 4.7), however, this position was among the few positions identified that seemed to be located in a region of conserved secondary structure, in this case an α-helix (Fig. 4.8). This α-helix is thought to be one of the helices which recognize the acceptor and TψC helices of the tRNA (Tomita and Yamashita, 2014) and acetylation at this position may impact the binding affinity between the CCA-adding enzyme and the tRNA.

```
Human          PDA-------------------TTRVCELLKYQGEHCLL----   375
A.thaliana     KDTKGKSIPVVNHIFKFSMKRKTSDAETVMNIHQTTERFRSLI   441
C.Albicans     RDIFNQYL-------RLGLTSKKSDIAKVSAINM---NSAELS   379
K.lactis       PAKPKNSIPLAGVITKEGLNFPNTQVDNVIACVESEDSYHNLV   372
C.glabrata     KKKLNNTLPVSESIVREGLKFNKASSIVVARCVENIAAYNSMV   403
S.cerevisiae   KKKINNLVSVTESIVKEGLKLSKNDAAVIAKTVDSICSYEEIL   418
                                           .      :
```

Figure 4.7: Multiple sequence alignment of the CCA-adding enzyme near position T407 (in highlight) from *Saccharomyces cerevisiae*, *Homo sapiens*, *Arabidopsis thaliana, Candida albicans, Kluyveromyces lactis*, and *Candida glabrata*. Standard one-letter abbreviations for amino acids. Numbers indicate position in each protein sequence. The alignment was performed using Clustal Omega (Madeira *et al*., 2019).

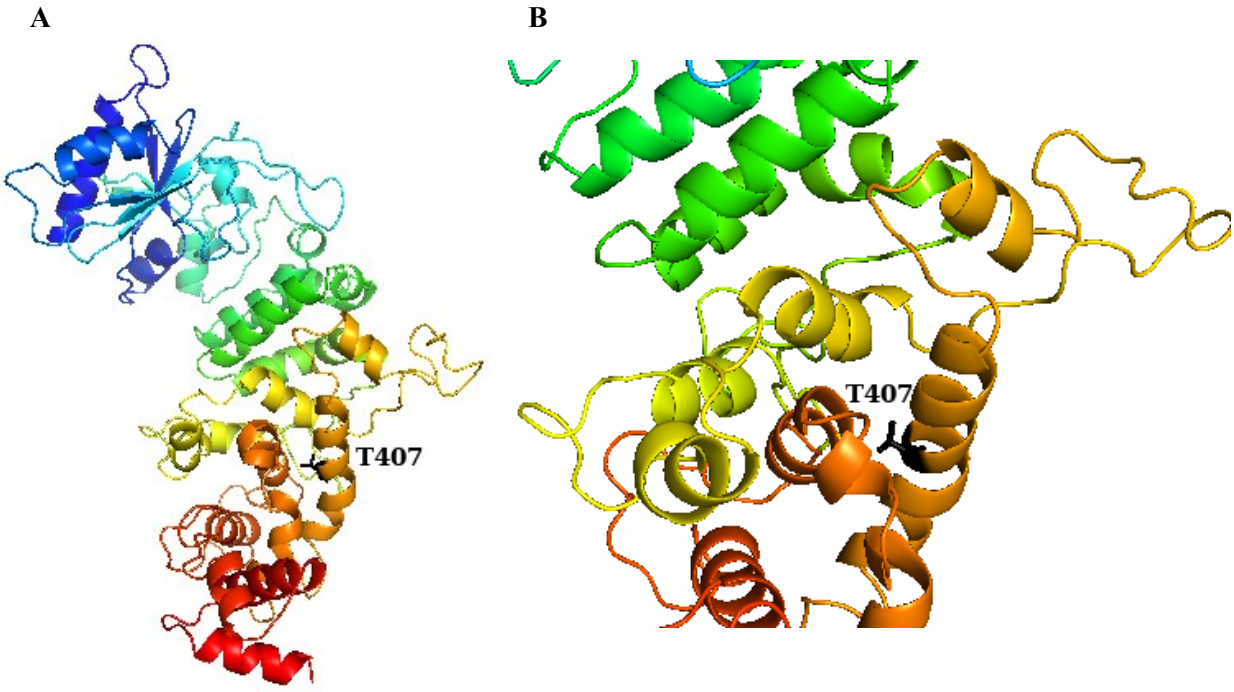

Figure 4.8: Model of *Saccharomyces cerevisiae* Cca1, presented in rainbow colour (N-terminus is blue and C-terminus is red), showing position T407 (black stick) in the body domain of the enzyme. A) Whole protein. B) Close up of body domain. This model was made based on the crystal structure of *Thermotoga maritima* using SWISS-MODEL (Waterhouse *et al*., 2018) and visualized by PyMol (v2.3.2) (Schrödinger).

4.1.2 PTMs that change depending on experimental conditions

Changes in the PTMs in response to the different cellular conditions and in different cellular compartments might occur to regulate enzyme function and/or localization. Many PTMs were conserved in most conditions tested with some exceptions. The potential significance of these differences will be discussed in the following sections.

4.1.2.1 Modifications of the N-terminal targeting signal (S4, T5, S7)

All mitochondrial targeting signals share common features. They usually are amphipathic α-helices with one non-polar and one positively charged face, and are rich in hydrophobic, hydroxylated and basic amino acid residues (Gavel *et al*., 1988). If one shows the amino-terminal 21 amino acids of Cca1 in a helical wheel conformation these features are evident (Fig. 4.9). As PTMs, particularly phosphorylations, have been shown to inhibit mitochondrial import of other proteins (Lee *et al*., 2006), I was interested in determining whether the mitochondrial targeting signal of Cca1 contained any PTMs. Previous research has shown that the amino-terminal 17 residues of Cca1 are necessary for its efficient import into yeast mitochondria (Chen *et al.*, 1992; Wolfe *et al*., 1994; Hansen and Herrmann, 2019). Except for the nuclear fraction from cells grown on glucose to an OD_{600} of 1 and one replicate of cells tested at OD_{600} of 0.3, acetylation and/or phosphorylation at different positions of this targeting sequence occurred under all of the conditions tested (Tables 3.1-3.10). Phosphorylation of S4, T5 and S7 in the targeting signal may play a role in decreasing the mitochondrial import of Cca1 as after subcellular fractionation, the cytosolic form of the enzyme showed acetylation in all three biological replicates tested compared with the mitochondrial fraction, which in only one instance showed phosphorylation or acetylation (Table 3.10). Perhaps acetylation at this targeting signal decreases mitochondrial import such that the protein accumulates in the cytosol (Tables 3.9). It is worth mentioning that MS analysis revealed that in each case only one of these amino acids (S4, T5, or S7) was modified in any one peptide (shown as 1X in Tables 3.9 and 3.10). Once a single modification has been made in these closely spaced amino acids it seems that this region is no longer a substrate for further modifications.

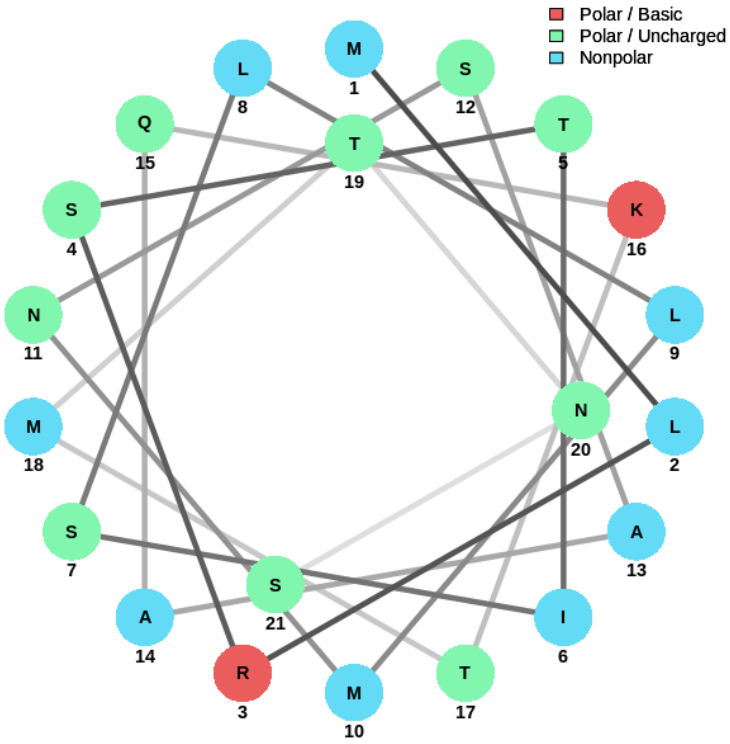

Figure 4.9: Helical wheel representation of the amino-terminal 21 residues of *Saccharomyces cerevisiae* CCA-adding enzyme. Polar/basic residues, polar/uncharged residues and nonpolar residues are red, green and cyan, respectively. Helical wheel generated using NetWheels (http://lbqp.unb.br/NetWheels/).

Phosphopeptide enrichment of extracts from yeast cells grown on glucose to OD_{600} of 1.0 and 2.5 using TiO_2 magnetic beads helped to identify phosphorylation of S4, T5 and S7. This observation is consistent with that of Helbig *et al*. (2010) who showed phosphorylation at positions S4 and T5 of Cca1 in wild-type and NatB (N-acetyltransferase)-defective *S. cerevisiae* cells. That study also showed competition between phosphorylation and acetylation with an obvious increase in phosphorylation observed in the *nat3*Δ strain. It would be interesting to see if any difference in the localization of Cca1 is evident in a *nat3*Δ strain. The lower abundance of phosphopeptides as compared to acetylated peptides may suggest that acetylation happens more frequently than phosphorylation or that experimentally it is easier to identify acetylation in an MS/MS spectrum as phosphoryl groups can be lost during the MS process which also includes one additional step (MS^3). Thus, my data suggest that phosphorylation and/or acetylation of a mitochondrial targeting signal reduces mitochondrial import such that the protein can accumulate in the nucleus and cytosol even in the presence of the mitochondrial targeting signal. This may explain why Wolfe *et al.,* (1994) found a functional pool of the longer form of Cca1 containing the mitochondrial

targeting signal in the nucleus even though they had anticipated that it would be directed to the mitochondrion. If mitochondrial import of Cca1 is post-translational and not co-translational, then perhaps phosphorylation and/or acetylation could modify the mitochondrial targeting signal to decrease the efficiency with which it is targeted to mitochondria so that cells which do not require this enzyme for mitochondrial respiration can direct it to the cytosol or nucleus to carry out its functions in these localizations. It would be interesting to repeat the experiments of Wolfe *et al*. (1994) in combination with site-directed mutagenesis to see if the distribution of Cca1 can be altered by changing S4, T5 and/or S7 to alanine. Also, it would be important to test available yeast kinases *in vitro* to see which of these kinases are responsible for phosphorylation of some or all of these residues.

4.1.2.2 Phosphorylation and/or acetylation of T17, T19 and S21

Although the first 17 residues of Cca1 are necessary for mitochondrial targeting it is possible that the complete targeting signal extends past residue 17 and into the mature portion of the protein. In this context, it was interesting that we also noted phosphorylation and/or acetylation of residues T17, T19, and S21. Consistent with the idea that these residues also form part of a mitochondrial targeting signal and that modification of these may affect localization we saw acetylation of these positions in nuclear and cytosolic fractions but not in any mitochondrial fractions. Specifically, acetylation at position 17 was absent in mitochondrial fractions but found in whole-cell lysates tested regardless of the carbon source. The ratio of peptides acetylated at position T17 to total abundance of that specific peptide was consistent (0.02%) from OD_{600} of 1.0 to 2.5 when the cells were grown with glucose as the carbon source. Surprisingly, similar results were seen when the cells were grown in glycerol, where aerobic respiration is a primary source of energy in the cell, and one would anticipate mitochondrial localization of the enzyme. So, acetylation of T17 alone is not sufficient to exclude Cca1 from mitochondria.

Finally, the cytosolic fractions also showed phosphorylation of positions T17, T19 and S21 which was not seen in the nuclear fractions. It is difficult to explain why if phosphorylation or acetylation reduces mitochondrial import efficiency, the phosphorylated proteins remain in the cytosol while the acetylated proteins enter the nucleus. Perhaps additional proteins can distinguish between phosphorylated and acetylated residues and direct the protein accordingly.

4.1.2.3 Acetylation of S328

A close inspection of extracts from cells grown to OD_{600} of 1.0 on glucose showed ratios of acetylated peptide to non-acetylated peptide containing S328 of 65%, 18% and 8% in mitochondrial, nuclear and cytosolic fractions, respectively. This enrichment in the mitochondrial enzyme suggests that this acetylation may enhance mitochondrial localization. In contrast, Soufi *et al*. (2009) reported phosphorylation of S328 of Cca1 under conditions of osmotic stress. These findings suggest that in response to cellular stress, acetylation at this position might be replaced by phosphorylation which may impact the localization of the enzyme or its interaction with other proteins. The higher ratio of acetylated to non-acetylated peptide also may show a potential role of S328 acetylation in mitochondrial targeting. This serine residue is predicted to be in a flexible loop on the surface of Cca1 (Fig. 4.10) although a sequence comparison suggests that this position is not conserved in the primary sequence (Fig. 4.11).

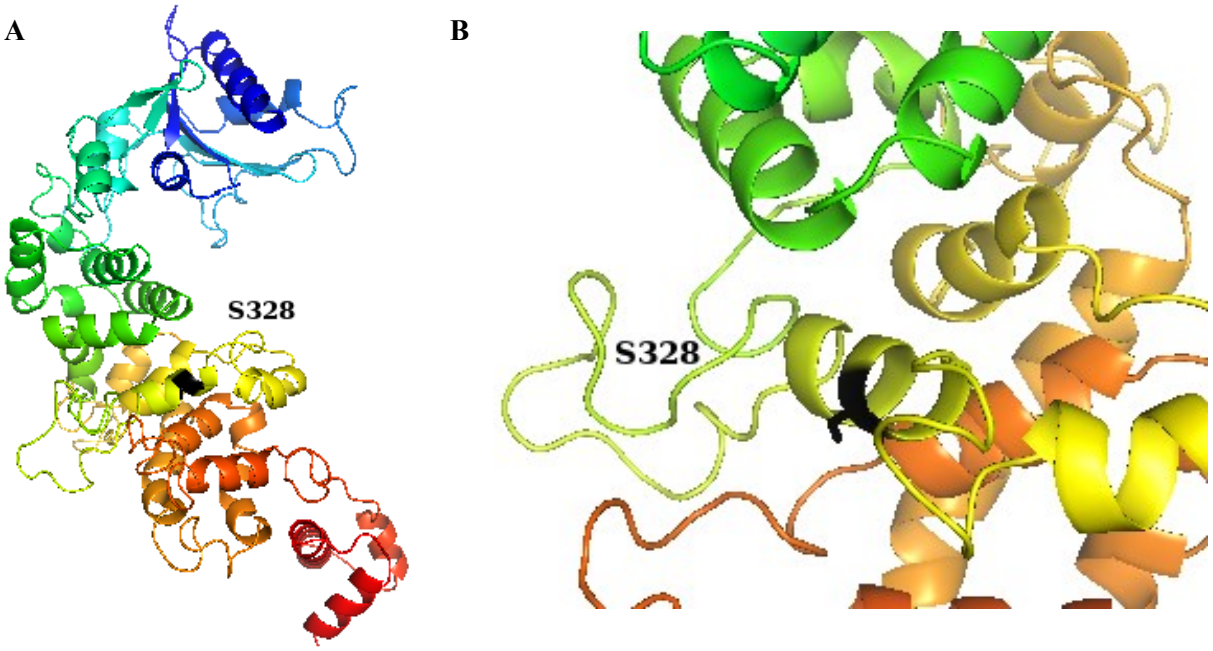

Figure 4.10: Model of *Saccharomyces cerevisiae* Cca1, presented in rainbow colour (N-terminus is blue and C-terminus is red), showing S328 (black stick) 60 amino acids C-terminal to motif E. A) Whole protein. B) Close up of body domain showing S328. This model was made based on the crystal structure of *Thermotoga maritima* using SWISS-MODEL (Waterhouse *et al*., 2018) and viewed by PyMol (v2.3.2) (Schrödinger).

```
H. sapiens          VSKNVDGFSPKPVTLLASLFKVQDDVTKLDLRLKIAKEE    319
C.glabrata          YKKGIFNHHLKNFIHHYKDFLSRYLKLRQAIETKDKSFQ    339
C.albicans          EARSQLACHMEIASLIYPNFKQTINNSTEKFKNEFAALM    319
A.thaliana          PRPGKFSGEQRRLALYAAMFLPFRKTVYKDTKGKSIPVV    409
K.lactis            YEN--LDQHLKSLVETIPKLLKSHTTFASVFPGMQEPLI    314
S.cerevisiae        YNDNILNSHLKSFIELYPMFLEKLPILREKIGRSP-GFQ    354
                                  .        :
```

Figure 4.11: Multiple sequence alignment of CCA-adding enzymes around residue S328 from *Saccharomyces cerevisiae*, *Homo sapiens*, *Arabidopsis thaliana, Candida albicans, Kluyveromyces lactis*, and *Candida glabrata*. S328 shown in bold. Standard one-letter abbreviations for amino acids are used. (:) indicates highly conserved and (.) indicates lower conservation. (-) indicates a gap introduced to optimize alignments. Numbers indicate position in each protein sequence. The alignment was performed using Clustal Omega (Madeira *et al*., 2019).

4.1.2.4 Acetylation of K57

Lysine 57 is found seven residues upstream of Motif A. As explained in Section 1.2, this motif has two conserved aspartic acid residues that coordinate the magnesium ions required for catalysis and the binding of incoming nucleotide triphosphates (Steitz, 1998; Li *et al.*, 2002; Betat *et al*., 2010). That this residue is not conserved among CCA-adding enzymes (Fig. 4.12) suggests that it is not important in enzyme function. In fact, despite the proximity of K57 to Motif A, structural modelling (Fig 4.13) predicts that this residue is far from any conserved residues and may not directly affect enzyme activity. However, acetylation of K57 was seen only in cells grown on glycerol or in a mitochondrial fraction suggesting that acetylation at this position is required for mitochondrial import.

```
H.sapiens       L--PKQYLFTMKLQSPEFQSLFTEGLKSLTEL------FVKENH    57
A.thaliana      KQSIPSIELKENIELTDKERKIFDRLLST-------LRYCNLDT   113
C.albicans      ----MKRPVSNSIVLTTTEEKIRNVLVGYCDYYNKT---NNDSL    37
K.lactis        ----MFKMVASKIQLNKVESEICTLVKEFCSHYNK-ANAETEPL    39
C.glabrata      KAIRRVFTMIPRIQLTEKETRICNLLKDYTAHYNS-LHYGQEPL    45
S.cerevisiae    MTNSNFVLNAPKITLTKVEQNICNLLNDYTDLYNQKYHNKPEPL    61
                                :     :  .   :
```

Figure 4.12: Alignment of the CCA-adding enzyme sequences around residue K57 from *Saccharomyces cerevisiae*, *Homo sapiens*, *Arabidopsis thaliana, Candida albicans, Kluyveromyces lactis*, and *Candida glabrata*. K57 is in bold. Standard one-letter abbreviations for amino acids are used. (:) indicates highly conserved and (.) indicates lower conservation. (-) indicates a gap introduced to optimize alignments. Numbers indicate position in each protein sequence. The alignment was performed using Clustal Omega (Madeira *et al*., 2019).

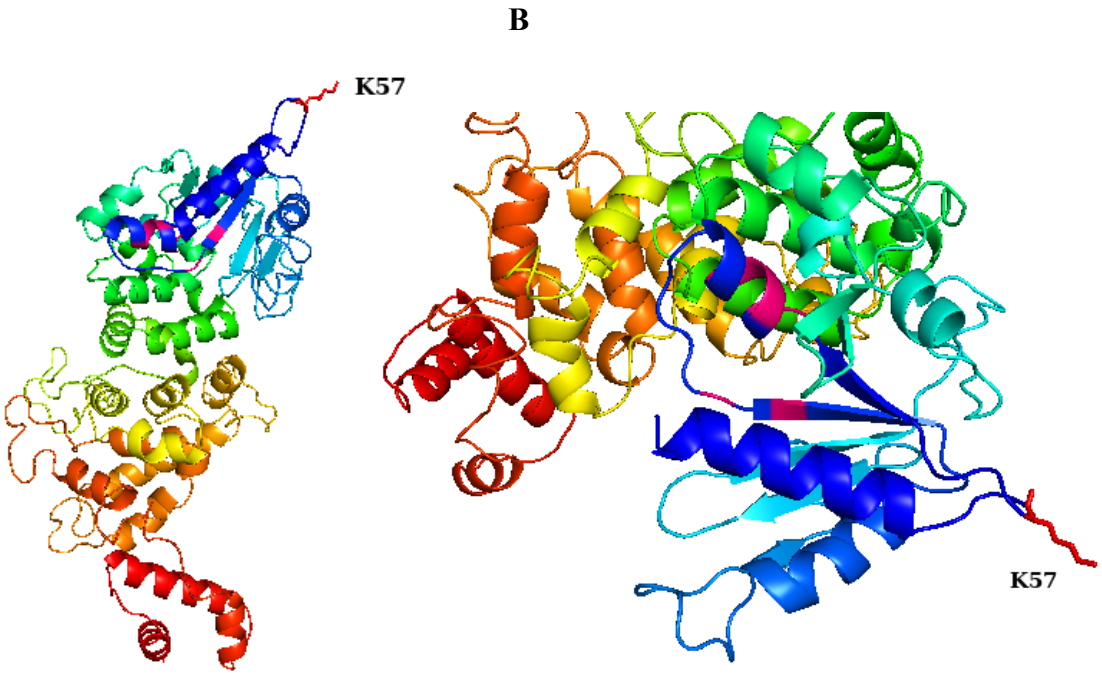

Figure 4.13: Model of *Saccharomyces cerevisiae* Cca1, presented in rainbow colour (N-terminus is blue and C-terminus is red), showing position of K57 (red stick) located seven residues upstream of conserved Motif A. Conserved residues of motif A are coloured in pink. A) Whole protein. B) Close up of the top view of the enzyme. This model was made based on the crystal structure of *Thermotoga maritima* using SWISS-MODEL (Waterhouse *et al*., 2018) and viewed by PyMol (v2.3.2) (Schrödinger).

4.1.2.5 Acetylation of K118

As with K150, K118 (bolded in Fig. 4.14) is located in the flexible loop between Motifs A and B in the head domain of Cca1. Acetylation at this position was seen in samples grown to an OD_{600} of 1.0 in both glucose and glycerol, but not at very early and late growth stages (OD_{600} of 0.3, 2.5, 3.0). Ratios of modified peptide to the total peptide containing this position ranged from about 20% in the mitochondrial fraction to 47% in both the nuclear and cytosolic fractions. The modification ratio at this position was more than double in the nuclear and cytosolic fractions compared to the mitochondrial fractions suggesting that acetylation reduced mitochondrial import either by blocking import to mitochondria or by sequestering the protein in the nucleus and cytosol. Again, given the importance of this flexible loop in Cca1 function, it is interesting that this residue is conserved in the yeasts *C. albicans, C. glabrata, K. lactis* and *S. cerevisiae* (Fig. 4.14).

```
C.albicans      DIDIAVNHLTGEEFVNGLHDYLRQHEPELSMNHVHTI-KM--      93
K.lactis        DLDIAINNMTGEQFAEKLCAFLQDRGLET--HSLHTID K---     93
C.glabrata      DLDIAINIMSGEEFATGLNGYLLEHFDKYGV-KPHSIHKIDK     105
S.cerevisiae    DLDIAINVMSGEQFATGLNEYLQQHYAKYGA-KPHNIHKIDK     121
                *:***:* ::**:*.  *  :* *:  :      * * *
```

Figure 4.14: Alignment of the CCA-adding enzyme sequences around K118 from *Saccharomyces cerevisiae, Candida albicans, Kluyveromyces lactis*, and *Candida glabrata*. K118 and the equivalent K in the other proteins are in bold. Standard one-letter abbreviations for amino acids are used. (*) indicates a position that is perfectly conserved, (:) indicates highly conserved and (.) indicates lower conservation. (-) indicates a gap introduced to optimize alignments. Numbers indicate position in each protein sequence. The alignment was performed using Clustal Omega (Madeira *et al*., 2019).

A structural model of Cca1 showing the position of K118 (Fig. 4.15) reveals that this residue is near the single β-sheet in Cca1. This β-sheet has been proposed to play a role in organizing the enzyme active site such that amino acid substitutions near this sheet, *e.g*., R64W in yeast (Goring *et al*., 2013), and R99W in the human enzyme (Hull *et al.* 2016; Frans *et al*., 2017) can affect enzyme activity. The conserved lysine residue at this position may suggest that it has a role in enzyme activity. Perhaps acetylation at this position can affect the activity of Cca1.

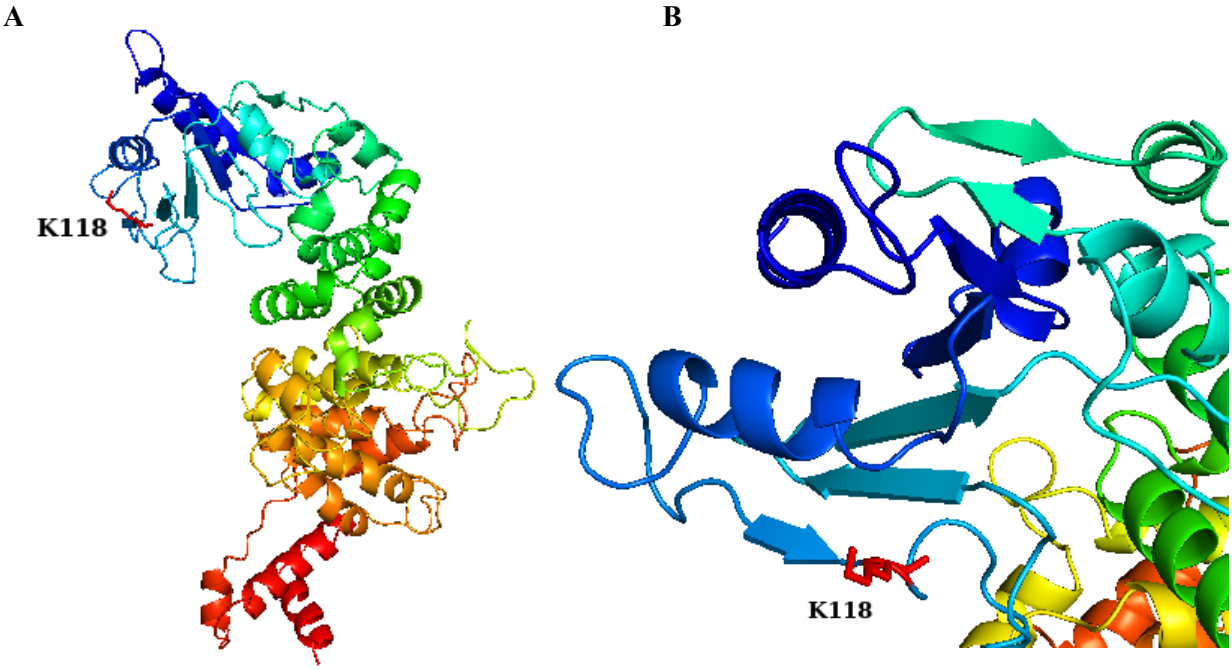

Figure 4.15: Model of *Saccharomyces cerevisiae* Cca1, presented in rainbow colour (N-terminus is blue and C-terminus is red), showing position of K118 (red stick) located in a large flexible loop between Motifs A and B. A) Whole protein. B) Close up of head and neck domains. This model was made based on the crystal structure of *Thermotoga maritima* using SWISS-MODEL (Waterhouse *et al*., 2018) and viewed by PyMol (v2.3.2) (Schrödinger).

4.1.3 Summary

PTMs were found at defined locations in Cca1. Some positions, *e.g.*, K150, K507 and T407 showed modifications under all conditions tested (perhaps reflecting a role of these positions and PTMs in the functioning of Cca1). Other positions showed variable levels of post-translational modification including competition between phosphorylation and acetylation, *e.g.*, S4, T5, S7, T19, and S21, suggesting that changes in the type and/or level of modification at these positions may affect enzyme activity or localization. The concentration of modified serine and threonine residues at the amino-terminus and the low level of modification elsewhere in the protein (Fig. 3.1) with the only other modified serine or threonine residues at positions 328 and 407, respectively, suggests that theses amino-terminal modifications are not artifactual. Their localization in or near the mitochondrial targeting signals suggests a role in the regulation of mitochondrial targeting. The switch between acetylation and phosphorylation at these positions may even be involved in altering the nucleocytosolic distribution of the longer form of Cca1 inside the cell.

4.2 Identification of proteins interacting with Cca1

Although many groups have used various high-throughput approaches to identify protein: protein interactions in yeast (Gavin *et al*., 2002; Ptacek *et al*., 2005; Krogan *et al*., 2006; Willmund *et al*., 2013; Jungfleisch *et al*., 2017) nobody has concentrated specifically on those proteins which interact with Cca1. Given the role of this enzyme in tRNA maturation (Deutscher, 1992), repair (Rosset and Monier, 1965) and quality control (Lund and Dahlberg, 1998; Steiner-Mosonyi and Mangroo, 2004; Wilusz *et al*., 2011) and its localization to the mitochondrion, nucleus and cytosol it seems reasonable that it will be shown to interact with accessory proteins linked either to its activities or its localization. In addition, here we compare a number of different conditions (cell density, carbon source, cellular fraction) to see if differences in interacting proteins can be identified which might provide additional information on Cca1 activity or localization. Proteins seen to interact with Cca1 in all conditions tested suggest that these proteins are integral to the basic functioning of Cca1. Other proteins that interact with Cca1 only under certain conditions may provide clues to the role of Cca1 under these conditions.

4.2.1 Proteins identified as interacting with Cca1 during growth in glucose or glycerol

Among all interacting proteins, 10 were co-purified with Cca1 in whole-cells extracts grown either on glucose or glycerol at OD_{600} of 1.0 in all three biological replicates tested. Of these proteins, Krs1, Ded81, Dps1, Gus1 are aminoacyl-tRNA synthetases which add an appropriate amino acid to their cognate tRNAs, Sah1 and Met6 are involved in amino-acid biogenesis, and Ape2, Pma1, Hsp82 and Imd4 are involved in the cellular supply of leucine, protein-export across plasma membranes, protein folding and purine biogenesis, respectively. Of these 10 proteins, only Gus1 has previously been identified in a proteomic or genetic screen (Costanzo *et al*., 2016) of Cca1. So, these experiments provide the first evidence of roles of these other proteins linked to Cca1. However, given the roles of proteins Met6, Krs1, Ded81, Dps1, Gus1 in the cell and the related functions of Cca1 it also is not surprising that these would be common to multiple conditions. Among these proteins, Krs1, Ape2, Dps1, Imd4 were eliminated from the list of interacting proteins by RNAseA treatment suggesting that they co-purified not directly with Cca1 but with RNA associated with it. Given the functions of these proteins in amino acid and/or protein biogenesis and their interactions with tRNA or other types of RNAs, it is interesting that they are lost on RNAse treatment.

It is not surprising that aminoacyl-tRNA synthetases (*e.g*., Ded81 Cytosolic asparaginyl-tRNA synthetase and Gus1 Glutamyl-tRNA synthetase) are shown to be interacting with Cca1 as CCA addition is the immediate precursor step to aminoacylation. This is consistent with the previous study that showed that aminoacylation of $tRNA^{Asn}$ is necessary for nuclear export of the cognate tRNA (Lund and Dahlberg, 1998). It is interesting that aminoacyl-tRNA synthetases were not identified for all 20 amino acids with only 11 aminoacyl-tRNA synthetases detected in this study in the different conditions and fractions. Furthermore, the two examples identified here interact with Cca1 even after RNAse treatment indicating that the synthetase may have other functions which require an interaction with Cca1. As with many enzymes involved in RNA metabolism (Anantharaman *et al*., 2002), a number of aminoacyl-tRNA synthetases have been identified with secondary functions (Guo *et al*., 2010; Cao *et al*., 2017). Alternatively, complexation of these proteins may exist for substrate channeling and direct transfer of the tRNA from one protein to another to increase the efficiency of tRNA charging inside the cell.

4.2.2 Proteins common to both the *in vitro* and *in vivo* assays

In order to define an interaction with Cca1 in more than one way, we used two different pull-down approaches. In one, labelled *in vivo*, a Cca1-TAP fusion protein was expressed in yeast such that interactions could occur in their natural locations within the cell. Given that Cca1 is found in the nucleus, mitochondrion and cytosol, this should allow for the greatest number of interactions to be identified. However, some interacting proteins may be expressed endogenously at levels so low that their interactions with Cca1 may be missed. To combat this possibility, a Cca1-GST fusion protein was expressed in *E. coli* and purified to homogeneity. This fusion protein was then bound to glutathione beds and cell extracts added. This allowed for increasing amounts of appropriate cell extracts to be added to show interactions that typically may involve low levels of specific proteins. While this *in vitro* approach may allow low-level interactions to be detected it must be noted that any interactions that require PTMs of Cca1 will be missed as expression of Cca1 in *E. coli* will not allow it to contain eukaryote-specific PTMs.

Using the *in vivo* approach 180 and 167 different proteins were identified as interacting with Cca1 when the cells were grown on glucose and glycerol, respectively. In contrast, 49 proteins interacting with Cca1 were identified in the *in vitro* approach in glucose. The difference in the number of proteins identified in these two approaches perhaps reflects the importance of PTMs in the interaction of Cca1 with its partners, as in the *in vitro* study, the number of identified proteins was much less than the *in vivo* assay. It also may reflect that the binding conditions for the proteins are optimized within the cell and not in the *in vitro* experiment. For example, there may be additional small molecules that are required for the interaction that are available *in vivo* but not *in vitro*. Something as simple as the temperature of the assay also could play a role in defining the interactions. So, while there are differences between the assays, perhaps it is the proteins that are common to both approaches that are the most interesting.

Six proteins (Arf1, Cyc1, Bat1, Gsp2, Nop56 and Pwp1) were common to both approaches when the cells were grown on glucose and 14 (Mck1, Shm2, Gvp36, Pnc1, Cyc1, Bat1, Prp43, Ydl124w, Ndi1, Nhp6B, Shm1, Efb1, Gsp2, and Pho88) were common when the cells were grown on glycerol. Moreover, Bat1, Cyc1, and Gsp2 were found using both approaches in cells grown either on glucose or glycerol. This suggests that these protein interactions are real.

These proteins (*e.g.*, Bat1) play roles, in amino-acid biosynthesis, Cyc1 in electron transport during cellular respiration and Gsp2 in nuclear import of proteins and export of RNA from the nucleus (Belhumeur *et al*., 1993). Of all of these interactions only the Gsp2 and Pwp1 interactions were eliminated upon RNAseA treatment suggesting that the interaction was mediated by RNA. This is not surprising as Gsp2 is a GTP binding protein involved in RNA processing and transport (Belhumeur *et al*., 1993). Perhaps Gsp2, tRNA and Cca1 interact during the export of tRNAs from the nucleus. Pwp1 is a WD-40 repeat protein involved in rRNA processing and it interacts with other proteins involved in ribosome synthesis (Zhang *et al*., 2004), so perhaps it interacts with other proteins that interact through an RNA with Cca1.

Among other proteins common between the *in vitro* and *in vivo* assays in glucose, Nop56 is a component of the box C/D snoRNP complex that directs 2'-O-methylation of pre-rRNA during its maturation (Hayano *et al*., 2003), thus similar to Pwp1, this protein might interact with Cca1 through RNA interacting proteins. Arf1 is a GTP-binding protein involved in protein trafficking and shown to be required for correct localization of *ASH1* mRNA (Trautwein *et al*., 2004). Co-purification of this protein with Cca1 might suggest a role of this protein in tRNA localization as well. Also, among the proteins reproduced in glycerol, Mck1 is a serine/tyrosine-specific kinase (Lim *et al*., 1993) which might mediate the serine/tyrosine phosphorylation that has been identified in this study.

Efb1 is one of the components of eEF-1A, the elongation factor which facilitates binding of aminoacyl-tRNA to the ribosomal A site (Carr-Schmid *et al*., 1999), and complexation between Efb1 and Cca1 might increase the efficiency of this interaction through substrate channeling. Gvp36 is associated with eukaryotic ribosomal complexes, and Prp43 is required for efficient biogenesis of both small- and large-subunit rRNAs (Leeds *et al*., 2006). Interactions with these proteins might suggest that Cca1 plays a role in tRNA maturation in the same area of the cell as ribosome assembly takes place. Nhp6B, required for transcriptional initiation fidelity of some tRNA genes (Braglia *et al*., 2007) suggests that an interaction between Cca1 and Nhp6B might induce the transcriptional initiation of some tRNA genes when the abundance of functional tRNAs is low inside the cell.

Pnc1 is a nicotinamidase that convert nicotinamide to nicotinic acid (Ghislain *et al*., 2001) and YDL124w is a NADPH-dependent alpha-keto amide reductase (Ishihara *et al*., 2004). Both have been shown to increase in abundances upon DNA replication stress (Tkach, *et al*., 2012). However, it is unclear why they would interact with Cca1. The reason for an interaction with Shm1 or Met10 also is unclear as these proteins are a mitochondrial serine hydroxy-methyltransferase which converts serine to glycine (Taylor *et al*., 1993) and a sulfite reductase (Hansen *et al*., 1994), respectively. Perhaps these interactions are non-specific.

Ndi1 which transfers electrons from NADH to ubiquinone in respiratory chain (Cui *et al.,* 2012) has been shown to be activated in mitochondria by N-terminal cleavage upon apoptotic stress such that it translocates to the cytoplasm to induce apoptosis (Cui *et al.*, 2012). Perhaps, Cca1 plays a role in sequestering tRNAs to reduce protein synthesis in response to the presence of activated Ndi1 in the cytosol. The sequestering of tRNAs in the nucleus to reduce protein synthesis is a common phenomenon in response to nutrient (Whitney *et al*., 2007) or other stress conditions (Shaheen e*t al.,* 2007; Hurto *et al*., 2007; Kramer and Hopper 2013; Watanabe *et al*., 2013; Chen *et al.,* 2016).

Finally, identification of Pho88 which is involved in signal recognition particle (SRP)-independent targeting of substrates to the ER (Aviram *et al.,* 2016) may suggest an interaction mediated by a tRNA that reflects the RNA component of the SRP. The RNA component of SRP is exported from the nucleus in yeast in a process mediated by Crm1 (Ciufo and Brown 2000; Grosshans *et al.,* 2001). This is interesting in the context of Crm1 interactions with Cca1 that I saw here related to nuclear export (see Section 4.2.3).

While in some cases it is reasonable to assume that the interactions identified are meaningful, it is less clear in the case of others. Most of the proteins identified on glucose are involved in amino acid and protein biogenesis in which Cca1 is an important component enabling protein synthesis by making functional tRNAs. It is not surprising that most of the proteins identified on glycerol are mitochondrial proteins, proteins involved in cellular respiration or proteins that are required in conditions of nutrition limitation, *e.g*., when glucose is limiting (Gasmi *et al*., 2014). However, the biological significance of the complexation of some of these proteins with Cca1 remains unclear

as they do not appear to function in processes that are related to known roles and functions of Cca1 within the cell.

4.2.3 Proteins involved in tRNA processing, turnover, and subcellular trafficking

In this study, a compilation of the proteins identified under all of the conditions tested showed 18 proteins with known functions in tRNA processing, turnover, and subcellular trafficking. Some proteins are involved in amino acid and/or protein biogenesis, such as aminoacyl-tRNA synthetases (Cdc60 cytosolic leucyl-tRNA synthetase, Ths1 cytosolic Threonyl-tRNA synthetase, Frs2 cytoplasmic phenylalanyl-tRNA synthetase). The significance of the interactions of aminoacyl-tRNA synthetases with Cca1 has been discussed in the previous section. Also, previous studies demonstrated that the presence of specific aminoacyl-tRNA synthetases in a temperature-sensitive strain could cause the accumulation of an end-matured unspliced noncognate $tRNA^{Ile}_{UAU}$ (Wu *et al*., 2015), which might be due to novel functions of these aaRS (Guo *et al*., 2010). These novel functions may be the reason for interaction of these proteins with Cca1.

Some proteins that were identified, *e.g*., Hyp2 translation elongation factor eIF-5A (Saini *et al*., 2009), Sup35 translation termination factor eRF3 (Gaudet *et al*., 2011), and Nop4 nucleolar protein essential for processing and maturation of 27S pre-rRNA and large ribosomal subunit (Sun, and Woolford, 1994) are involved in protein synthesis and ribosome biogenesis. These proteins are associated with the ribosome during its synthesis and function, so it would not be surprising if Cca1 also was found in these locations given its role in generating the functional tRNAs needed for protein synthesis. Although Xrn1, was first identified as a 5'-3' exonuclease that is a component of cytoplasmic processing (P) bodies involved in mRNA decay (Mitchell *et al*., 2013), it also can enter the nucleus and positively regulate transcription initiation and elongation to play a role in ribosome biogenesis and rRNA processing (Petfalski *et al*., 1998). So, again perhaps this protein interacts with Cca1 during ribosome biogenesis.

Although, no studies have yet shown the presence of Cca1 in the (P) body, as already mentioned in Section 1.3.3, Cca1 also plays a role in the degradation of RNA. It adds a CCACCA sequence to the 3’-end of unstable tRNAs (Wilusz *et al*., 2011; Kuhn *et al*., 2015) and flags them for degradation in the rapid tRNA decay (RTD) pathway mediated by the 5’-3’ exonucleases Rat1

and Xrn1 indirectly regulated by Met22 (Dichtl *et al*., 1997). Perhaps complexation of Xrn1 and Cca1 in the cytosol boosts the efficiency of the RTD pathway to ensure that damaged or hypomodified tRNAs do not reach the ribosome where they could deleteriously effect translation.

Bdf1 (bromodomain-containing factor 1), detected in the nuclear fraction of cells grown on glycerol, is involved in transcription initiation and impacts the expression of a broad class of genes (Lygerou *et al*., 1994). This study showed many acetylated sites on Cca1 and acetylation dependent protein-protein interactions are mainly studied in the context of bromodomain-containing proteins that interact with acetylated proteins (Josling *et al*., 2012). This result suggests that acetylated Cca1 may interact with Bdf1 to regulate transcription inside the nucleus. For instance, in response to a high abundance of Cca1 inside the cell, some positions of this protein could become acetylated such that modified Cca1 can interact with Bdf1 and decrease expression of specific target genes perhaps of other proteins required for protein synthesis.

Also, environmental stresses cause accumulation of pre-tRNA in the nucleus and block their export or re-export by retention of Los1 in the cytoplasm (Ghavidel *et al*., 2007). Alternatively, altered tRNA export/re-export can be due to a lower efficiency of the parallel tRNA export pathways in response to cellular stress (Lari *et al*., 2019). As already mentioned, in response to oxidative stress angiogenin removes the 3'-terminal adenosine residue from tRNAs by an endonucleolytic cleavage making those tRNAs non-functional (Czech *et al.,* 2013). Upon removal of the oxidative stress, Cca1 can then repair the CCA sequence so the tRNA can be used again in protein synthesis (Czech *et al.,* 2013). Thus, complexation of Cca1 with some export/import proteins seen in this study (*e.g*., Crm1, Cex1, Cse1, and Utp8) suggests that Cca1-dependent export of aminoacylated tRNAs might be an alternative pathway to export/re-export tRNA in parallel with the Los1 pathway in response to stress or the removal of stress.

Previous experiments (Strub *et al*., 2007) have shown that Utp8, a nucleolar tRNA-binding protein that forms a complex with the tRNA nuclear export machinery, interacts with Cca1. We also showed this interaction here. However, those earlier experiments did not show any interaction of Utp8 with Cse1, the protein that mediates importin-alpha re-export of proteins, RNAs, and ribosomal subunits from the nucleus to the cytoplasm after import substrates have been released

into the nucleoplasm (Hood and Silver 1998; Künzler and Hurt, 1999; Maurer *et al*., 2001; Johnson *et al*., 2002). Here, I show a Cse1:Cca1 interaction in addition to the Utp8:Cca1 interaction. Taken together these data may suggest a complex that contains Utp8, Cca1 and Cse1 (perhaps involved in tRNA export) such that the Cca1 interacts with both Utp8 and Cse1, but these two proteins do not interact with each other. Other components of this export process identified here as interacting with Cca1 include Nup57, a component of the central core of the nuclear pore complex (Frey and Görlich, 2009), Nup170, a component of the inner ring of the nuclear pore complex that also interacts with genomic regions that contain ribosomal protein, (Shulga and Goldfarb, 2003), Nup192, a subunit of the inner ring of the nuclear pore complex (Kosova *et al*., 1999), Mex67, a component of the nuclear pore involved in nuclear mRNA export (Segref *et al*., 1997), Rna1, a GTPase activating protein (GAP) for Gsp1 and involved in nuclear transport (Becker *et al*., 1995; Ryan *et al*., 2003), and Hrp1, an RRM-containing heteronuclear RNA binding protein that binds poly(A) (Kessler *et al*., 1997).

Of the proteins described in this section, Ths1, Sup35, Nop4, Cse1 and Crm1 were co-purified regardless of RNAseA treatment. This suggests that these proteins directly interact with Cca1 such that their complexations play important roles in tRNA processing. Also, one of the export proteins detected here might mediate nuclear transport of Cca1 within the cell. On the other hand, Hyp2 and Rna1, which are involved in translation elongation (Saini *et al*., 2009) and in nuclear transport (Corbett *et al*., 1995) respectively, showed up only in samples without RNAseA treatment which suggests a direct interaction of these proteins with tRNA, not Cca1. Alternatively, it is possible that the interactions between the proteins have been disrupted by removing tRNA as one of the components of the complex.

This study also identified Crm1 as interacting with Cca1 regardless of RNaseA treatment, suggesting that Crm1 directly interacts with Cca1, and not indirectly through the tRNA substrate. Interestingly, previous studies have shown that overexpression of the *CCA1* gene, complemented a defect in the nuclear export of tRNAs in *Los1Δ* cells, but did not correct a pre-tRNA splicing defect (Chatterjee *et al*., 2018). In contrast to *LOS1* which is not essential, *CRM1* is an essential gene and encodes Crm1 (Exportin-1) which is required for the export of proteins with leucine rich nuclear export signals (NES). As with the *Los1Δ* strain, a Crm1 strain with reduced activity also showed an accumulation of unsliced pre-tRNA at the nuclear periphery (Chatterjee *et al*., 2018).

Our study suggests a Cca1-dependent Crm1 export of aminoacylated tRNAs by complexation between Cca1 and Crm1. Alternatively, aminoacylation could occur after Crm1 exports Cca1-bound tRNA to the cytoplasm.

Cex1, a component of the nuclear aminoacylation-dependent tRNA export pathway (McGuire and Mangroo, 2007), also co-purified with Cca1 in 2 out of 3 replicates on glucose. This enzyme collects aminoacylated tRNAs from Los1 and Msn5 on the cytosolic face of the NPC and delivers them to eEF-1A in the cytoplasm (McGuire and Mangroo, 2007). In my study, Cex1 interacted with Cca1 even after RNAseA treatment suggesting a specific protein:protein interaction. As with the Utp8 interaction described above, perhaps this represents an indirect interaction through complexation with other proteins such as Crm1 as McGuire and Mangroo (2007) previously have reported that Cex1 does not co-purify with Cca1. Further experiments are required to validate this hypothesis.

Kap95, Kap104 and Kap123 co-purified with Cca1 even after RNAseA treatment suggesting that these proteins might associate together and interact with Cca1 directly to mediate transport of Cca1 across the nuclear membrane.

4.2.4 Identification of a potential nuclear targeting signal in Cca1

Different tools have been used to predict a potential nuclear localization signal (NLS) in Cca1 but to date none has been identified in any CCA-adding enzyme (Schmidt von Braun *et al*., 2007; Kalderon *et al*., 1984, Lanford and Butel, 1984; Soniat and Chook, 2015; Leibovitch *et al.*, 2013). The results of the pull-down experiments conducted here suggest multiple direct or indirect interactions of Cca1 with different import/export proteins such as Gsp2, Crm1, Kap95, Kap104, Kap123, and Cex1 suggesting the importance of nuclear import and export signals.

Knowing which proteins interacted with Cca1 allowed us to search for the NLS sequences recognized by these proteins. According to Fries *et al*. (2007), a proposed novel NLS with the consensus sequence R/KxxL$(x)_n$V/YxxV/IxK/RxxxK/R was shown to be able to interact with five yeast importins including Kap95, Kap104 and Kap123 which I identified in this study. A similar consensus sequence (KxxI/L$(x)_n$V/LxxxI/LxK/RxxxK) was detected in Cca1 from *S. cerevisiae*

(376-395), in the *S. pombe* CC-adding enzyme (331-345), and in the *Candida glabrata* (311-380) CCA-adding enzyme (Fig. 4.16) with a predicted α-helical structure at the core of the motif. This NLS is found on the surface of the protein as expected based on the predicted structure of Cca1 (Fig. 4.17).

```
S. pombe(cca1) PWYNWSILEKSKIKI-----LPPILIRDSLKYSKP---IMSQVEN  355
C. glabrata    PMADLKIIALPKKKLNNTLPVSESIVREGLKFNKASSIVVARCVE  394
S. cerevisiae  PMANLQIIGNPKKKINNLVSVTESIVKEGLKLSKNDAAVIAKTVD  409
               *  : .*:  .* *:     :.  ::::.** .*    :::.  :
```

Figure 4.16: Alignment of yeast *Schizosaccharomyces pombe (Cca1), Candida glabrata* and *Saccharomyces cerevisiae* CC- or CCA-adding enzymes showing the predicted NLS. Conserved nucleotides of the NLS motif shown in bold. Standard one-letter abbreviations for amino acids are used. (*) indicates a position that is perfectly conserved, (:) indicates highly conserved and (.) indicates lower conservation. (-) indicates a gap introduced to optimize alignments. Numbers indicate position in each protein sequence. The alignment was performed using Clustal Omega (Madeira *et al*., 2019).

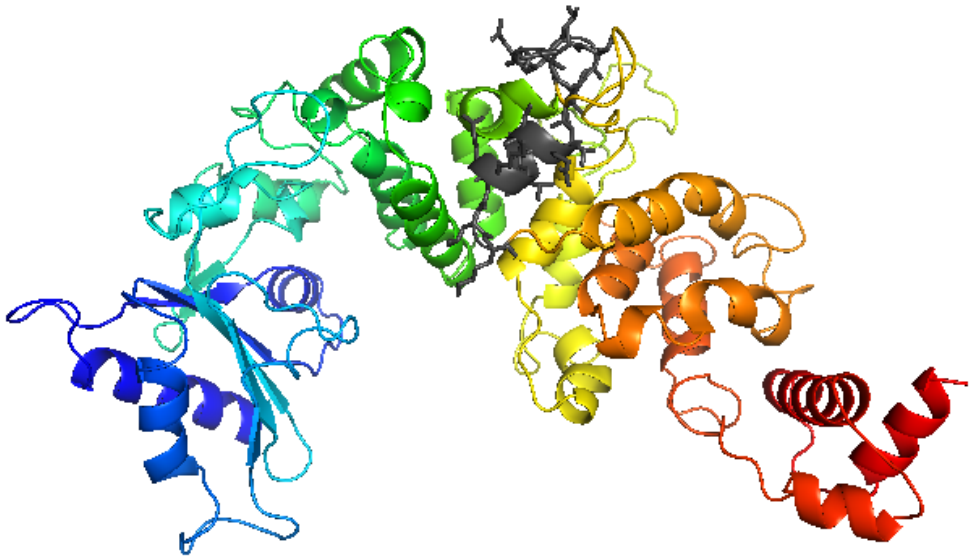

Figure 4.17: Cca1 structural model showing potential NLS (highlighted in gray). The protein is rainbow colored (blue to red from N to C terminus). This model was made based on the crystal structure of the *Thermotoga maritima* CCA-adding enzyme using SWISS-MODEL (Waterhouse *et al*., 2018) and viewed by PyMol (v2.3.2) (Schrödinger).

So, identifying karyopherins that interact with Cca1 has for the first time highlighted a potential nuclear import signal in this protein. Site-directed mutagenesis of this region of the protein will support the identification of this sequence.

4.2.5 Identification of the proteins of the RNAseP/RNAseZ supercomplex

During tRNA maturation, precursor tRNAs must undergo both 5' and 3'-processing by the endonucleases RNAseP (Lai *et al*., 2010) and RNAseZ (Zhao *et al*., 2009), respectively. Previous studies using a combination of detergent-free Blue Native Gel Electrophoresis, proteomics and *in vitro* testing of pre-tRNA maturation have suggested a large number of proteins (up to 130) in an RNAseP/RNAseZ stable supercomplex (Daoud *et al*., 2012). In total, 32 proteins of this complex were identified in this study as interacting with Cca1. These proteins exhibit diverse functions inside the cell. My study revealed twelve proteins of the citric acid cycle (Aco1, Cit1, Fum1, Idp1, Idh1, Idh2, Kgd1, Kgd2, Lpd1, Lsc1, Lsc2 Mdh1) of the 16 identified by Daoud *et al*. (2012). In addition, of the 29 proteins that Daoud *et al*. (2012) identified as involved in amino acid, acetate and ethanol metabolism, choline metabolism, and pyrimidine synthesis, 10 (Agx1, Ade3, Adh2, Ald4, Aat2, Bat1, Bat2, Leu4, Shm1, and Shm2) were also found in this study. Of the 35 proteins identified by Daoud *et al*. (2012) with roles in translation, three ribosomal proteins (Mrp1, Rps5, Rpl8) were identified in this study. While Rps5 and Rpl8 are components of the cytosolic ribosome, Mrp1 is found in the mitochondrial ribosome. Here, I identified three (Aap1, Ape2 and Dug1) of the five peptidases that Daoud *et al*. (2012) found although it is difficult to appreciate why peptidases would be involved in tRNA maturation. Daoud *et al*. (2012) identified six subunits of the oxidative phosphorylation complex and here this study identified two subunits of the mitochondrial F_1F_0 ATP synthase (Atp1 and Atp2). Daoud *et al*. (2012) also identified six proteins involved in genome maintenance and eight proteins involved in glycolysis. Here we identified one protein in each of these processes, Mmf1 and Eno1, respectively. Although, Cca1 has not been reported as one of the components of this complex, its important role in tRNA processing cannot be ignored. The presence of Cca1 in this complex would increase the efficiency of tRNA processing by adding the C-terminal second CCA sequence to target tRNAs for degradation.

4.2.6 Proteins identified as interacting with Cca1 in specific conditions

Among all of the proteins detected in cells grown to an OD_{600} of one in glucose and in glycerol, 144 and 295, respectively, were specific to one of the two conditions. Of these identified interacting proteins, proteins important in the context of interaction with Cca1 have been discussed in the previous sections. Cex1, Cse1, Frs2, Hrp1, Nop4, Rna1, supp35, Ths1, Tys1, Arc1, and Ncl1

were identified only in glucose and Prp43, Nup170, Nup191, Nup49, Nup57, Kgd2, Kre33 and Xrn1 were identified only in glycerol. Many proteins involved in amino acid and protein biosynthesis have been identified in glucose grown cells consistent with the high level of growth under this condition. As expected for cells grown on glycerol (such that fermentation is downregulated), the number of proteins involved in the citric acid cycle, cellular respiration, and the stress response was increased. It is not clear why more nuclear proteins are detected in this condition in which aerobic respiration is the main energy production and promotes mitochondrial localization of the Cca1.

5. CONCLUSIONS AND FUTURE WORK

This study has been conducted to better understand the factors that may impact the distribution or function of Cca1 inside the cell using *S. cerevisiae* as a model organism and mass spectrometry as a proteomic tool to identify PTMs and potential Cca1 partners in different conditions.

This study found PTMs at specific positions in Cca1 including some positions that have been identified before as well as some positions that are reported here for a first time. Of the positions showing modifications, seven (S4, T5, S7, S12, T17, T19, and S21) are found near the amino terminus and may play some role in protein targeting. Two of the other modifications (K105 and K118) are found in the loop between conserved motifs A and B such that these modifications may play some role in protein function. The other positions are scattered throughout the protein and could be involved either in protein localization or function.

Also, *in vivo* and *in vitro* pull-down assays under different conditions were used to identify proteins that interact with Cca1. As expected, we showed potential interactions of Cca1 with proteins involved in tRNA processing, maturation and turnover. Also, we showed interactions between Cca1 and many components of the protein import/export machinery at the nuclear membrane. This suggests that Cca1 import and/or export are controlled at the nuclear pore complex and may be regulated as tRNA import and export are regulated. Some of these interacting proteins were identified multiple times in different conditions (*e.g.,* carbon source, RNaseA treatment) providing support for a real and important interaction with Cca1 inside the cell. Moreover, some of the interactions detected were specific to defined experimental conditions such as the presence of glucose or glycerol, *i.e*., fermentation versus aerobic respiration as the main source of energy. Also, large differences in the number of interacting proteins were seen in comparing the *in vivo* and *in vitro* pull-down studies, perhaps suggesting an important role for PTMs in the interactions of Cca1 with its partners in the cell. Further study of these proteins may reveal important features required for Cca1 activity and localization. Already as a result of these protein:protein interaction studies we have identified for the first time a potential nuclear localization signal in any eukaryotic tRNA nucleotidyltransferase.

Further experiment such as site-directed mutagenesis of the post-translationally modified resdues of Cca1 identified in this study can be used to screen for the importance of these modifications in enzyme localization or phenotype *in vivo* or to measure changes in enzyme activity *in vitro*. Secondary approaches such as cross-linking, two hybrid assays or genetic screens could be used to confirm the interactions identified in this study. Finally, gene fusions and site-directed mutagenesis can be used to confirm the predicted NLS in Cca1.

6. BIBLIOGRAPHY

Aebi, M., Kirchner, G., Chen, J. Y., Vijayraghavan, U., Jacobson, A., Martin, N. C., and Abelson, J. (1990). Isolation of a temperature-sensitive mutant with an altered transfer RNA nucleotidyltransferase and cloning of the gene encoding tRNA nucleotidyltransferase in the Yeast *Saccharomyces cerevisiae*. *J Biol Chem*, *265*, 16216–16220.

Aksentijevich, I., Zhou, Q., Giannelou, A., Sediva, A., Stone, D., Rosenzweig, S., Edwan, J., Pelletier, M., Monique, S., Šrámková, L., *et al*. (2014). *TRNT1* missense mutations define an autoinflammatory disease characterized by recurrent fever, severe anemia, and B-cell immunodeficiency. *Pediatr Rheumatol Online J. 12* (Suppl 1), O21.

Albuquerque, C. P., Smolka, M. B., Payne, S. H., Bafna, V., Eng, J., and Zhou H. (2008). A multidimensional chromatography technology for in-depth phosphoproteome analysis. *Mol Cell Proteomics, 7*, 1389-1396.

Alexandrov, A., Chernyakov, I., Gu. W., Hiley, S. L., Hughes, T. R., Grayhack, E. J., and Phizicky, E. M. (2006). Rapid tRNA decay can result from lack of nonessential modifications. *Mol Cell*, *21*, 87-96.

Anantharaman, V., Koonin, E. V., and Aravind, L. (2002). Comparative genomics and evolution of proteins involved in RNA metabolism. *Nucleic Acids Res*, *30*, 1427–1464.

Aravind, L., and Koonin, E. V. (1999). Novel predicted RNA-binding domains associated with the translation machinery. *J Mol Evol*, *48*, 291-302.

Arthur, J. (2009). The role of arginine 244 in *Candida glabrata* tRNA nucleotidyltransferase. Master's thesis, Chemistry and Biochemistry, Concordia University.

Arts, G. J., Kuersten, S., Romby, P., Ehresmann, B., and Mattaj, I. W. (1998). The role of exportin-t in selective nuclear export of mature tRNAs. *EMBO J*, *17*, 7430–7441.

Augustin, M. A., Reichert, A. S., Betat, H., Huber, R., Mörl, M., and Steegborn, C. (2003). Crystal structure of the human CCA-adding enzyme: Insights into template-independent polymerization. *J Mol Biol*, *328*, 985–994.

Ausubel, F. M., Brent, R., Kingston, R. E., Moore, D. D., Seidman, J. G., and Struhl, K. (1989). Current Protocols in Molecular Biology. New York: Wiley.

Aviram, N., Ast, T., Costa, E. A., Arakel, E. C., *et al*. (2016). The SND proteins constitute an alternative targeting route to the endoplasmic reticulum. *Nature*, *540*, 134–138.

Babazadeh, R., Lahtvee, P. J., Adiels, C. B., Goksör, M., Nielsen, J. B., and Hohmann, S. (2017). The yeast osmostress response is carbon source dependent. *Sci Rep*, *7*, 990. doi:10.1038/s41598-017-01141-4.

Bader-Meunier, B., Rieux-Laucat, F., Touzot, F., Frémond, M-L, André-Schmutz, I., Fraitag, S., and Bodemer, C. (2018). Inherited immunodeficiency: A new association with early-onset childhood panniculitis. *Pediatrics*, *141*(Supplement 5), S496–S500.

Bannister, A. J., Miska, E. A., Görlich, D and Kouzarides, T. (2000). Acetylation of importin-α nuclear import factors by CBP/p300. *Curr Biol*, *10*, 467–470.

Becker, J., Melchior, F., Gerke, V., Bischoff, F. R., Ponstingl, H., and Wittinghofer, A. (1995). *RNA1* encodes a GTPase-activating protein specific for Gsp1p, the Ran/TC4 homologue of *Saccharomyces cerevisiae*. *J Biol Chem.*, *270*, 11860-11865.

Belhumeur, P., Lee, A., Tam, R., DiPaolo, T., Fortin, N., and Clark, M. W. (1993). *GSP1* and *GSP2*, genetic suppressors of the *prp20-1* mutant in *Saccharomyces cerevisiae*: GTP-binding proteins involved in the maintenance of nuclear organization. *Mol Cell Biol*, *13*, 2152–2161.

Betat, H., Rammelt, C., and Mörl, M. (2010). tRNA nucleotidyltransferases: ancient catalysts with an unusual mechanism of polymerization. *Cell Mol Life Sci*, *67*, 1447–1463.

Bio-Rad protein assay. 2018a. [accessed 2018 Dec 9].
https://www.bio rad.com/webroot/web/pdf/lsr/literature/LIT33.pdf.

Bradford, M. M. (1976). A rapid and sensitive method for the quantitation of microgram quantities of protein utilizing the principle of protein-dye binding. *Anal Biochem, 72*, 248–254.

Braglia, P., Dugas, S. L., Donze, D., and Dieci, G. (2007). Requirement of Nhp6 proteins for transcription of a subset of tRNA genes and heterochromatin barrier function in *Saccharomyces cerevisiae*. *Mol Cell Biol, 27*, 1545–1557.

Breitkreutz, A., Choi, H., Sharom, J. R., Boucher, L., *et al*. (2010). A global protein kinase and phosphatase interaction network in yeast. *Science*, *328*, 1043–1046.

Brewer, B. J., Chlebowicz-Sledziewska, E. and Fangman, W. L. (1984). Cell cycle phases in the unequal mother/daughter cell cycles of *Saccharomyces cerevisiae*. *Mol Cell Biol*, *4*, 2529-2531.

Cao, X. Y., Li, C. Q., Xiao, S. Y., Tang, Y. L., Huang, J., Zhao, S., Li, X. Y., Li, J., Zhang, R., and Yu, W. (2017). Acetylation promotes TyrRS nuclear translocation to prevent oxidative damage. *Proc Natl Acad Sci USA*, *114*, 687-692.

Capage, M., and Hill, C. W. (1979). Preferential unequal recombination in the glyS region of the *Escherichia coli* chromosome. *J Mol Biol*, *127*, 73-87.

Carr-Schmid, A., Valente, L., Loik, V. I., Williams, T., Starita, L. M., and Kinzy, T. G. (1999). Mutations in elongation factor 1beta, a guanine nucleotide exchange factor, enhance translational fidelity. *Mol Cell Biol*, *19*, 5257–5266.

Chakraborty, P. K., Schmitz-Abe, K., Kennedy, E. K., *et al*. (2014). Mutations in TRNT1 cause congenital sideroblastic anemia with immunodeficiency, fevers, and developmental delay (SIFD). *Blood*, *124*, 2867–2871.

Chatterjee, K., Nostramo, R. T., Wan, Y., and Hopper A. K. (2018). tRNA dynamics between the nucleus, cytoplasm and mitochondrial surface: Location, location, location. *Biochim Biophys Acta*, *1861*, 373-386.

Chen, J. Y., Joyce, P. B. M., Wolfe, C. L., Steffen, M. C., and Martin, N. C. (1992). Cytoplasmic and mitochondrial tRNA nucleotidyltransferase activities are derived from the same gene in the yeast *Saccharomyces cerevisiae*. *J Biol Chem*, *267*, 14879-14883.

Chen, J. Y., Kirchner, G., Aebi, M., and Martin, N.C. (1990). Purification and properties of yeast ATP (CTP): tRNA nucleotidyltransferase from wild-type and overproducing cells. *J Biol Chem, 265*, 16221-16224.

Chen, Q., Yan, M., Cao, Z., Li, X., Zhang, Y., Shi, J., Feng, G., Peng, H., Zhang, X., Zhang, Y., Qian, J., Duan, E., Zhai, Q., and Zhou, Q. (2016). Sperm tsRNAs contribute to intergenerational inheritance of an acquired metabolic disorder. *Science, 351*, 397-400.

Chernyakov, I., Whipple, J. M., Kotelawala, L., Grayhack, E. J., and Phizicky, E. M. (2008). Degradation of several hypomodified mature tRNA species in *Saccharomyces cerevisiae* is mediated by Met22 and the 5'-3' exonucleases Rat1 and Xrn1. *Genes and Dev*, *22*, 1369–1380.

Cho, H. D., Verlinde, C. L., and Weiner, A. M. (2007). Reengineering CCA-adding enzymes to function as (U,G)- or dCdCdA-adding enzymes or poly(C,A) and poly(U,G) polymerases. *Proc Natl Acad Sci USA*, *104*, 54–59.

Ciufo, L. F., and Brown, J. D. (2000). Nuclear export of yeast signal recognition particle lacking srp54p by the Xpo1p/Crm1p NES-dependent pathway. *Curr Biol, 10*, 1256-1264.

Chung, M. (2019). Biophysical and biochemical characterization of human tRNA nucleotidyltransferase variants. Master's thesis, Biology, Concordia University.

Cook, A. G., Fukuhara, N., Jinek, M., and Conti, E. (2009). Structures of the tRNA export factor in the nuclear and cytosolic states. *Nature*, *461*, 60–65.

Corbett, A. H., Koepp, D. M., Schlenstedt, G., Lee, M. S., Hopper, A. K., and Silver, P. A. (1995). Rna1p, a Ran/TC4 GTPase activating protein, is required for nuclear import. *J Cell Biol*, *130*, 1017–1026.

Costanzo, M., VanderSluis, B., Koch, E. N., Baryshnikova, A., *et al*. (2016). A global genetic interaction network maps a wiring diagram of cellular function. *Science*, *353*. pii: aaf1420.

Crick, F. H. C. (1958). On protein synthesis. *Symp Soc Exp Biol, 12*, 138-163.

Cui, H., Kong, Y., and Zhang, H. (2012). Oxidative stress, mitochondrial dysfunction, and aging. *J Signal Transduct*, 646354. doi: 10.1155/2012/646354.

Curto, P. (1994). Comparative Characterization of the Fermentation Pathway of *Saccharomyces cerevisiae* Using Biochemical Systems Theory and Metabolic Control Analysis: Model Definition and Nomenclature. *Math Biosci*, *130*, 25-50.

Czech, A., Wende, S., Morl, M., Pan, T. and Ignatova, Z. (2013). Reversible and rapid transfer-RNA deactivation as a mechanism of translational repression in stress. *PLoS Genet*, *9*, e1003767.

Dagert, M., and Ehrlich, S. D. (1979). Prolonged incubation in calcium chloride improves the competence of *E. coli* cells. *Gene*, *6*, 23-28.

Danpure, C. J. (1995). How can the products of a single gene be localized to more than one intracellular compartment? *Trends Cell Biol*, *5*, 230–238.

Daoud, R., Forget, L., and Lang, B. F. (2012). Yeast mitochondrial RNase P, RNase Z and the RNA degradosome are part of a stable supercomplex. *Nucleic Acids Res*, *40*, 1728–1736.

DeLuca, A. P., Whitmore, S. S., Barnes, J., Sharma, T. P., *et al*. (2016). Hypomorphic mutations in *TRNT1* cause retinitis pigmentosa with erythrocytic microcytosis. *Hum Mol Genet*, *25*, 44–56.

Deng, X.Y., Hanic-Joyce, P. J., and Joyce, P. B. (2000). Isolation and nucleotide sequence of a gene encoding tRNA nucleotidyltransferase from *Kluyveromyces lactis*. *Yeast*, *16*, 945-52.

Deutscher, M. P. (1992). tRNA nucleotidyltransferase. *The Enzymes*, *15*, 183–215.

Dichtl, B., Stevens, A., and Tollervey, D. (1997). Lithium toxicity in yeast is due to the inhibition of RNA processing enzymes. *EMBO J*, *16*, 7184–7195.

Dohmen, R. J., Strasser, A. W., Höner, C. B., and Hollenberg, C. P. (1991). An efficient transformation procedure enabling long-term storage of competent cells of various yeast genera. *Yeast*, *7*, 691-692.

Domon, B., and Aebersold, R. (2010). Options and considerations when selecting a quantitative proteomics strategy. *Nature Biotech*, *28*, 710-721.

Drazic, A., Myklebust, L. M., Ree, R., and Arnesen, T. (2016). World of protein acetylation. *Biochim Biophys Acta*, *1864*, 1372-401.

Dupasquier, M., Sangbumn, K., Konstantine, H., Howard, G., and Hou, Y.M. (2008). tRNA integrity is a prerequisite for rapid CCA addition: implication for quality control. *J Mol Biol*, *379*, 579-588.

Ernst, F. G., Rickert, C., Bluschke, A., Betat, H., Steinhoff, H. J., and Morl, M. (2015). Domain movements during CCA-addition: a new function for motif C in the catalytic core of the human tRNA nucleotidyltransferases. *RNA Biol*, *12*, 435-446.

Frans, G., Moens, L., Schaballie, H., Wuyts, G., *et al.* (2017). Homozygous N-terminal missense mutation in *TRNT1* leads to progressive B-cell immunodeficiency in adulthood. *J Allergy Clin Immunol*, *139*, 360-363.e6.

Frey, S., and Görlich, D. (2009). FG/FxFG as well as GLFG repeats form a selective permeability barrier with self-healing properties. *EMBO J*, *28*, 2554–2567.

Fries, T., Betz, C., Sohn, K., Caesar, S., Schlenstedt, G., and Bailer, S. M. (2007). Novel conserved nuclear localization signal is recognized by a group of yeast importins. *J Biol Chem*, *282*, 19292–19301.

Garrels, J. I., McLaughlin, C. S., Warner, J. R., Futcher, B., *et al*. (1997). Proteome studies of *Saccharomyces cerevisiae*: identification and characterization of abundant proteins. *Electrophoresis*, *18*, 1347-1360.

Gasmi, N., Jacques, P. E., Klimova, N., Guo, X., Ricciardi, A., Robertand, F., and Turcotte, B. (2014). The switch from fermentation to respiration in *Saccharomyces cerevisiae* is regulated by the Ert1 transcriptional activator/repressor. *Genetics*, *198*, 547–560.

Gaudet, P., Livstone, M. S., Lewis, S. E., and Thomas, P. D. (2011). Phylogenetic-based propagation of functional annotations within the Gene Ontology Consortium. *Brief Bioinform*, *12*, 449–462.

Gavel, Y., Nilsson, L., and Hejine, G. H. (1988). Mitochondrial targeting sequences. Why 'non-amphiphilic' peptides may still be amphiphilic. *FEBS Lett*, *235*, 173-177.

Gavin, A., Bösche, M., Krause, R. *et al.* (2002). Functional organization of the yeast proteome by systematic analysis of protein complexes. *Nature, 415***,** 141–147.

GE Healthcare. (2009). Instruction 28-9537-65 AB, TiO2 Mag Sepharose^{TM}.

Ghaemmaghami, S., Huh, W-K., Bower, K., Howson, R. W., Belle, A., Dephoure, N., O'Shea, E. K., and Weissman, J. S. (2003). Global analysis of protein expression in yeast. *Nature*, *425*, 737–41.

Ghavidel, A., Kislinger, T., Pogoutse, O., Sopko, R., Jurisica, I., and Emili, A. (2007). Impaired tRNA nuclear export links DNA damage and cell cycle checkpoint. *Cell, 131*, 915-26.

Ghislain, M., Talla, E., and François, J. M. (2001). Identification and functional analysis of the *Saccharomyces cerevisiae* nicotinamidase gene, *PNC1*. *Yeast, 19*, 215-224.

Giannelou, A., Wang, H., Zhou, Q., Park, Y. H., *et al.* (2018). Aberrant tRNA processing causes an autoinflammatory syndrome responsive to TNF inhibitors. *Ann Rheum Dis*, *77*, 612–619.

Goffeau, A., Barrell, B. G., Bussey, H., Davis, R. W., *et al*. (1996). Life with 6000 genes. *Science*, *274*, 546, 563-7.

Goring, M. E., Leibovitch, M., Gea-Mallorqui, E., Karls, S., Richard, F., Hanic-Joyce, P. J., and Joyce, P. B. M. (2013). The ability of an arginine to tryptophan substitution in *Saccharomyces cerevisiae* tRNA nucleotidyltransferase to alleviate a temperature-sensitive phenotype suggests a role for motif C in active site organization. *Biochim Biophys Acta - Proteins and Proteomics*, *1834*, 2097-2106.

Görlich, D and Kutay, U. (1999). Transport between the cell nucleus and the cytoplasm. *Cell Dev Biol*, *15*, 607-660.

Gorodetsky, C., Morel, C. F., and Tein, I. (2018). Expanding the phenotype of *TRNT1* mutations to include Leigh syndrome. *Can J Neurol Sci*, Suppl, *2*(S51), p.133.

Green, R., and Noller, H. F. (1997). Ribosomes and translation. *Annu Rev Biochem*. *66*, 679-716.

Gregg, C., Kyryakov, P., and Titorenko V. (2009). Purification of mitochondria from yeast cells. *J Vis Exp*: *JoVE*, (30), 1417. doi:10.3791/1417.

Grosshans, H., Deinert, K., Hurt, E., and Simos, G. (2001). Biogenesis of the signal recognition particle (SRP) involves import of SRP proteins into the nucleolus, assembly with the SRP-RNA, and Xpo1p-mediated export. *J Cell Biol*, *153*, 745–762.

Guo, M., Yang, X. L., and Schimmel, P. (2010). New functions of aminoacyl- tRNA synthetases beyond translation. *Nat Rev Mol Cell Biol*, *11*, 668–674.

Guan, T. L. (2018). A LC-MS/MS-Based Approach to Studying the *Saccharomyces cerevisiae* Cca1 Protein. Master's thesis, Chemistry and Biochemistry, Concordia University.

Gurtubay J. I., Goni F. M., Gomez-Fernandez J. C., Otamendi J. J., and Macarulla J. M. (1980). Triton X-100 Solubilization of Mitochondrial Inner and Outer Membranes. *J Bioenerg Biomembr*, *12*, 47-70.

Guthrie, C., and G. Fink. (1991). Guide to Yeast Genetics and Molecular Biology. *Methods in Enzymology*. Vol. 194. Academic Press, San Diego.

Hanic-Joyce, P. J. and Joyce, P. B. M. (2002). Characterization of a gene encoding tRNA nucleotidyltransferase from *Candida glabrata*. *Yeast*, *19*, 1399-1411.

Hansen, J., Cherest, H., and Kielland-Brandt, M. C. (1994). Two divergent *MET10* genes, one from *Saccharomyces cerevisiae* and one from *Saccharomyces carlsbergensis*, encode the alpha

subunit of sulfite reductase and specify potential binding sites for FAD and NADPH. *J bacterial, 176*, 6050–6058.

Hansen, K. G., and Herrmann, J. M. (2019). Transport of proteins into mitochondria. *Protein J*, *38*, 330-342.

Harju, S., Fedosyuk, H., and Peterson, K. R. (2004). Rapid isolation of yeast genomic DNA: Bust n' Grab. *BMC Biotechnol*, *4*, 8. doi: 10.1186/1472-6750-4-8.

Harper, S., and Speicher, D. W. (2011). Purification of proteins fused to glutathione S-transferase. *Methods Mol Biol, 681*, 259–280.

Hayano, T., Yanagida, M., Yamauchi, Y., Shinkawa, T., Isobe, T., and Takahashi, N. (2003). Proteomic Analysis of Human Nop56p-associated Pre-ribosomal Ribonucleoprotein Complexes. *J Biol Chem*, *278*, 34309–34319.

Helbig, A. O., Rosati, S., Pijnappel, P. W. W. M, Breukelen, B.V., Timmers, M. H. T. H., Mohammed, S., Slijper, M., and Heck A. J. R. (2010). Perturbation of the yeast N-acetyltransferase NatB induces elevation of protein phosphorylation levels. *BMC Genomics*, *11*, 685.

Hennekes, H., Peter, M., Weber, K., and Nigg, E. A. (1993). Phosphorylation on protein kinase C sites inhibits nuclear import of lamin B2. *J Cell Biol*, *120*, 1293-1304.

Henriksen, P., Wagner, S. A., Weinert, B. T., Sharma, S., Bacinskaja, G., Rehman, M., Juffer, A. H., Walther, T. C., Lisby, M., and Choudhary, C. (2012). Proteome-wide Analysis of Lysine Acetylation Suggests its Broad Regulatory Scope in *Saccharomyces cerevisiae*. *Mol Cell Proteomics*, *11*, 1510-1522.

Henzel, W. J., Billeci, T. M., Stults, J. T., and Wong, S. C. (1993). Identifying proteins from two-dimensional gels by molecular mass searching of peptide fragments in protein sequence databases. *Proc Natl Acad Sci USA*, *90*, 5011–5015.

Hoagland, M. B, Stephenson, M. L, Scott, J. F, Hecht, L. I, and Zamecnik, P. C. (1958). A soluble ribonucleic acid intermediate in protein synthesis. *J Biol Chem*, *231*, 241-257.

Hoffmeier, A., Betat, H., Bluschke, A., Günther, R., Junghanns, S., Hofmann, H. J., and Mörl, M. (2010). Unusual evolution of a catalytic core element in CCA-adding enzymes. *Nucleic Acids Res, 38*, 4436-4447.

Holm, L., and Sander, C. (1995). DNA polymerase β belongs to an ancient nucleotidyltransferase superfamily. *Trends Biochem Sci*, *20*, 345-347.

Hood, J. K., and Silver, P. A. (1998). Cse1p is required for export of Srp1p/importin-alpha from the nucleus in *Saccharomyces cerevisiae*. *J Biol Chem, 273*, 35142-6.

Hopper, A. K., and Huang, H-Y. (2015). Quality Control Pathways for Nucleus-Encoded Eukaryotic tRNA Biosynthesis and Subcellular Trafficking. *Mol Cell Biol, 35*, 2052-2058.

Hull, S., Malik, A. N. J., Arno, G., Mackay, D.S., *et al.* (2016). Expanding the phenotype of *TRNT1*-related immunodeficiency to include childhood cataract and inner retinal dysfunction. *JAMA Ophthalmol*, *134*, 1049-1053.

Hurt, J. K., Fitzpatrick, B. J., Norris-Drouin, J., and Zylka, M. J. (2012). Secretion and N-linked glycosylation are required for prostatic acid phosphatase catalytic and antinociceptive activity. *PLoS One*, *7*, e32741.

Hurto, R. L., Tong, A. H. Y., Boone, C., and Hopper, A. K. (2007). Inorganic Phosphate Deprivation Causes tRNA Nuclear Accumulation via Retrograde Transport in *Saccharomyces cerevisiae*. *Genetics*, *176*, 841–852.

Ishihara, K., Yamamoto, H., Mitsuhashi, K., Nishikawa, K., Tsuboi, S., Tsuji, H., and Nakajima, N. (2004). Purification and Characterization of α-Keto Amide Reductase from *Saccharomyces cerevisiae*. *Biosci Biotechnol Biochem*, *68*, 2306-2312.

James, P., Quadroni, M., Carafoli E., and Gonnet, G. (1993). Protein identification by mass profile fingerprinting. *Biochem Biophys Res Commun*, *195*, 58–64.

Jans, D. A., Ackermann, M. J., Bischoff, J. R., Beach, D. H., and Peters, R. (1991). p34cdc2-mediated phosphorylation at T124 inhibits nuclear import of SV-40 T antigen proteins. *J Cell Biol*, *115*, 1203-12.

Jfri, A., El-Helou, T., Watters, K. I., and Netchiporouk, E. (2019). Mucocutaneous Features of Congenital Sideroblastic Anemia Associated with B Cell Immunodeficiency, Periodic Fevers, and Developmental Delay (SIFD). *SAGE Open Med Case Rep*, 7, 2050313X19876710.

Johnson, A. W., Lund, E., and Dahlberg, J. (2002). Nuclear export of ribosomal subunits. *Trends Biochem Sci, 27*, 580-585.

Johnson, E. A., and Echavarri-Erasun, C. (2011). Yeast Biotechnology, in The Yeasts (*fourth edition)*, a Taxonomic Study, Elsevier B. V., Eds: Kurtzman, P. C., Fell, J. W., Boekhout, T. London. Chapter 3, pp. 21-44.

Josling, G. A., Selvarajah, S. A., Petter, M., and Duffy, M. F. (2012). The role of bromodomain proteins in regulating gene expression. *Genes*, *3*, 320–343.

Juhling, F., Morl, M., Hartmann, R. K., Sprinzl, M., Stadler, P. F., and Putz, J. (2009). tRNAdb 2009: compilation of tRNA sequences and tRNA genes. *Nucleic Acids Res*, *37*(database issue), D159-D162.

Jungfleisch, J., Nedialkova, D. D., Dotu, I., Sloan, K. E., *et al*. (2017). A novel translational control mechanism involving RNA structures within coding sequences. *Genome Res, 27*, 95–106.

Just, A., Butter, F., Trenkmann, M., Heitkam, T., Morl, M., and Betat, H. (2008). A comparative analysis of two conserved motifs in bacterial poly(A) polymerase and CCA-adding enzyme. *Nucleic Acids Res*, *36*, 5212–5220.

Kachroo, A. H., Laurent, J. M., Yellman, C. M., Meyer, A. G., Wilke, C. O., and Marcotte, E. M. (2015). Evolution. systematic humanization of yeast genes reveals conserved functions and genetic modularity. *Science, 348*, 921-925.

Kalderon, D., Roberts, B. L., Richardson, W. D., and Smith, A. E. (1984). A short amino acid sequence able to specify nuclear location. *Cell*, *39*, 499-509.

Kanerva, P. A., and Maenpaa, P. H. (1981). Codon-specific serine transfer ribonucleic acid degradation in avian liver during vitellogenin induction. *Acta Chem Scand B*, *35*, 379-385.

Karnahl, U., and Wasternack. (1992). Half-life of cytoplasmic rRNA and tRNA, of plastid rRNA and of uridine nucleotides in heterotrophically and photoorganotrophically grown cells of *Euglena gracilis* and its apoplastic mutant W3BUL. *Int J Biochem*, *24*, 493-497.

Kessler, B. M, and Edelmann, M. J. (2011). PTMs in conversation: activity and function of deubiquitinating enzymes regulated via post-translational modifications. *Cell Biochem Biophys*, *60*, 21–38.

Kessler, M. M., Henry, M. F., Shen, E., Zhao, J., Gross, S., Silver, P. A., and Moore, C. L. (1997). Hrp1, a sequence-specific RNA-binding protein that shuttles between the nucleus and the cytoplasm, is required for mRNA 3'-end formation in yeast. *Genes Dev*, *11*, 2545–2556.

Kim, D. F., and Green, R. (1999). Base-pairing between 23S rRNA and tRNA in the ribosomal A site. *Mol Cell*, *4*, 859–864.

Kohrer, K and Domdey, H. (1991). Preparation of high molecular weight RNA. *Methods in Enzymology, 194*, 398-405.

Kosova, B., Panté, N., Rollenhagen, C., and Hurt, E. (1999). Nup192p is a conserved nucleoporin with a preferential location at the inner site of the nuclear membrane. *J Biol Chem*, *274*, 22646-51.

Kotelawala, L., Grayhack, E. J., and Phizicky, E. M. (2008). Identification of yeast tRNA Um (44) 2'-O-methyltransferase (Trm44) and demonstration of a Trm44 role in sustaining levels of specific tRNA (Ser) species. *RNA*, *14*, 158-69.

Kramer, E. B., and Hopper, A. K. (2013). Retrograde transfer RNA nuclear import provides a new level of tRNA quality control in *Saccharomyces cerevisiae. Proc Natl Acad Sci USA*, *110*, 21042-21047.

Krogan, N., Cagney, G., Yu, H. Zhong, G., *et al.* (2006). Global landscape of protein complexes in the yeast *Saccharomyces cerevisiae*. *Nature*, *440*, 637–643.

Kuhn C-D., Wilusz J. E., Zheng Y., Beal, P. A., and Joshua-Tor, L. (2015). On enzyme refolding permits small RNA and tRNA surveillance by the CCA-adding enzyme. *Cell, 160*, 644-658.

Kumaki, E., Tanaka, K., Imai, K., Aoki-Nogami, Y., Ishiguro, A., Okada, S., Kanegane, H., Ishikawa, F., and Morio, T. (2019). Atypical SIFD with novel *TRNT1* mutations: A case study on the pathogenesis of B-cell deficiency. *Int J Hematol*. *109*, 382-389.

Kumar, S., Kim, Y. R., Vikram, A., Naqvi, A., *et al*. (2017). Sirtuin1-regulated lysine acetylation of p66Shc governs diabetes-induced vascular oxidative stress and endothelial dysfunction. *Proc Natl Acad Sci USA*, *114*, 1714–1719.

Künzler, M., and Hurt, E. C. (1999). Cselp functions as the nuclear export receptor for importin α in yeast. *FEBS Lett*, *433*, 185-190.

Lai, L. B., Vioque, A., Kirsebom, L. A. and Gopalan, V. (2010). Unexpected diversity of RNase P, an ancient tRNA processing enzyme: challenges and prospects. *FEBS Lett*, *584*, 287–296.

Lamberti, G., Gügel, I. L., Meurer, J., Soll, J., and Schwenkert, S. (2011). The cytosolic kinases STY8, STY17, and STY46 are involved in chloroplast differentiation in Arabidopsis. *Plant Physiol*, *157*, 70–85.

Lanford, R. E., and Butel, J. S. (1984). Construction and characterization of an SV40 mutant defective in nuclear transport of T antigen. *Cell*, *37*, 801-13.

Lari, A., Rajan, A. A. N., Sandhu, R., Reiter, T., Montpetit, R., Young, B.P., Loewen, C. J. R., and Montpetit, B. (2019). A nuclear role for the DEAD-box protein Dbp5 in tRNA export. *eLife*. doi: https://doi.org/10.7554/eLife.48410.

Larsen, M. R., and Roepstorff, P. (2000). Mass spectrometric identification of proteins and characterization of their post-translational modifications in proteome analysis. *Fresenius J Anal Chem, 366*, 677–690.

Lavova, B., Urminska, D., Sillerova, S. (2014). Diauxic growth of *Saccharomyces cerevisiae. JMBFS, 3,* 122-123.

Leach, M. D., and Brown, A. J. P. (2012). Posttranslational Modifications of Proteins in the Pathobiology of Medically Relevant Fungi. *Eukaryot Cell, 11*, 98–108.

Lee, J., O'Neill, R. C., Park, M. W., Gravel, M., and Braun, P. E. (2006). Mitochondrial localization of CNP2 is regulated by phosphorylation of the N-terminal targeting signal by PKC: Implications of a mitochondrial function for CNP2 in glial and non-glial cells. *Mol Cell Neurosci*, *31*, 446-462.

Leeds, N. B., Small, E. C., Hiley, S. L., Hughes, T. R., and Staley, J. P. (2006). The splicing factor Prp43p, a DEAH box ATPase, functions in ribosome biogenesis. *Mol Cell Biol*, *26*, 513-522.

Leibovitch, M., Bublak, D., Hanic-Joyce, P. J., Tillmann, B., Flinner, N., Amsel, D., and Schleiff, E. (2013). The folding capacity of the mature domain of the dual-targeted plant tRNA nucleotidyltransferase influences organelle selection. *Biochem J*, *453*, 401–412.

Leibovitch, M., Hanic-Joyce, P. J., and Joyce, P. B. M. (2018). *In vitro* studies of disease-linked variants of human tRNA nucleotidyltransferase reveal decreased thermal stability and altered catalytic activity. *Biochim Biophys Acta- Proteins and Proteomics, 1866*, 527-540.

Leibovitch, M., Reid, N. E., Victoria, J, Hanic-Joyce, P.J., and Joyce, P. B. M. (2019). Analysis of the pathogenic I326T variant of human tRNA nucleotidyltransferase reveals reduced catalytic activity and thermal stability *in vitro* linked to a conformational change. *Biochim Biophys Acta-Proteins and Proteomics*, *1867*, 616-626.

Leibovitch. (2016). Exploring the interplay of structure, stability, activity and localization in tRNA nucleotidyltransferase function. PhD thesis, Chemistry and Biochemistry, Concordia University.

Li, F., Xiong, Y., Wang, J., Cho, H. D., Tomita, K., Weiner, A. M., and Steitz, T. A. (2002). Crystal structures of the *Bacillus stearothermophilus* CCA-adding enzyme and its complexes with ATP or CTP. *Cell*, *111*, 815-824.

Li, X., Foley, E. A., Kawashima, S. A., Molloy, K. R., Li. Y., Chait, B. T., and Kapoor, T. M. (2012). Examining post-translational modification-mediated protein-protein interactions using a chemical proteomics approach. *Protein Sci*, *22*, 287–295.

Lim, M.Y., Dailey, D., Martin, G. S., and Thorner, J. (1993). Yeast *MCK1* protein kinase autophosphorylates at tyrosine and serine but phosphorylates exogenous substrates at serine and threonine. *J Biol Chem*, *268*, 21155-21164.

Lin, S., (2008). Expression and purification of fusion-tag proteins. Adapted from AEG-0095.3. *AEGERA*.

Lipowsky, G., Bischoff, F. R, Izaurralde, E., Kutay, U., Schafer, S., Gross, H. J., Beier, H., and Gorlich, D. (1999). Coordination of tRNA nuclear export with processing of tRNA. *RNA*, *5*, 539-549.

Liu, J. C., Liu, M., and Horowitz, J. (1998). Recognition of the universally conserved 3'-CCA end of tRNA by elongation factor EF-Tu. *RNA*, *4*, 639-646.

Lizano, E., Scheibe, M., Rammelt, C., Betat, H., and Mörl, M. (2008). A comparative analysis of CCA-adding enzymes from human and *E. coli*: differences in CCA addition and tRNA 3′-end repair. *Biochimie*, *90*, 762–772.

Lougaris, V., Chou, J., Baronio, M., *et al*. (2018). Novel biallelic TRNT1 mutations resulting in sideroblastic anemia, combined B and T cell defects, hypogammaglobulinemia, recurrent infections, hypertrophic cardiomyopathy and developmental delay. *Clin Immunol*, *188*, 20–22.

Lund, E., and Dahlberg, J. E. (1998). Proofreading and aminoacylation of tRNAs before export from the nucleus. *Science, 282*, 2082-2085.

Lygerou, Z., Conesa, C., Lesage, P., Swanson, R. N., *et al*. (1994). The yeast *BDF1* gene encodes a transcription factor involved in the expression of a broad class of genes including snRNAs. *Nucleic Acids Res*, *22*, 5332–5340.

Madeira, F., Park, Y. M., Lee, J., Buso, N., *et al*. (2019). The EMBL-EBI search and sequence analysis tools APIs in 2019. *Nucleic Acids Res*, *47*, W636-W641.

Mann, M., Hojrup, P., and Roepstorff, P. (1993). Use of mass spectrometric molecular weight information to identify proteins in sequence databases. *Biol Mass Spectrom*, *22,* 338–345.

Martin, N. C., and Hopper A. K., (1994). How single genes provide tRNA processing enzymes to mitochondria, nuclei and cytosol. *Biochimie, 76*, 1161-1167.

Martin, G. and Keller, W. (2007). RNA-specific ribonucleotidyl transferases. *RNA*, *13*, 1834-1849.

Martinez-Gil, L., Vera-Velasco, N. M., and Mingarro, I. (2017). Exploring the Human-Nipah Virus Protein-Protein Interactome. *J Virol*, *91*. pii: e01461-17.

Maurer, P., Redd, M., Solsbacher, J., Bischoff, F. R., *et al*. (2001). The nuclear export receptor Xpo1p forms distinct complexes with NES transport substrates and the yeast Ran binding protein 1 (Yrb1p). *Mol Biol Cell*, *12*, 539–549.

McGann, R.G, and Deutscher M.P. (1980). Purification and characterization of a mutant tRNA nucleotidyltransferase. *Eur J Biochem*, *106*, 321–328.

McGuire, A. T., and Mangroo, D. (2007). Cex1p is a novel cytoplasmic component of the *Saccharomyces cerevisiae* nuclear tRNA export machinery. *EMBO J*, *26*, 288–300.

Melton, D. A., De Robertis, E. M., and Cortese, R. (1980). Order and intracellular location of the events involved in the maturation of a spliced tRNA, *Nature*, *284*, 143-8.

Mitchell, S. F., Jain, S., She, M., and Parker, R. (2013). Global analysis of yeast mRNPs. *Nat Struct Mol Biol*, *20*, 127–133.

Mól, A. R., Castro, M, S. and Fontes, W. NetWheels: A web application to create high quality peptide helical wheel and net projections. bioRxiv 416347; doi: https://doi.org/10.1101/416347 (preprint).

Moll, T., Tebb, G., Surana, U., Robitsch, H., and Nasmyth, K. (1991). The role of phosphorylation and the CDC28 protein kinase in cell cycle-regulated nuclear import of the *S. cerevisiae* transcription factor *SW15*. *Cell, 66*, 743-758.

Moore, K. E., Carlson, S. M., Camp, N. D., Cheung, P., James, R. G., Chua, K. F., Wolf-Yadlin, A., and Gozani, O. (2013). A General Molecular Affinity Strategy for Global Detection and Proteomic Analysis of Lysine Methylation. *Mol Cell*, *50*, 444–456.

Mortimer, R. K., and Schild, D. (1980). Genetic Map of *Saccharomyces cerevisiae*. *Microbiol Rev*, *44*, 519-571.

Mumberg, D., Müller, R., and Funk, M. (1995). Yeast vectors for the controlled expression of heterologous proteins in different genetic backgrounds. *Gene*, *156*, 119-22.

Nagaike, T., Suzuki, T., Tomari, Y., Takemoto-Hori, C., Negayama, F., Watanabe, K., and Ueda, T. (2001). Identification and characterization of mammalian mitochondrial tRNA nucleotidyltransferases. *J Biol Chem*, *276*, 40041-40049.

Nardozzi, J. D., Lott, K., and Cingolani, G. (2010). Phosphorylation meets nuclear import: a review. *Cell Commun Signal, 8*. doi: 10.1186/1478-811X-8-32.

Narita, T., Weinert, B. T., and Choudhary, C. (2019). Functions and mechanisms of non-histone protein acetylation. *Nat Review Mol Cell Biol*, *20*, 156-174.

Nasmyth, K., Adolf, G., Lydall, D., and Seddon, A. (1990). The identification of a second cell cycle control on the *HO* promoter in yeast: Cell cycle regulation of *SWI5* nuclear entry. *Cell*, *62*(4), 631-647.

Neuenfeldt, A., Just, A., Betat, H., and Mörl, M. (2008). Evolution of tRNA nucleotidyltransferases: A small deletion generated CC-adding enzymes. *Proc Natl Acad Sci USA*, *105*, 7953-7958.

Nwagwu, M., and Nana, M. (1980). Ribonucleic acid synthesis in embryonic chick muscle, rates of synthesis and half-lives of transfer and ribosomal RNA species. *J Embryol Exp Morphol*, *56*, 253-267.

Pappin, D. J. C., Hojrup, P., and Bleasby A. J. (1993). Rapid identification of proteins by peptide-mass fingerprinting. *Curr Biol*, *3*, 327– 332.

Parker, C. E., Mocanu, V., Mocanu, M., Dicheva, N., and Warren, M.R. (2010). Mass Spectrometry for Post-Translational Modifications. In: Alzate O, editor. *Neuroproteomics*. Boca Raton (FL): CRC Press/Taylor & Francis. Chapter 6.
https://www.ncbi.nlm.nih.gov/books/NBK56012/

Pasteur, L., Constable, R. D., tr, Faulkner, F., tr (1879). Studies on fermentation: the diseases of beer, their causes, and the means of preventing them. MacMillan & Co., London.

Peltz, S. W., Donahue, J. L., and Jacobson, A. (1992). A mutation in the tRNA nucleotidyltransferase gene promotes stabilization of mRNAs in *Saccharomyces cerevisiae*. *Mol Cell Biol*, *12*, 5778–5784.

Petfalski, E., Dandekar, T., Henry, Y., and Tollervey, D. (1998). Processing of the precursors to small nucleolar RNAs and rRNAs requires common components. *Mol Cell Biol*, *18*, 1181–1189.

Ptacek, J., Devgan, G., Michaud, G. *et al.* (2005). Global analysis of protein phosphorylation in yeast. *Nature, 438*, 679–684.

Rahman, M. S. (2017). Biophysical and biochemical characterization of yeast tRNA nucleotidyltransferase variants. Master's thesis, Chemistry and Biochemistry, Concordia University.

Reichert, A. S., Thurlow, D. L. and Morl, M. (2001). A eubacterial origin for the human tRNA nucleotidyltransferase? *Biol Chem*, *382*, 1431-1438.

Reid, N. E., Ngou, J. S., Joyce, P. B. M. (2019). *Schizosaccharomyces pombe* contains separate CC- and A-adding tRNA nucleotidyltransferases. *Biochem Biophys Res Commun, 508*, 785-790.

Rihs, H. P., Jans, D. A., Fan, H., and Peters, R. (1991). The rate of nuclear cytoplasmic protein transport is determined by the casein kinase II site flanking the nuclear localization sequence of the SV40 T-antigen. *EMBO J*, *10*, 633-639.

Rogers, L.D., and Overall, C.M. (2013). Proteolytic Post-translational Modification of Proteins: Proteomic Tools and Methodology. *Mol Cell Proteomics*, *12*, 3532–3542.

Rosset, R., and Monier, R. (1965). Instability of the terminal 3′-hydroxy sequence of transfer RNA in microorganisms. I. Turnover of terminal AMP in *Saccharomyces cerevisiae. Biochem Biophys Acta*. *108*, 376-384.

Ryan, K. J., McCaffery, J. M., and Wente, S. R. (2003). The Ran GTPase cycle is required for yeast nuclear pore complex assembly. *J Cell Biol*, *160*, 1041–1053.

Saini, P., Eyler, D. E., Green, R., and Dever, T. E. (2009). Hypusine-containing protein eIF5A promotes translation elongation. *Nature*, *459*, 118–121.

Sambrook, J., Maniatis, T., and Fritch, E. F. (1989). Molecular Cloning (2nd ed.). Cold Spring Harbor Laboratory Press.

Sarkar, S., Azad, A.K., and Hopper, A. K. (1999). Nuclear tRNA aminoacylation and its role in nuclear export of endogenous tRNAs in *Saccharomyces cerevisiae*. *Proc Natl Acad Sci USA, 96*, 14366-14371.

Sasarman, F., Thiffault, I., Weraarpachai, W., Salomon, S., *et al*. (2015). The 3′ addition of CCA to mitochondrial $tRNA^{Ser}$ (AGY) is specifically impaired in patients with mutations in the tRNA nucleotidyl transferase *TRNT1*. *Hum Mol Genet*, *24*(10), 2841–2847.

Schindelin, J., Arganda-Carreras, I., and Frise, E. *et al*. (2012), "Fiji: an open-source platform for biological-image analysis", *Nat Methods, 9*, 676-682.

Schmidt von Braun, S., Sabetti, A., Hanic-Joyce, P. J., Gu, J., Schleiff, E., and Joyce, P. B. M. (2007). Dual targeting of the tRNA nucleotidyltransfrase in plants: not just the signal. *J Exp Bot*, *58*, 4083-4093.

Schmidt, O., Harbauer, A. B., Rao, S., Eyrich, B., Zahedi, R. P., Stojanovski, D., Schonfisch, B., Guiard, B., Sickmann, A., Pfanner, N., and Meisinger, C. (2011). Regulation of mitochondrial protein import by cytosolic kinases. *Cell*, *144*, 227-239.

Schmidt, O., Pfanner, N., and Meisinger, C. (2010). Mitochondrial protein import: from proteomics to functional mechanisms. *Nat Rev Mol Cell Biol, 11*, 655-67.

Schrödinger. The PyMol molecular graphics system. Version 2.3.2, LLC.

Schwenzer, H., Jühling, F., Chu, A., Pallett, L. J., Baumert, T. F., Maini, M., and Fassati, A. (2019). Oxidative stress triggers selective tRNA retrograde transport in human cells during the integrated stress response. *Cell Rep*, *26*, 3416–3428.e5.

Segref, A., Sharma, K., Doye, V., Hellwig, A., Huber, J., Lührmann, R., and Hurt, E. (1997). Mex67p, a novel factor for nuclear mRNA export, binds to both poly(A)+ RNA and nuclear pores. *EMBO J*, *16*, 3256–3271.

Shaheen, H. H., Horetsky, R. L., Kimball, S. R., Murthi, A., Jefferson, L. S., and Hopper, A. K. (2007). Retrograde nuclear accumulation of cytoplasmic tRNA in rat hepatoma cells in response to amino acid deprivation. *Proc Natl Acad Sci USA*, *104*, 8845– 8850.

Shaheen, H. H., and Hopper, A. K. (2005). Retrograde movement of tRNAs from the cytoplasm to the nucleus in *Saccharomyces cerevisiae*. *Proc Natl Acad Sci USA*, *102*, 11290-11295.

Shan, X., Russell, T. A., Paul, S. M., Kushner, D. B., and Joyce, P. B. M. (2008). Characterization of a temperature-sensitive mutation that impairs the function of yeast tRNA nucleotidyltransferase. *Yeast*, *25*, 219–233.

Shanmugam, K., Hanic-Joyce, P., and Joyce, P. B. M. (1996). Purification and characterization of a tRNA nucleotidyltransferase from *Lupinus albus* and functional complementation of a yeast mutation by the corresponding cDNA. *Plant Mol Biol*, *30*, 281-295.

Sharma, U., and Rando, J. R. (2017). Metabolic Inputs into the Epigenome. *Cell Metab*, *25*, 544-558.

Shuai, K., Horvath, C. M., Huang, L. H., Qureshi, S. A., Cowburn, D., and Darnell, J. E. Jr. (1994). Interferon activation of the transcription factor Stat91 involves dimerization through SH2-phosphotyrosyl peptide interactions. *Cell*, *76*, 821-828.

Shulga, N., and Goldfarb, D. S. (2003). Binding dynamics of structural nucleoporins govern nuclear pore complex permeability and may mediate channel gating. *Mol Cell Biol, 23*, 534–542.

Simonovic, M., and Steitz, T. A. (2008). Peptidyl-CCA deacylation on the ribosome promoted by induced fit and the O3'-hydroxyl group of A76 of the unacylated A-site tRNA. *RNA*, *14*, 2372-2378.

Soniat, M., and Chook, Y. M. (2015). Nuclear localization signals for four distinct karyopherin-β nuclear import systems. *Biochem J*, *468*, 353-362.

Soufi, B., Kelstrup, C. D., Stoehr, G., Frohlich, F., Waltherd, T. C and Olsen, J. V. (2009). Global analysis of the yeast osmotic stress response by quantitative proteomics. *Mol BioSyst*, *5*, 1337–1346.

Sprinzl, M., and Cramer, F. (1979). The -C-C-A end of tRNA and its role in protein biosynthesis. *Mol Biol*, *22*, 1-69.

Steiner-Mosonyi, M., and Mangroo, D. (2004). The nuclear tRNA aminoacylation-dependent pathway may be the principal route used to export tRNA from the nucleus in *Saccharomyces cerevisiae*. *Biochem J*, *378*, 809–816.

Steitz, T. A. (1998). A mechanism for all polymerases. *Nature*, *391*, 231–232.

Strub, B. R., Eswara, M. B. K., Pierce, J. B., and Mangroo, D. (2007). Utp8p Is a Nucleolar tRNA-binding protein that forms a complex with components of the nuclear tRNA export machinery in *Saccharomyces cerevisiae*. *Mol Biol Cell*, *18*, 3845–3859.

Sun, C., and Woolford, J. L., Jr. (1994). The yeast *NOP4* gene product is an essential nucleolar protein required for pre-rRNA processing and accumulation of 60S ribosomal subunits. *EMBO J*, *13*, 3127–3135.

Takano, A., Endo, T., and Yoshihisa, T. (2005). tRNA actively shuttles between the nucleus and cytosol in yeast. *Science*, *309*, 140–142.

Tatara, Y., Terakawa, T., and Uchida, T. (2010). Identification of Pin1-Binding Phosphorylated Proteins in the Mouse Brain. *Biosci Biotechnol Biochem*, *74*, 2480–2483.

Taylor, B. V., McNeil, J. B., McIntosh, E. M., Zhang, F. R., and Bognar, A. L. (1993). Cloning of the genes encoding the serine hydroxymethyltransferases from *Saccharomyces cerevisiae*. *Adv Exp Med Biol*, *338*, 711-4.

Tkach, J. M., Yimit, A., Lee, A. Y., *et al*. (2012). Dissecting DNA damage response pathways by analysing protein localization and abundance changes during DNA replication stress. *Nat Cell Biol*, *14*, 966–976.

Thermo Proteome Discoverer User Guide Software Version 2.2_XCALI-97808. (2017), pp. 12.

Toh, Y., Takeshita, D., Numata, T., Fukai, S., Nureki, O., and Tomita, K. (2009). Mechanism for the definition of elongation and termination by the class II CCA-adding enzyme. *EMBO J*, *28*, 3353-3365.

Tomita, K., and Weiner, A. M. (2001). Collaboration between CC- and A-adding enzymes to build and repair the 3'-terminal CCA of tRNA in *Aquifex aeolicus*. *Science, 294*, 1334-1336.

Tomita, K., and Yamashita, S. (2014). Molecular mechanisms of template-independent RNA polymerization by tRNA nucleotidyltransferases. *Front Genet*, *5*, 36.
doi: 10.3389/fgene.2014.00036.

Tomita, K., Fukai, S., Ishitani, R., Ueda, T., Takeuchi, N., Vassylyev, D. G., and Nureki, O. (2004). Structural basis for template-independent RNA polymerization. *Nature*, *430*, 700–704.

Tomita, K., Ishitani, R., Fukai S., and Nureki, O. (2006). Complete crystallographic analysis of the dynamics of CCA sequence addition. *Nature*, *443*, 956–960.

Trautwein, M., Dengjel, J., Schirle, M., and Spang, A. (2004). Arf1p provides an unexpected link between COPI vesicles and mRNA in *Saccharomyces cerevisiae*. *Mol Biol Cell*, *15*, 5021–5037.

Using Multistage Activation in an Ion Trap Mass Spectrometer. Product support bulletin 122. Thermo scientific. p1-2. Available from: www.thermo.com/ms

Vasylkovska, R., Petriv, N., and Semchyshyn, H. (2015). Carbon sources for yeast growth as a precondition of hydrogen peroxide induced hormetic phenotype. *Int J Microbiol*, *2015*, 697813.
doi:10.1155/2015/697813.

Ventura, M., Mateo, F., Serratosa, J., Salaet, I., Carujo, S., Bachs, O., *et al*. (2010). Nuclear translocation of glyceraldehyde-3-phosphate dehydrogenase is regulated by acetylation. *Int J Biochem Cell Biol*, *42*, 1672–80.

Vörtler, S., and Mörl, M. (2010). tRNA nucleotidyltransferases: Highly unusual RNA polymerases with vital functions. *FEBS Lett*, *584*, 297-302.

Waegemann, K., and Soll, J. (1996). Phosphorylation of the transit sequence of chloroplast precursor proteins. *J Biol Chem*, *271*, 6545-6554.

Walker, J. M., ed. (2002). The Protein Protocols Handbook (2nd edition.), Humana Press. Chapter 11, pp. 61-67.

Watanabe, S., Radman-Livaja, M., Rando, O.J., and Peterson, C. L. (2013). A histone acetylation switch regulates H2A.Z deposition by the SWR-C remodeling enzyme. *Science*, *340*, 195-9.

Waterhouse, A., Bertoni, M., Bienert, S., Studer, G., *et al*. (2018). SWISS-MODEL: homology modelling of protein structures and complexes. *Nucleic Acids Res*, *46*(W1), W296-W303.

Wedatilake, Y., Niazi, R., Fassone, E., Powell, C. A., Pearce, S., Plagnol, V., Saldanha, J. W., Kleta, R., Chong, W. K., Footitt, E., *et al.* (2016). *TRNT1* deficiency: Clinical, biochemical and molecular genetic features. *Orphanet J Rare Dis*, *11*, 90. doi: 10.1186/s13023-016-0477-0.

Wellner, K., Betat, H., and Mörl. M. (2018). A tRNA's fate is decided at its 3′ end: Collaborative actions of CCA-adding enzyme and RNases involved in tRNA processing and degradation. *Biochim Biophy Acta Gene Regul Mech*, *1861*, 433-441.

Wenta, N., Strauss, H., Meyer, S and Vinkemeier, U. (2008). Tyrosine phosphorylation regulates the partitioning of STAT1 between different dimer conformations. *Proc Natl Acad Sci USA*, *105*, 9238–924.

Whipple, J. M., Lane, E. A., Chernyakov, I., D'Silva, S., and Phizicky, E. M. (2011). The yeast rapid tRNA decay pathway primarily monitors the structural integrity of the acceptor and T-stems of mature tRNA. *Genes Dev, 25*, 1173– 1184.

Whitney, M. L., Hurto, R. L., Shaheen, H. H., and Hopper, A. K. (2007). Rapid reversible nuclear accumulation of cytoplasmic tRNA in response to nutrient availability. *Mol Biol Cell*, *18*, 2678–2686.

Willmund, F., del Alamo, M., Pechmann, S., Chen, T., *et al*. (2013). The cotranslational function of ribosome-associated Hsp70 in eukaryotic protein homeostasis. *Cell*, *152*. 196–209.

Wilusz, J. E., Whipple, J. M., Phizicky, E. M., and Sharp, P. A. (2011). tRNAs marked with CCACCA are targeted for degradation. *Science*, *334*, 817-821.

Wiseman, D. H., May, A., Jolles, S., Connor, P., *et al.* 2013. A novel syndrome of congenital sideroblastic anemia, B-cell immunodeficiency, periodic fevers, and developmental delay (SIFD). *Blood*. *122*, 112–123.

Wolfe, C. L., Lou, Y-C., Hopper, A. K., and Martin, N. C. (1994). Interplay of heterogeneous transcriptional start sites and translational selection of AUGs dictate the production of mitochondrial and cytosolic/nuclear tRNA nucleotidyltransferase from the same gene in yeast. *J Biol Chem*, *269*, 13361-6.

Wolfe, C.L., Hopper, A. K., and Martin, N. C. 1996. Mechanisms leading to and the consequences of altering the normal distribution of ATP(CTP): tRNA nucleotidyltransferase. *J Biol Chem*, *271*, 4679-4686.

Wong, C., Sridhara, S., Bardwell, J. C., and Jakob, U. (2000). Heating greatly speeds Coomassie blue staining and destaining. *Biotechniques*, *28*, 426–8, 430, 432.

Wu, J., Bao, A., Chatterjee, K., Wan, Y., and Hopper, A. K. (2015). Genome-wide screen uncovers novel pathways for tRNA processing and nuclear-cytoplasmic dynamics. *Genes Dev*, *29*, 2633-2644.

Xin, F., and Radivojac, P. (2012). Post-translational modifications induce significant yet not extreme changes to protein structure. *Bioinformatics*, *28*, 2905-13.

Xiong, Y., Li, F., Wange, J., Weiner, A. M., and Steitz, A. (2003). Crystal Structures of an Archaeal Class I CCA-Adding Enzyme and Its Nucleotide Complexes. *Mol Cell*, *12*, 1165–1172.

Xiong, Y., and Steitz, T. A. (2006). A story with a good ending: tRNA 3′-end maturation by CCA-adding enzymes. *Curr Opin Struct Biol*, *16*, 12–17.

Yogev, O., Naamati, A. and Pines, O. (2011). Fumarase: a paradigm of dual targeting and dual localizedfunctions. *FEBS J*, *278*, 4230-4242.

Yue, D., Maizels, N., and Weiner, A. M. (1996). CCA-adding enzymes and poly(A) polymerases are all members of the same nucleotidyltransferase superfamily: characterization of the CCA-adding enzyme from the archaeal hyperthermophile *Sulfolobus shibatae*. *RNA*, *2*, 895–908.

Zhang, W., Morris, Q. D., Chang, R., Shai, O., *et al*. (2004). The functional landscape of mouse gene expression. *J Biol*, *3*, 21. doi: 10.1186/jbiol16.

Zhao, L-J., Subramanian, T., Zhou, Y., and Chinnadurai, G. (2006). Acetylation by p300 regulates nuclear localization and function of the transcriptional corepressor CtBP2. *J Biol Chem*, *281*, 4183–9.

Zhao, Z., Su, W., Yuan, S. and Huang, Y. (2009). Functional conservation of tRNase ZL among *Saccharomyces cerevisiae*, *Schizosaccharomyces pombe* and humans. *Biochem J, 422*, 483–492.

Zhu, L., Cudny, H., Deutscher, and M. P. (1986). A mutation in *Escherichia coli* tRNA nucleotidyltransferase that affects only AMP incorporation is in a sequence often associated with nucleotide-binding proteins. *J Biol Chem*, *261*, 14875–14877.

Zhu, L., and Deutscher, M. P. (1987). tRNA nucleotidyltransferase is not essential for *Escherichia coli* viability. *EMBO J*, *6*, 2473-2477.

7. APPENDICES

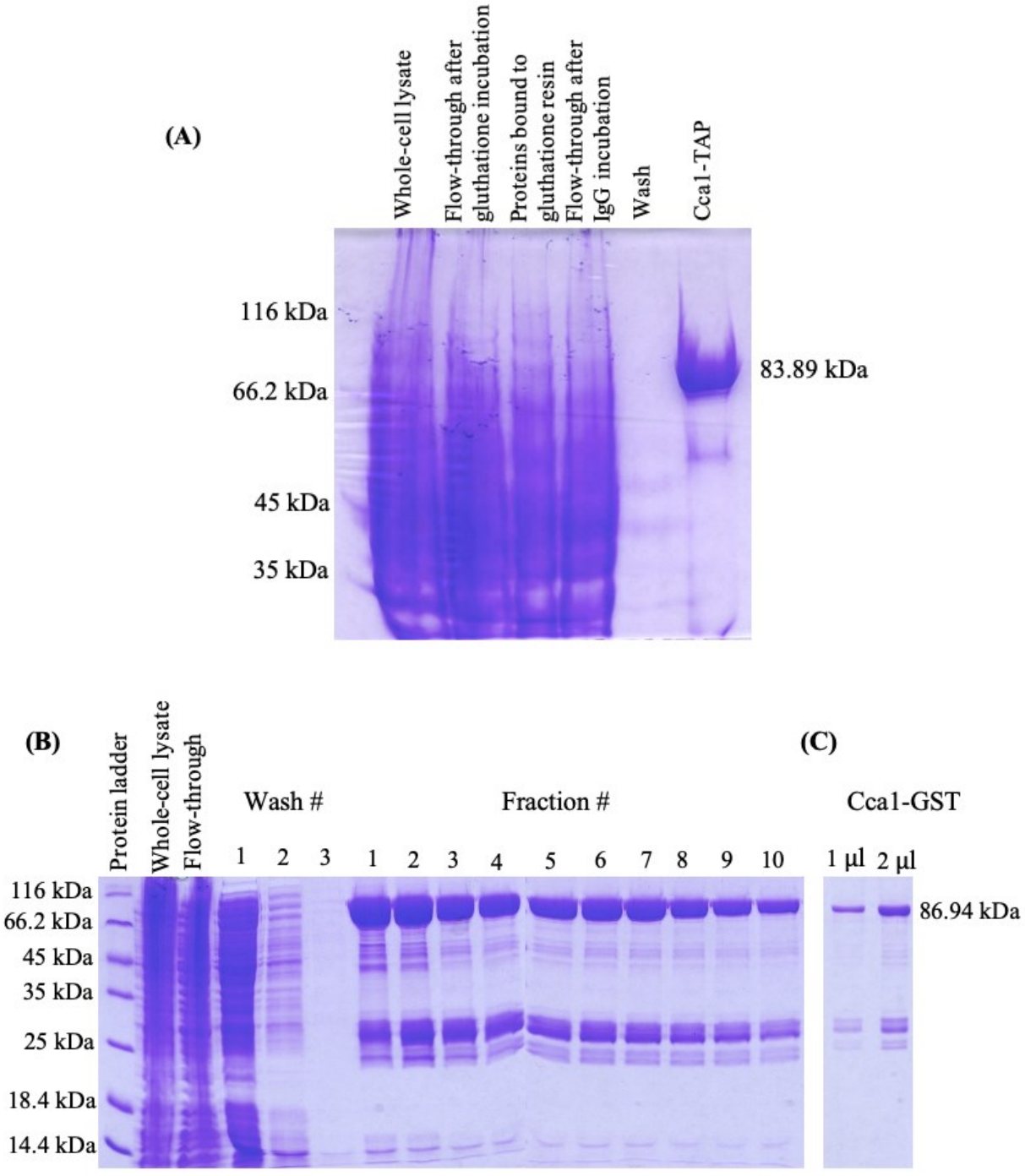

Appendix 1: Purified proteins used in this study. (A) Cca1-TAP overexpressed in yeast cells grown on glucose to the OD_{600} of 1.0 (replicate 1). (B) Cca1-GST recombinant protein purified from *E. coli*. (C) Fractions 1-10 after pooling and dialysis.

Appendix 2: Proteins interacting with Cca1 detected in the *in vitro* GST pull-down study with (A) 1:10, (B) 1:20 and (C) 1:100 bait:prey ratios (10 µg of bait used). Proteins previously identified as being involved in tRNA biogenesis or as physically interacting with Cca1 have been bolded while proteins reported as interacting with Cca1 through genetic screens are italicized.

(A)

	Gene name	Protein name	Number of unique peptides	Sequence coverage (%)
Transport Proteins	*ARF1*	ADP-ribosylation factor 1	1	8
	SAR1	Small COPII coat GTPase	1	6
	SEC4	Ras-related protein	1	7
Ribosome biogenesis	*RPS14B*	40S ribosomal protein S14-B	1	9
	RPL11A	60S ribosomal protein L11-A	1	8
	RPS5	40S ribosomal protein S5	1	7
Transferase	*DPM1*	dolichol-phosphate mannosyltransferase	1	5
	SHM2	Serine hydroxymethyl-transferase, cytosolic	1	3
Other proteins	*PNC1*	Nicotinamidase	1	9
	GPP2	Glycerol-1-phosphate phosphohydrolase 2	1	6
	DED1	ATP-dependent RNA helicase	1	5
	GVP36	Golgi Vesicle Protein 36	1	3

(B)

	Gene name	Protein name	Number of unique peptides	Sequence coverage (%)
Transport Proteins	*CYC1*	Cytochrome c iso-1	2	16
	COG1	conserved oligomeric Golgi complex subunit 1	1	3
Transferase	*ARO8*	Aromatic/aminoadipate aminotransferase 1	2	5
	SHM1	Serine hydroxymethyl-transferase, mitochondrial	1	3

Amino-acid biosynthesis	*EFB1*	Elongation factor 1-beta	1	5
	BAT1	Branched-chain-amino-acid aminotransferase, mitochondrial	1	2
Other proteins	*DDP1*	Diphosphoinositol polyphosphate phosphohydrolase	2	15
	GRX5	Monothiol glutaredoxin-5, mitochondrial	1	10
	GPP2	Glycerol-1-phosphate phosphohydrolase 2	1	6
	RPS31	Ubiquitin-40S ribosomal protein S31	1	6
	YSA1	ADP-ribose pyrophosphatase	1	5
	MCM4	DNA replication licensing factor MCM4	1	4
	GRP78	78 kDa glucose-regulated protein homolog	1	3
	GND2	6-phosphogluconate dehydrogenase, decarboxylating 2	1	2

(C)

	Gene name	**Protein name**	**Number of unique peptides**	**Sequence coverage (%)**
Transport proteins	*PHO88*	SRP-independent targeting protein 3	2	15
	DID2	vacuolar protein-sorting-associated protein 46	1	7
	VPS21	Vacuolar protein sorting-associated protein 21	1	7
	YPT7	GTP-binding protein ypt7	1	6
	GSP2	GTP-binding nuclear protein GSP2/CNR2	1	5
	MEX67	**mRNA export factor**	**1**	**3**
Ribosome biogenesis	*RPL25*	60S ribosomal protein L25	1	9
	NOP56	Nucleolar protein 56	1	2
	RRP12	Ribosomal RNA-processing protein 12	1	1
Transferasee	*MCK1*	protein kinase MCK1	2	8
	APT1	Adenine phosphoribosyl-transferase 1	1	7
	NAT2	Putative N-terminal acetyltransferase 2	1	5

	LCB1	serine palmitoyltransferase 1	1	3
Other proteins	*PWP1*	Periodic tryptophan protein 1	2	6
	MSC7	Putative aldehyde dehydrogenase-like protein YHR039C	2	3
	NCP1	NADPH--cytochrome P450 reductase	2	3
	TOP1	DNA topoisomerase 1	2	3
	NHP6B	Non-histone chromosomal protein 6B	1	13
	GPP2	Glycerol-1-phosphate phosphohydrolase 2	1	6
	YDL124W	NADPH-dependent alpha-keto amide reductase	1	4
	NDI1	Rotenone-insensitive NADH-ubiquinone oxidoreductase, mitochondrial	1	2
	PRP43	**pre-mRNA-splicing factor ATP-dependent RNA helicase PRP43**	**1**	**2**
	MET10	**sulfite reductase [NADPH] flavoprotein component**	**1**	**1**
	EMW1	Essential for maintenance of the cell wall protein 1	1	1
	RAD26	DNA repair and recombination protein RAD26	1	1
	UBA1	ubiquitin-activating enzyme E1 1	1	1

Appendix 3: Proteins interacting with Cca1 reproduced in two or all biological replicates from yeast cells grown on glucose to OD_{600} of 1.0. Proteins previously identified as being involved in tRNA biogenesis or as physically interacting with Cca1 have been bolded while proteins reported as interacting with Cca1 through genetic screens are italicized.

	Gene name	Protein name	Number of unique peptides	Sequence coverage (%)
Amino-acid/protein biosynthesis	*YNL247W*	Cysteine-tRNA ligase	27, 8	45, 13
	VAS1	Valine-tRNA ligase, mitochondrial	18, 1	21, 1
	KRS1	lysine-tRNA ligase, cytoplasmic	10, 17, 8	22, 37, 18
	MET6	5-methyltetrahydropteroyl-triglutamate-homocysteine methyltransferase	2, 7, 17	4, 13, 28
	DPS1	Aspartate-tRNA ligase, cytoplasmic	2, 15, 9	6, 32, 20
	THS1	**Threonine-tRNA ligase, cytoplasmic**	**9, 12, 14**	**15, 22, 23**
	ADE3	C-1-tetrahydrofolate synthase, cytoplasmic	14, 2	21, 2
	CDC60	**Leucine-tRNA ligase, cytoplasmic**	**14, 1**	**20, 1**
	DED81	Asparagine-tRNA ligase, cytoplasmic	2, 4, 9	6, 10, 9
	GUS1	*Glutamate-tRNA ligase, cytoplasmic*	*3, 2, 9*	*5, 4, 15*
	BAT1	Branched-chain-amino-acid aminotransferase, mitochondrial	1, 5	3, 18
	AIM10	Probable proline--tRNA ligase, mitochondrial	1, 2, 1	3, 6, 3
	TRP5	Tryptophan synthase	1, 2	2, 5
	MET17	Homocysteine/cysteine synthase	1, 1	3, 3
	ASN1	Asparagine synthetase [glutamine-hydrolyzing] 1	1, 1	2, 2
	LYS4	Homoaconitase, mitochondrial	1, 1	1, 2
	HYP2	**Eukaryotic translation initiation factor 5A-1**	**1, 1, 1**	**11, 11, 11**
Transport protein	*PMA1*	plasma membrane ATPase 1	8, 9, 12	10, 9,14
	SEC18	vesicular-fusion protein SEC18	3, 1, 4	4, 2, 5
	KAP95	Importin subunit beta-1	3, 4	4, 5
	CPR1	peptidyl-prolyl *cis-trans* isomerase	3, 2	22, 13
	GGC1	Mitochondrial GTP/GDP carrier protein 1	3, 2	12, 8

	ARF1	ADP-ribosylation factor 1	1, 3	4, 19
	MIR1	mitochondrial phosphate carrier protein	1, 3	4, 9
	CEX1	Cytoplasmic export protein 1	2, 1	3, 2
	CYC1	Cytochrome c iso-1	1, 1	16, 16
	CRM1	**Exportin-1**	**1, 1**	**1, 1**
Stress response	*HSP82*	ATP-dependent molecular chaperone HSP82	2, 1, 3	27, 27, 34
	AHP1	Peroxiredoxin	2, 1, 1	13, 6, 6
	HSP78	Heat shock protein 78, mitochondrial	1, 2	1, 4
Other Proteins	*FAA1*	Long-chain-fatty-acid--CoA ligase 1	4, 15, 7	7, 27, 15
	AAP1	Alanine/arginine aminopeptidase	4, 4, 12	6, 6, 16
	ADE5,7	Bifunctional purine biosynthetic protein ADE5,7	3, 12	5, 18
	TRM44	tRNA (uracil-O(2)-)-methyltransferase	5, 6, 1	12, 12, 2
	SAH1	Adenosylhomocysteinase	6, 3, 2	19, 9, 5
	PWP1	Periodic tryptophan protein 1	2, 4	4, 8
	ACO1	Aconitate hydratase, mitochondrial	1, 4, 1	3, 8, 2
	SAN1	Protein SAN1	1, 3	3, 7
	RNR1	ribonucleoside-diphosphate reductase large chain 1	3, 1	4, 1
	APE2	Aminopeptidase 2, mitochondrial	2, 1, 2	3, 1, 3
	IMD4	Inosine-5'-monophosphate dehydrogenase 4	1, 2, 1	2, 6, 3
	PYC2	pyruvate carboxylase 2	1, 2	9, 2
	ARO10	transaminated amino acid decarboxylase	1, 2	2, 3
	NOC3	nucleolar complex-associated protein 3	1, 2	2, 3
	VPS1	vacuolar protein sorting-associated protein 1	2, 1	3, 2
	IPP1	Inorganic pyrophosphatase, cytosolic	1, 1	7, 6
	PPH22	serine/threonine-protein phosphatase PP2A-2 catalytic subunit	1, 1	3, 3
	NRP1	Asparagine-rich protein	1, 1	3, 2

Appendix 4: Common proteins interacting with Cca1 detected in the with and without RNAseA treatment samples from yeast cells grown on glucose to OD_{600} of 1.0. Proteins previously identified as being involved in tRNA biogenesis or as physically interacting with Cca1 have been bolded while proteins reported as interacting with Cca1 through genetic screens are italicized. The first values in each column are the samples with RNase treatment and second values are the samples without RNase treatment.

	Gene name	Protein name	Number of unique peptides	Sequence coverage (%)
Transport Proteins	*PMA1*	plasma membrane ATPase 1	11, 12	12, 14
	KAP123	Importin subunit beta-4	7, 5	8, 6
	KAP95	Importin subunit beta-1	6, 4	8, 5
	MIR1	mitochondrial phosphate carrier protein	6, 3	19, 9
	PUF6	Pumilio homology domain family member 6	5, 7	9, 13
	GGC1	Mitochondrial GTP/GDP carrier protein 1	5, 2	19, 8
	SEC18	vesicular-fusion protein	2, 4	3, 5
	ARF1	ADP-ribosylation factor 1	3, 3	19, 19
	KAP104	Importin subunit beta-2	2, 2	3, 3
	CEX1	Cytoplasmic export protein 1	1, 1	2,2
	CRM1	**Exportin-1**	**1, 1**	**1, 1**
Amino-acid/ protein biosynthesis	*MET6*	5-methyltetrahydropteroyltriglutamate-homocysteine methyltransferase	12, 17	18, 28
	THS1	**Threonine-tRNA ligase, cytoplasmic**	**8, 14**	**12, 23**
	GUS1	*Glutamate-tRNA ligase, cytoplasmic*	*11, 9*	*18, 15*
	SUP35	**Eukaryotic peptide chain release factor GTP-binding subunit**	**10, 9**	**21, 19**
	PRT1	Eukaryotic translation initiation factor 3 subunit B	3, 1	5, 2
	ARO10	transaminated amino acid decarboxylase	2, 2	3, 3
	DED81	Asparagine-tRNA ligase, cytoplasmic	1, 1	2, 2
Ribosome biogenesis	*NOC3*	nucleolar complex-associated protein 3	4, 2	7, 3
	UTP4	U3 small nucleolar RNA-associated protein 4	3, 2	5, 3
	RPL14A	60S ribosomal protein L14-A	2, 1	9, 8
	ENP2	ribosome biogenesis protein ENP2	1, 1	2, 2

Other Proteins	*ACO1*	Aconitate hydratase, mitochondrial	12, 16	17, 26
	AAP1	Alanine/arginine aminopeptidase	13, 12	16, 16
	ADE5,7	Bifunctional purine biosynthetic protein ADE5,7	12, 12	18, 18
	YPK1	Serine/threonine-protein kinase YPK1	8, 8	14, 15
	FAA1	Long-chain-fatty-acid--CoA ligase 1	8, 7	17, 15
	SAH1	Adenosylhomocysteinase	8, 4	19, 7
	ALD5	Aldehyde dehydrogenase 5, mitochondrial	2, 5	5, 13
	SAN1	Protein SAN1	2, 3	5, 7
	HSP82	ATP-dependent molecular chaperone HSP82	1, 3	25, 34
	CRH1	Probable glycosidase CRH1	3, 1	6, 2
	VPS1	vacuolar protein sorting-associated protein 1	3, 1	5, 2
	ECM33	Cell wall protein Ecm33	2, 2	6, 6
	SCH9	serine/threonine-protein kinase SCH9	2, 1	3, 2
	AHP1	Peroxiredoxin AHP1	1, 1	6, 6

Appendix 5: Proteins interacting with Cca1 reproduced in three biological replicates from yeast cells grown on glycerol to OD_{600} of 1.0. Proteins previously identified as being involved in tRNA biogenesis or as physically interacting with Cca1 have been bolded while proteins reported as interacting with Cca1 through genetic screens are italicized.

	Gene name	Protein name	Number of unique peptides	Sequence coverage (%)
Amino acid/Protein biosynthesis	*MET6*	5-methyltetrahydropteroyl-triglutamate-homocysteine methyltransferase	23, 18, 24	37, 31, 40
	ARG1	Argininosuccinate synthase	9, 9, 8	22, 22, 20
	TUF1	elongation factor Tu, mitochondrial	5, 6, 9	17, 20, 29
	DPS1	Aspartate-tRNA ligase, cytoplasmic	8, 5, 4	19, 17, 12
	ARO4	Phospho-2-dehydro-3-deoxyheptonate aldolase, tyrosine-inhibited	6, 6, 7	21, 17, 23
	THR4	threonine synthase	7, 6, 6	15, 13, 12
	KRS1	lysine-tRNA ligase, cytoplasmic	5, 6, 7	12, 13, 15
	DED81	Asparagine-tRNA ligase, cytoplasmic	7, 5, 6	14, 12, 14
	HOM2	Aspartate-semialdehyde dehydrogenase	7, 5, 4	22, 17, 12
	BAT1	Branched-chain-amino-acid aminotransferase, mitochondrial	6, 6, 5	29, 29, 26
	HYP2	**Eukaryotic translation initiation factor 5A-1**	**6, 6, 4**	**36, 25, 24**
	TMA19	Translationally-controlled tumor protein homolog	5, 6, 5	34, 35, 34
	LEU4	2-isopropylmalate synthase	6, 4, 5	12, 6, 8
	YDR341C	arginine-tRNA synthetase, mitochondrial, RRS1	6, 3, 3	12, 5, 5
	ARG4	argininosuccinate lyase	3, 5, 4	9, 16, 13
	TRP5	Tryptophan synthase	4, 3, 5	9, 6, 11
	HOM6	Homoserine dehydrogenase	4, 5, 2	11, 18, 10
	ILV3	Dihydroxy-acid dehydratase, mitochondrial	2, 5, 4	6, 11, 13
	SES1	Serine--tRNA ligase, cytoplasmic	4, 3, 4	12, 10, 13
	ASN2	Asparagine synthetase [glutamine-hydrolyzing] 2	4, 4, 3	12, 11, 10
	GUS1	*Glutamate-tRNA ligase, cytoplasmic*	*3, 4, 4*	*5, 7, 7*
	VAS1	Valine-tRNA ligase, mitochondrial	3, 4, 4	3, 4, 4

	ASN1	Asparagine synthetase [glutamine-hydrolyzing] 1	3, 4, 3	8, 12, 8
	MET17	Homocysteine/cysteine synthase	3, 2, 3	8, 5, 7
	CDC60	**Leucine-tRNA ligase, cytoplasmic**	**3, 2, 3**	**3, 2, 3**
	EFB1	Elongation factor 1-beta	2, 2, 2	10, 10, 10
	BAT2	Branched-chain-amino-acid aminotransferase, cytosolic	2, 1, 1	15, 10, 10
	TEF4	Elongation factor 1-gamma 2	1, 1, 2	3, 3, 6
	TRP2	anthranilate synthase component 1	1, 1, 2	2, 2, 4
	LYS1	Saccharopine dehydrogenase [NAD(+), L-lysine-forming]	1, 1, 1	5, 5, 5
Transport Proteins	*POR1*	Mitochondrial outer membrane protein porin 1	8, 7,11	41, 37, 49
	PMA1	plasma membrane ATPase 1	8, 9, 9	11, 11, 11
	KAP123	Importin subunit beta-4	4, 4, 8	4, 5, 9
	CPR1	peptidyl-prolyl *cis-trans* isomerase	7, 6, 6	42, 42, 42
	GGC1	Mitochondrial GTP/GDP carrier protein 1	5, 5, 2	18, 19, 6
	YHM2	Citrate/oxoglutarate carrier protein	4, 3, 5	14, 11, 21
	GSP2	GTP-binding nuclear protein GSP2/CNR2	4, 4, 4	21, 21, 21
	SUB2	ATP-dependent RNA helicase	3, 4, 3	9, 13, 9
	PBI2	Protease B inhibitor 2	2, 3, 2	49, 52, 49
	ODC1	Mitochondrial 2-oxodicarboxylate carrier 1	2, 1, 3	8, 4, 13
	CYC1	Cytochrome c iso-1	2, 2, 2	16, 16, 16
	MIC60	MICOS complex subunit	2, 1, 2	5, 2, 5
	ARL1	ADP-ribosylation factor-like protein 1	1, 1, 1	8, 8, 8
	TOM40	Mitochondrial import receptor subunit TOM40	1, 1, 1	4, 4, 4
TCA Cycle Proteins	*ICL1*	isocitrate lyase	19, 16, 17	40, 32, 39
	MLS1	Malate synthase 1, glyoxysomal	13, 11, 12	25, 24, 26
	CIT1	citrate synthase, mitochondrial	10, 11, 11	23, 27, 27
	LPD1	Dihydrolipoyl dehydrogenase, mitochondrial	11, 10, 10	26, 25, 28
	KGD1	2-oxoglutarate dehydrogenase, mitochondrial	8, 6, 10	11, 7, 13
	MDH1	Malate dehydrogenase, mitochondrial	9, 8, 9	42, 37, 40

	IDH1	Isocitrate dehydrogenase [NAD] subunit 1, mitochondrial	9, 8, 9	29, 23, 26
	MDH2	Malate dehydrogenase, cytoplasmic	8, 7, 6	21, 21, 18
	IDP1	Isocitrate dehydrogenase [NADP], mitochondrial	8, 4, 4	33, 25, 25
	LSC2	Succinate--CoA ligase [ADP-forming] subunit beta, mitochondrial	8, 4, 3	22, 12, 11
	FUM1	fumarate hydratase, mitochondrial	7, 7, 7	16, 18, 17
	LSC1	Succinate--CoA ligase [ADP-forming] subunit alpha, mitochondrial	5, 3, 6	22, 15, 22
	SDH2	Succinate dehydrogenase [ubiquinone] iron-sulfur subunit, mitochondrial	2, 4, 2	9, 17, 9
	COX6	Cytochrome c oxidase subunit 6, mitochondrial	3, 2, 2	24, 13, 13
	KGD2	*Dihydrolipoyllysine-residue succinyltransferase component of 2-oxoglutarate dehydrogenase complex, mitochondrial*	*2, 3, 2*	*5, 8, 5*
	MDH3	Malate dehydrogenase, peroxisomal	1, 2, 3	5, 11, 14
	IDH2	Isocitrate dehydrogenase [NAD] subunit 2, mitochondrial	2, 2, 2	8, 8, 8
	SDH3	Succinate dehydrogenase [ubiquinone] cytochrome b subunit, mitochondrial	1, 1, 1	6, 6, 6
Stress response	*MDJ1*	DnaJ homolog 1, mitochondrial	1, 3, 5	2, 8, 15
	LSP1	Sphingolipid long chain base-responsive protein	4, 4, 3	12, 12, 8
	PIL1	sphingolipid long chain base-responsive protein	4, 4, 3	12, 12, 8
	HSP82	ATP-dependent molecular chaperone	2, 4, 3	34, 38, 38
	PRX1	Peroxiredoxin, mitochondrial	3, 3, 3	15, 15, 15
	TRX1	thioredoxin-1	1, 3, 1	22, 30, 30
	STI1	Heat shock protein STI1	2, 1, 2	5, 2, 6
	GRE3	NADPH-dependent aldose reductase	1, 1, 2	5, 5, 9
	HYR1	Glutathione peroxidase-like peroxiredoxin	1, 1, 1	8, 8, 8
	UBC1	ubiquitin-conjugating enzyme E2 1	1, 1, 1	6, 6, 6
	GND1	6-phosphogluconate dehydrogenase, decarboxylating 1	9, 10, 10	25, 28, 28
	SOD1	Superoxide dismutase [Cu-Zn]	8, 6, 7	71, 60, 66

Oxidoreductase	*GDH2*	NAD-specific glutamate dehydrogenase	4, 5, 4	5, 7, 5
	RNR4	Ribonucleoside-diphosphate reductase small chain 2	3, 3, 2	8, 12, 6
	YDL124W	NADPH-dependent alpha-keto amide reductase	2, 1, 3	9, 8, 19
	TRR1	thioredoxin reductase 1	1, 1, 3	5, 5, 15
	NDE1	External NADH-ubiquinone oxidoreductase 1, mitochondrial	2, 2, 2	3, 3, 4
	YMR226C	NADP-dependent 3-hydroxy acid dehydrogenase	2, 2, 1	10, 10, 5
	SOD2	Superoxide dismutase [Mn], mitochondrial	2, 1, 2	10, 4, 10
	ARA1	D-arabinose dehydrogenase [NAD(P)+] heavy chain	2, 2, 1	6, 8, 4
	GDH3	NADP-specific glutamate dehydrogenase 2	1, 1, 1	12, 9, 16
	GDH1	NADP-specific glutamate dehydrogenase 1	1, 1, 1	11, 9, 16
Transferase	*TAL1*	Transaldolase	11, 10, 10	41, 38, 37
	AAT2	Aspartate aminotransferase, cytoplasmic	6, 6, 9	20, 19, 32
	CIT2	Citrate synthase, peroxisomal	8, 8, 7	23, 25, 21
	TKL1	transketolase 1	8, 7, 7	16, 16, 12
	PSA1	mannose-1-phosphate guanyltransferase	2, 5, 5	8, 21, 22
	ARO9	Aromatic amino acid aminotransferase 2	4, 4, 3	8, 8, 6
	AGX1	Alanine-glyoxylate aminotransferase 1	4, 3, 3	15, 12, 12
	SHM2	Serine hydroxymethyl-transferase, cytosolic	4, 3, 3	9, 7, 7
	RIB4	6,7-dimethyl-8-ribityllumazine synthase	3, 2, 2	33, 17, 17
	MCK1	protein kinase MCK1	2, 2, 3	6, 6, 8
	GUT1	glycerol kinase	1, 2, 1	2, 3, 2
	INO1	inositol-3-phosphate synthase	9, 10, 9	20, 23, 20
	ACH1	acetyl-CoA hydrolase	9, 9, 9	21, 22, 23
	ACC1	Acetyl-CoA carboxylase	9, 6, 3	5, 4, 2

Lipid metabolism	*ERG20*	Farnesyl pyrophosphate synthase	6, 5, 7	20, 18, 23
	CAT2	Carnitine O-acetyltransferase, mitochondrial	6, 3, 4	10, 5, 8
	ERG13	Hydroxymethylglutaryl-CoA synthase	5, 4, 5	13, 10, 12
	YAT1	Putative mitochondrial carnitine O-acetyltransferase	4, 3, 3	8, 6, 6
	ERG6	Sterol 24-C-methyltransferase	2, 2, 1	8, 7, 4
	ETR1	Enoyl-[acyl-carrier-protein] reductase, mitochondrial	2, 1, 1	6, 3, 3
	MVD1	Diphosphomevalonate decarboxylase	1, 1, 1	3, 3, 3
Glycolysis and gluconeogenesis	*PCK1*	Phosphoenolpyruvate carboxykinase (ATP)	11, 8, 11	27, 20, 26
	HXK1	Hexokinase-1	7, 8, 10	19, 26, 26
	ENO1	Enolase 1	6, 8, 8	36, 44, 46
	PYC1	pyruvate carboxylase 1	8, 8, 6	10, 9, 7
	GLK1	Glucokinase-1	5, 4, 7	13, 9, 19
	PGM2	Phosphoglucomutase 2	6, 5, 5	13, 11, 11
	PDB1	*Pyruvate dehydrogenase E1 component subunit beta, mitochondrial*	*5, 5, 4*	*17, 17, 13*
Nucleotide biosynthesis	*URA5*	Orotate phosphoribosyl- transferase 1	2, 1, 3	12, 4, 18
	GUA1	GMP synthase [glutamine-hydrolyzing]	3, 1, 1	6, 2, 2
	PNC1	Nicotinamidase	2, 2, 1	15, 15, 9
	SPE3	spermidine synthase	1, 1, 2	4, 4, 9
	IMD4	Inosine-5'-monophosphate dehydrogenase 4	1, 1, 1	3, 3, 3
DNA repair/damage proteins	*YNK1*	Nucleoside diphosphate kinase	7, 2, 4	55, 17, 36
	HTA1	Histone H2A.1	2, 2, 3	12, 12, 17
	HTB1	Histone H2B.1	2, 1, 1	15, 8, 8
	POL30	proliferating cell nuclear antigen	1, 1, 1	4, 4, 4
	LAP3	Cysteine proteinase 1, mitochondrial	1, 1, 1	3, 3, 3
Ribosome biogenesis	*RPL43B*	60S ribosomal protein L43-B	2, 1, 2	33, 20, 33
	RPL33A	60S ribosomal protein L33-A	1, 1, 1	32, 24, 40
	RPL33B	60S ribosomal protein L33-B	1, 1, 1	32, 24, 40

	RPL38	60s ribosomal protein l38	1, 1, 1	19, 19, 19
	OM14	Mitochondrial outer membrane protein OM14	1, 1, 1	16, 16, 16
	RPP1B	60S acidic ribosomal protein P1-beta	1, 1, 1	15, 15, 15
	MRP1	37S ribosomal protein MRP1, mitochondrial	1, 1, 1	4, 4, 4
	NPL3	Nucleolar protein 3	1, 1, 1	3, 3, 3
Electron Transport Chain proteins	*ATP5*	ATP synthase subunit 5, mitochondrial	5, 3, 2	31, 18, 12
	COR1	Cytochrome b-c1 complex subunit 1, mitochondrial	5, 2, 3	13, 5, 8
	ATP4	ATP synthase subunit 4, mitochondrial	3, 2, 3	16, 10, 13
	CYT1	*Cytochrome c1, heme protein, mitochondrial*	*2, 1, 1*	*8, 5, 5*
	ATP7	ATP synthase subunit d, mitochondrial	1, 1, 1	7, 7, 7
Other Proteins	*SAH1*	Adenosylhomocysteinase	13, 12, 13	30, 28, 36
	PDH1	Probable 2-methylcitrate dehydratase	9, 10, 7	22, 27, 16
	IPP1	Inorganic pyrophosphatase, cytosolic	8, 7, 8	37, 30, 41
	ARO10	transaminated amino acid decarboxylase	5, 6, 3	8, 10, 6
	WTM1	Transcriptional modulator WTM1	6, 5, 3	17, 14, 8
	APE2	Aminopeptidase 2, mitochondrial	6, 2, 3	7, 2, 3
	GVP36	Golgi Vesicle Protein 36	5, 5, 4	18, 17, 15
	SEC53	phosphomannomutase	5, 4, 4	22, 19, 19
	MMF1	Protein mmf1, mitochondrial	5, 2, 3	41, 17, 26
	COF1	Cofilin	4, 4, 4	38, 38, 38
	PEP4	Saccharopepsin	2, 4, 3	8, 12, 12
	PRB1	Cerevisin	3, 3, 3	5, 5, 5
	BMH2	Protein BMH2	3, 3, 2	50, 43, 42
	FPR1	FK506-binding protein 1	3, 3, 2	26, 26, 19
	HNT1	Hit family protein 1	3, 1, 1	28, 8, 8
	DUG1	Cys-Gly metallodipeptidase	3, 1, 1	6, 2, 2
	YMR099C	glucose-6-phosphate 1-epimerase	1, 2, 3	4, 7, 14
	RNA1	**Ran-specific GTPase-activating protein 1**	**2, 2, 2**	**15, 15, 15**
	FBP1	fructose-1,6-bisphosphatase	2, 2, 1	9, 9, 4

	MBF1	multiprotein-bridging factor 1	2, 1, 1	16, 6, 6
	BFR1	nuclear segregation protein Bfr1	1, 2, 1	3, 6, 3
	HSP10	10 kDa heat shock protein, mitochondrial	1, 1, 1	15, 15, 15
	ZEO1	protein ZEO1	1, 1, 1	10, 10, 10
	CDC33	Eukaryotic translation initiation factor 4E	1, 1, 1	8, 8, 8
	RGI1	Respiratory growth induced protein 1	1, 1, 1	8, 8, 8
	ISU1	iron sulfur cluster assembly protein 1, mitochondrial	1, 1, 1	7, 7, 7
	YNL134C	Uncharacterized protein	1, 1, 1	4, 2, 7
	ABP1	actin-binding protein	1, 1, 1	4, 4, 4
	PDX1	Pyruvate dehydrogenase complex protein X component, mitochondrial	1, 1, 1	4, 4, 4
	SGT2	Small glutamine-rich tetratricopeptide repeat-containing protein 2	1, 1, 1	3, 3, 3
	VPS1	vacuolar protein sorting-associated protein 1	1, 1, 1	2, 2, 2

Appendix 6: Proteins interacting with Cca1 detected in mitochondrial fraction from yeast cells grown on glucose to OD_{600} of 1.0. Proteins previously identified as being involved in tRNA biogenesis or as physically interacting with Cca1 have been bolded while proteins reported as interacting with Cca1 through genetic screens are italicized.

	Gene name	Protein name	Number of unique peptides	Sequence coverage (%)
Transport Proteins	*ATP1*	ATP synthase subunit alpha, mitochondrial	4	9
	MDM38	Mitochondrial distribution and morphology protein 38	2	8
	ATP2	*ATP synthase subunit beta, mitochondrial*	*2*	*6*
	GGC1	Mitochondrial GTP/GDP carrier protein 1	1	4
	MIR1	mitochondrial phosphate carrier protein	1	4
Amino-acid/Protein biosynthesis	*ILV6*	Acetolactate synthase small subunit, mitochondrial	4	15
	SUP35	**Eukaryotic peptide chain release factor GTP-binding subunit**	**3**	**6**
	BAT1	Branched-chain-amino-acid aminotransferase, mitochondrial	1	4
	ILV3	Dihydroxy-acid dehydratase, mitochondrial	1	2
	LYS4	Homoaconitase, mitochondrial	1	2
	VAS1	Valine-tRNA ligase, mitochondrial	1	1
Other proteins	*ACO1*	Aconitate hydratase, mitochondrial	6	10
	ALD5	Aldehyde dehydrogenase 5, mitochondrial	5	13
	DUG1	Cys-Gly metallodipeptidase dug1	1	4
	GND1	6-phosphogluconate dehydrogenase, decarboxylating 1	1	4
	YLR283W	Uncharacterized protein YLR283W, mitochondrial	1	4
	AI2	putative COX1/OXI3 intron 2 protein	1	3
	SYG1	Protein SYG1	1	3
	ALD4	Potassium-activated aldehyde dehydrogenase, mitochondrial	1	2
	FAA1	Long-chain-fatty-acid--CoA ligase 1	1	2
	MDJ1	DnaJ homolog 1, mitochondrial	1	2
	MSS116	ATP-dependent RNA helicase MSS116, mitochondrial	1	2
	PUF3	mRNA-binding protein puf3	1	2

Appendix 7: Proteins interacting with Cca1 detected in nuclear fraction from yeast cells grown on glucose to OD_{600} of 1.0. Proteins previously identified as being involved in tRNA biogenesis or as physically interacting with Cca1 have been bolded while proteins reported as interacting with Cca1 through genetic screens are italicized.

	Gene name	Protein name	Number of unique peptides	Sequence coverage (%)
Ribosome biogenesis and rRNA processing	*NOP56*	Nucleolar protein 56	5	12
	NOP1	rRNA 2'-O-methyltransferase fibrillarin	4	15
	MAK21	Ribosome biogenesis protein Mak21	3	4
	NPL3	Nucleolar protein 3	2	7
	NOP58	Nucleolar protein 58	2	6
	DBP3	ATP-dependent RNA helicase dbp3	2	5
	CBF5	H/ACA ribonucleoprotein complex subunit 1	1	6
	DBP2	*ATP-dependent RNA helicase dbp2*	*1*	*3*
	KRI1	Protein Kri1	1	2
	MPP10	U3 small nucleolar RNA-associated protein MPP10	1	2
	NOC2	nucleolar complex protein 2	1	2
	NOC3	nucleolar complex-associated protein 3	1	2
	NOP4	**Nucleolar protein 4**	**1**	**2**
	MAK5	ATP-dependent RNA helicase Mak5	1	1
	NOP9	Nucleolar protein 9	1	1
Transport Proteins	*KAP123*	Importin subunit beta-4	6	7
	KAP95	Importin subunit beta-1	5	6
	NSP1	nucleoporin nsp1	3	8
	BFR2	protein Bfr2	2	6
	CSE1	**importin alpha re-exporter**	**2**	**2**
	NUG1	nuclear GTP-binding protein NUG1	1	3
	SEC63	protein translocation protein SEC63	1	2
	SET2	Large subunit GTPase 1	1	2

	CRM1	**Exportin-1**	**1**	**1**
	NIC96	nucleoporin NIC96	1	1
Transcription Regulation	*MSN4*	Zinc finger protein MSN4	1	3
	RSC8	*Chromatin structure-remodeling complex protein RSC8*	*1*	*3*
	WTM1	Transcriptional modulator WTM1	1	3
	TAF12	Transcription initiation factor TFIID subunit 12	1	2
	TFG1	Transcription initiation factor IIF subunit alpha	1	2
	TAF5	*Transcription initiation factor TFIID subunit 5*	*1*	*1*
mRNA processing	*BFR1*	nuclear segregation protein Bfr1	4	9
	SCP160	Protein SCP160	3	3
	HRP1	**Nuclear polyadenylated RNA-binding protein 4**	**1**	**4**
	PPZ1	Serine/threonine-protein phosphatase PP-Z1	1	3
Other proteins	*MKT1*	protein MKT1	5	8
	ARO4	Phospho-2-dehydro-3-deoxyheptonate aldolase, tyrosine-inhibited	3	9
	SUI3	Eukaryotic translation initiation factor 2 subunit beta	2	7
	ZUO1	Zuotin	2	6
	FPR3	FK506-binding nuclear protein	1	5
	SAN1	Protein SAN1	1	3
	FRA1	*Putative Xaa-Pro aminopeptidase FRA1*	*1*	*2*
	NCL1	**Multisite-specific tRNA:(cytosine-C (5))-methyltransferase**	**1**	**2**
	TKL1	transketolase 1	1	2
	UBP14	Ubiquitin carboxyl-terminal hydrolase 14	1	2

Appendix 8: Proteins interacting with Cca1 detected in cytosolic fraction from yeast cells grown on glucose to OD_{600} of 1.0. Proteins previously identified as being involved in tRNA biogenesis or as physically interacting with Cca1 have been bolded while proteins reported as interacting with Cca1 through genetic screens are italicized.

	Gene name	Protein name	Number of unique peptides	Sequence coverage (%)
Amino-acid/ protein biosynthesis	***THS1***	**Threonine--tRNA ligase, cytoplasmic**	**20**	**31**
	DPS1	Aspartate--tRNA ligase, cytoplasmic	17	37
	KRS1	lysine--tRNA ligase, cytoplasmic	16	33
	YNL247W	Cysteine--tRNA ligase	16	24
	ADE3	C-1-tetrahydrofolate synthase, cytoplasmic	12	15
	SES1	Serine-tRNA ligase, cytoplasmic	9	3
	CDC60	**Leucine--tRNA ligase, cytoplasmic**	**7**	**9**
	ASN1	Asparagine synthetase [glutamine-hydrolyzing] 1	6	15
	PRO3	Pyrroline-5-carboxylate reductase	5	20
	ARO4	Phospho-2-dehydro-3-deoxyheptonate aldolase, tyrosine-inhibited	5	17
	ARG1	Argininosuccinate synthase	5	16
	TRP2	anthranilate synthase component 1	4	9
	TRP3	Multifunctional tryptophan biosynthesis protein	4	9
	GUS1	*Glutamate--tRNA ligase, cytoplasmic*	*4*	*7*
	YDR341C	Arginine--tRNA ligase, cytoplasmic	4	7
	ASN2	Asparagine synthetase [glutamine-hydrolyzing] 2	3	12
	LYS2	L-2-aminoadipate reductase	3	3
	ARG4	argininosuccinate lyase	2	6
	DED81	Asparagine--tRNA ligase, cytoplasmic	2	5
	FRS2	**Phenylalanine--tRNA ligase alpha subunit**	**2**	**5**
	MET17	Homocysteine/cysteine synthase	1	3
	TYS1	**Tyrosine--tRNA ligase, cytoplasmic**	**1**	**3**

	BPL1	biotin-protein ligase	1	2
Nucleotide biosynthesis	*ADE6*	Phosphoribosylformyl-glycinamidine synthase	5	6
	GUA1	GMP synthase [glutamine-hydrolyzing]	4	8
	IMD2	inosine-5'-monophosphate dehydrogenase 2	3	9
	ADE5,7	Bifunctional purine biosynthetic protein ADE5,7	1	1
Ribosomal proteins	*RPL27A*	60S ribosomal protein L27-A	1	10
	RPS16B	40S ribosomal protein S16-B	1	10
	ASC1	Guanine nucleotide-binding protein subunit beta-like protein	1	7
	RPS1A	40S ribosomal protein S1-A	1	5
Oxidoreductase	*GDH1*	NADP-specific glutamate dehydrogenase 1	7	24
	DLD3	D-2-hydroxyglutarate--pyruvate transhydrogenase DLD3	5	14
	GND1	6-phosphogluconate dehydrogenase, decarboxylating 1	4	9
	RNR1	ribonucleoside-diphosphate reductase large chain 1	1	1
Glycolysis and Gluconeogenesis	*PGI1*	glucose-6-phosphate isomerase	11	26
	ENO1	Enolase 1	5	36
	PYC1	pyruvate carboxylase 1	1	2
Stress response	*HSP82*	ATP-dependent molecular chaperone HSP82	6	45
	STI1	Heat shock protein STI1	4	8
Other Proteins	*TRM44*	tRNA (uracil-O (2)-)-methyltransferase	12	23
	TKL1	transketolase 1	10	18
	SHM2	Serine hydroxymethyl-transferase, cytosolic	6	12
	ARC1	**tRNA-aminoacylation cofactor ARC1**	**3**	**10**
	RNA1	**Ran-specific GTPase-activating protein 1**	**2**	**15**
	CPR6	Peptidyl-prolyl *cis-trans* isomerase CPR6	2	7
	INO1	inositol-3-phosphate synthase	2	5
	NCL1	**Multisite-specific tRNA:(cytosine-C (5))-methyltransferase**	**2**	**4**

	GLY1	Low specificity L-threonine aldolase	1	4
	PAN5	2-dehydropantoate 2-reductase	1	4
	AAT2	Aspartate aminotransferase, cytoplasmic	1	3
	ERG20	Farnesyl pyrophosphate synthase	1	3
	MVD1	Diphosphomevalonate decarboxylase	1	3
	PGM1	Phosphoglucomutase 1	1	2

Appendix 9: Proteins interacting with Cca1 detected in mitochondrial fraction from yeast cells grown on glycerol to OD_{600} of 1.0. Proteins previously identified as being involved in tRNA biogenesis or as physically interacting with Cca1 have been bolded while proteins reported as interacting with Cca1 through genetic screens are italicized.

	Gene name	Protein name	Number of unique peptides	Sequence coverage (%)
Transport proteins	*POR1*	Mitochondrial outer membrane protein porin 1	16	64
	YHM2	Citrate/oxoglutarate carrier protein	6	22
	ODC1	Mitochondrial 2-oxodicarboxylate carrier 1	5	18
	RIP1	*cytochrome b-c1 complex subunit Rieske, mitochondrial*	*4*	*27*
	QCR7	Cytochrome b-c1 complex subunit 7	3	33
	CIR1	Probable electron transfer flavoprotein subunit beta	3	19
	YMC1	Carrier protein YMC1, mitochondrial	3	13
	CRC1	mitochondrial carnitine carrier	3	14
	OAC1	Mitochondrial oxaloacetate transport protein	3	14
	QCR10	cytochrome b-c1 complex subunit 10	2	26
	CYC1	Cytochrome c iso-1	2	16
	NCE102	Non-classical export protein 2	2	13
	AIM45	Probable electron transfer flavoprotein subunit alpha, mitochondrial	2	11
	PHO88	SRP-independent targeting protein 3	2	11
	GGC1	Mitochondrial GTP/GDP carrier protein 1	2	10
	TOM40	Mitochondrial import receptor subunit TOM40	2	10
	TIM44	Translocase of the inner mitochondrial membrane 44	2	6
	PAM16	Mitochondrial import inner membrane translocase subunit TIM16	1	18
	TOM20	mitochondrial import receptor subunit Tom20	1	7
	ODC2	Mitochondrial 2-oxodicarboxylate carrier 2	1	3

	TIM50	Translocase of the inner mitochondrial membrane 50	1	3
	CIR2	Probable electron transfer flavoprotein-ubiquinone oxidoreductase, mitochondrial	1	2
TCA cycle proteins	*LPD1*	Dihydrolipoyl dehydrogenase, mitochondrial	21	52
	MDH1	Malate dehydrogenase, mitochondrial	12	53
	CIT1	citrate synthase, mitochondrial	12	31
	IDP1	Isocitrate dehydrogenase [NADP], mitochondrial	9	44
	SDH2	Succinate dehydrogenase [ubiquinone] iron-sulfur subunit, mitochondrial	9	34
	FUM1	fumarate hydratase, mitochondrial	8	25
	KGD2	*Dihydrolipoyllysine-residue succinyltransferase component of 2-oxoglutarate dehydrogenase complex, mitochondrial*	*8*	*25*
	LSC1	Succinate--CoA ligase [ADP-forming] subunit alpha, mitochondrial	7	35
	IDH1	Isocitrate dehydrogenase [NAD] subunit 1, mitochondrial	7	24
	IDH2	Isocitrate dehydrogenase [NAD] subunit 2, mitochondrial	6	22
	LSC2	Succinate--CoA ligase [ADP-forming] subunit beta, mitochondrial	6	21
	COX4	*cytochrome c oxidase subunit 4, mitochondrial*	*5*	*45*
	COX2	Cytochrome c oxidase subunit 2	5	26
	CIT3	Citrate synthase 3, mitochondrial	5	14
	SDH4	Succinate dehydrogenase [ubiquinone] cytochrome b small subunit, mitochondrial	4	24
	COX6	Cytochrome c oxidase subunit 6, mitochondrial	3	30
	IDP3	isocitrate dehydrogenase [NADP]	2	14
	SHH4	Mitochondrial inner membrane protein SHH4	1	14
	COX13	Cytochrome c oxidase subunit 6A, mitochondrial	1	8
	COX1	Cytochrome c oxidase subunit 1	1	3

Oxidoreductase	*DLD1*	D-lactate dehydrogenase [cytochrome] 1, mitochondrial	14	35
	NDI1	Rotenone-insensitive NADH-ubiquinone oxidoreductase, mitochondrial	12	30
	NDE1	External NADH-ubiquinone oxidoreductase 1, mitochondrial	5	12
	NDE2	External NADH-ubiquinone oxidoreductase 2, mitochondrial	3	8
	SOD2	Superoxide dismutase [Mn], mitochondrial	2	12
	AIM17	Probable oxidoreductase, mitochondrial	2	6
	GCV3	Glycine cleavage system H protein, mitochondrial	1	9
	DLD2	D-2-hydroxyglutarate--pyruvate transhydrogenase DLD2	1	3
Amino-acid/protein biosynthesis	*TUF1*	elongation factor Tu, mitochondrial	9	33
	BAT1	Branched-chain-amino-acid aminotransferase, mitochondrial	5	20
	RRF1	Ribosome-recycling factor, mitochondrial	1	9
	LYS12	Homoisocitrate dehydrogenase, mitochondrial	1	3
	LYS4	Homoaconitase, mitochondrial	1	2
	MSY1	**Tyrosine--tRNA ligase, mitochondrial**	**1**	**2**
Stress response	*HSP78*	Heat shock protein 78, mitochondrial	14	24
	LSP1	Sphingolipid long chain base-responsive protein LSP1	8	35
	PRX1	Peroxiredoxin PRX1, mitochondrial	7	33
	MDJ1	DnaJ homolog 1, mitochondrial	3	9
	FMP45	SUR7 family protein FMP45	1	5
	SSQ1	Heat shock protein SSQ1, mitochondrial	1	2
Lipid metabolism	*CAT2*	Carnitine O-acetyltransferase, mitochondrial	10	20
	FAA2	Long-chain-fatty-acid--CoA ligase 2	3	6
	OPI3	phosphatidyl-N-methylethanolamine N-methyltransferase	2	12
	ERG6	Sterol 24-C-methyltransferase	2	7

	ETR1	Enoyl-[acyl-carrier-protein] reductase, mitochondrial	2	7
	PSD1	Phosphatidylserine decarboxylase proenzyme 1, mitochondrial	1	4
RNA processing	*YME2*	Mitochondrial escape protein 2	5	8
	CBP6	*cytochrome B pre-mRNA-processing protein 6*	*2*	*14*
	MSS51	*Protein MSS51, mitochondrial*	*1*	*4*
	DSS1	Exoribonuclease II, mitochondrial	1	1
Other Proteins	*MIC60*	MICOS complex subunit Mic60	17	36
	COR1	Cytochrome b-c1 complex subunit 1, mitochondrial	13	34
	PDH1	Probable 2-methylcitrate dehydratase	9	20
	PDB1	*Pyruvate dehydrogenase E1 component subunit beta, mitochondrial*	*7*	*28*
	MGM101	*Mitochondrial genome maintenance protein MGM101*	*5*	*24*
	PDX1	Pyruvate dehydrogenase complex protein X component, mitochondrial	5	12
	CYT1	*Cytochrome c1, heme protein, mitochondrial*	*4*	*24*
	ICL2	Mitochondrial 2-methylisocitrate lyase	4	13
	MAS2	Mitochondrial-processing peptidase subunit alpha	4	12
	VAR1	Ribosomal protein VAR1, mitochondrial	3	11
	SHY1	*Cytochrome oxidase assembly protein SHY1*	*3*	*9*
	SHM1	Serine hydroxymethyltransferase, mitochondrial	3	8
	MMF1	Protein Mmf1, mitochondrial	2	17
	PHB2	*Prohibitin-2*	*2*	*8*
	MDM38	Mitochondrial distribution and morphology protein 38	2	6
	FIS1	mitochondrial fission 1 protein	1	10
	MIC10	MICOS complex subunit Mic10	1	10
	MIC26	MICOS subunit MIC26	1	6
	CBP3	Protein CBP3, mitochondrial	1	5

	MGR1	Mitochondrial inner membrane i-AAA protease supercomplex subunit MGR1	1	4
	RCF2	Respiratory supercomplex factor 2, mitochondrial	1	4
	MGR3	Mitochondrial inner membrane i-AAA protease supercomplex subunit MGR3	1	3
	YLH47	LETM1 domain-containing protein YLH47, mitochondrial	1	3
	AFG3	*Mitochondrial respiratory chain complexes assembly protein AFG3*	*1*	*2*
	RSM22	Probable S-adenosyl-L-methionine-dependent RNA methyltransferase RSM22, mitochondrial	1	2

Appendix 10: Proteins interacting with Cca1 detected in nuclear fraction from yeast cells grown on glycerol to OD_{600} of 1.0. Proteins previously identified as being involved in tRNA biogenesis or as physically interacting with Cca1 have been bolded while proteins reported as interacting with Cca1 through genetic screens are italicized.

	Gene name	Protein name	Number of unique peptides	Sequence coverage (%)
Ribosome biogenesis and rRNA processing	*RRP5*	rRNA biogenesis protein Rrp5	8	6
	NOP1	rRNA 2'-O-methyltransferase fibrillarin	7	28
	NOP58	Nucleolar protein 58	6	18
	UTP6	U3 small nucleolar RNA-associated protein 6	3	1
	BRX1	ribosome biogenesis protein Brx1	2	9
	CIC1	proteasome-interacting protein CIC1	2	9
	NPL3	Nucleolar protein 3	2	7
	UTP4	U3 small nucleolar RNA-associated protein 4	2	4
	GAR1	H/ACA ribonucleoprotein complex subunit 1	1	6
	DBP2	*ATP-dependent RNA helicase dbp2*	*1*	*5*
	RRB1	Ribosome assembly protein Rrb1	1	4
	UTP11	U3 small nucleolar RNA-associated protein 11	1	4
	ERB1	Ribosome biogenesis protein ERB1	1	3
	UTP15	U3 small nucleolar RNA-associated protein 15	1	3
	UTP8	**U3 small nucleolar RNA-associated protein 8**	**1**	**3**
	UTP9	U3 small nucleolar RNA-associated protein 9	1	3
	YTM1	Ribosome biogenesis protein Ytm1	1	3
	NOC3	nucleolar complex-associated protein 3	1	2
	RIX1	Pre-rRNA-processing protein Rix1	1	2
	UTP22	U3 small nucleolar RNA-associated protein 22	1	1
	NIC96	nucleoporin NIC96	9	12
	NSP1	**nucleoporin nsp1**	**6**	**10**

Transport protein	***NUP170***	**Nucleoporin NUP170**	**3**	**3**
	CPR1	peptidyl-prolyl *cis-trans* isomerase	2	21
	GSP2	GTP-binding nuclear protein GSP2/CNR2	2	11
	ASM4	Nucleoporin Asm4	2	6
	BFR2	protein Bfr2	2	6
	NUP57	***Nucleoporin NUP57***	***1***	***5***
	POM33	Pore membrane protein of 33 kDa	1	5
	JEN1	Carboxylic acid transporter protein homolog	1	4
	NUP49	**Nucleoporin NUP49/NSP49**	**1**	**3**
	NUP53	Nucleoporin NUP53	1	3
	SEC63	protein translocation protein SEC63	1	2
	BDF1	**bromodomain-containing factor 1**	**1**	**1**
	KAP123	Importin subunit beta-4	1	1
	KAP95	Importin subunit beta-1	1	1
	NUP157	Nucleoporin NUP157	1	1
	NUP192	**Nucleoporin NUP192**	**1**	**1**
	SUB2	ATP-dependent RNA helicase SUB2	1	1
Transcription Regulation	*RVB2*	RuvB-like protein 2	10	27
	YRA1	RNA annealing protein Yra1	4	20
	UME1	Transcriptional regulatory protein UME1	4	12
	RPD3	histone deacetylase RPD3	3	10
	SIN3	*transcriptional regulatory protein SIN3*	*3*	*3*
	NHP6B	Non-histone chromosomal protein 6B	2	26
	RXT3	transcriptional regulatory protein Rxt3	2	11
	RSC8	*Chromatin structure-remodeling complex protein RSC8*	*2*	*5*
	TAF5	*Transcription initiation factor TFIID subunit 5*	*2*	*4*
	IES2	Ino eighty subunit 2	1	6
	PHO23	Transcriptional regulatory protein PHO23	1	4

	TAF12	Transcription initiation factor TFIID subunit 12	1	4
	WTM1	Transcriptional modulator WTM1	1	3
	MOT2	General negative regulator of transcription subunit 4	1	2
	POB3	FACT complex subunit pob3	1	2
	CDC33	Eukaryotic translation initiation factor 4E	1	1
	CTR9	RNA polymerase-associated protein CTR9	1	1
	SPT16	FACT complex subunit SPT16	1	1
RNA processing	*GBP2*	Single-strand telomeric DNA-binding protein Gbp2	4	14
RNA processing	***XRN1***	***5'-3' exoribonuclease 1***	***4***	***5***
RNA processing	*PWP1*	Periodic tryptophan protein 1	3	6
RNA processing	*YGR250C*	Uncharacterized RNA-binding protein YGR250C	2	3
RNA processing	*SNU13*	13 kDa ribonucleoprotein-associated protein	1	17
RNA processing	*GLC7*	Serine/threonine-protein phosphatase PP1-2	1	6
RNA processing	*NAP1*	nucleosome assembly protein	1	6
RNA processing	*HRB1*	Protein HRB1	1	3
RNA processing	*ZUO1*	zuotin	1	3
RNA processing	***PRP43***	**pre-mRNA-splicing factor ATP-dependent RNA helicase PRP43**	**1**	**2**
RNA processing	***KRE33***	**RNA cytidine acetyltransferase**	**1**	**1**
Transferase	*ARO9*	Aromatic amino acid aminotransferase 2	10	21
Transferase	*NQM1*	Transaldolase Nqm1	3	11
Transferase	*CKA2*	casein kinase II subunit alpha'	2	7
Transferase	*TAL1*	Transaldolase	2	6
Transferase	*GLC3*	1,4-alpha-glucan-branching enzyme	2	2
	RPN11	Ubiquitin carboxyl-terminal hydrolase Rpn11	3	13
	RPN7	*26S proteasome regulatory subunit RPN7*	*3*	*10*

Ubiquitin conjugation pathway	*RPN3*	26S proteasome regulatory subunit RPN3	3	8
	SUI3	**Eukaryotic translation initiation factor 2 subunit beta**	**1**	**3**
	UBP15	ubiquitin carboxyl-terminal hydrolase 15	1	2
	UBP6	Ubiquitin carboxyl-terminal hydrolase 6	1	2
	GID7	Glucose-induced degradation protein 7	1	1
DNA Replication	*RFC3*	replication factor C subunit 3	4	16
	RFC2	Replication factor C subunit 2	3	10
	RFC4	replication factor C subunit 4	2	10
	RFC5	Replication factor C subunit 5	2	8
	RFC1	Replication factor C subunit 1	2	3
Stress response	*SBP1*	Single-stranded nucleic acid-binding protein	3	15
	TRX1	thioredoxin-1	1	13
	GRE3	NADPH-dependent aldose reductase GRE3	1	5
	SDS23	Protein SDS23	1	4
Other proteins	*ENO1*	Enolase 1	4	34
	HTB1	Histone H2B.1	4	29
	HMG1	3-hydroxy-3-methylglutaryl-coenzyme A reductase 1	4	5
	HTA1	Histone H2A.1	3	17
	BMH2	Protein BMH2	2	36
	COF1	Cofilin	2	22
	IPP1	Inorganic pyrophosphatase, cytosolic	2	9
	TEF4	Elongation factor 1-gamma 2	2	7
	FPR4	FK506-binding protein 4	2	7
	ERG13	Hydroxymethylglutaryl-CoA synthase	2	4
	TKL1	transketolase 1	2	3
	PNC1	Nicotinamidase	1	9
	YDL124W	NADPH-dependent alpha-keto amide	1	8

		reductase		
	PRE1	Proteasome subunit beta type-4	1	6
	CKB2	Casein kinase II subunit beta	1	4
	POL30	proliferating cell nuclear antigen	1	4
	MAK16	Protein MAK16	1	3
	REP1	Partitioning protein Rep1	1	3
	CDC14	tyrosine-protein phosphatase CDC14	1	2

Appendix 11: Proteins interacting with Cca1 detected in cytosolic fraction from yeast cells grown on glycerol to OD_{600} of 1.0. Proteins previously identified as being involved in tRNA biogenesis or as physically interacting with Cca1 have been bolded while proteins reported as interacting with Cca1 through genetic screens are italicized.

	Gene name	protein name	Number of unique peptides	Sequence coverage (%)
Amino-acid/protein biosynthesis	*EFT2*	Elongation factor 2	7	10
	PDC1	pyruvate decarboxylase isozyme 1	5	11
	HYP2	**Eukaryotic translation initiation factor 5A-1**	**2**	**19**
	GUS1	*Glutamate--tRNA ligase, cytoplasmic*	*1*	*2*
Ribosome biosynthesis	*RPL8A*	60S ribosomal protein L8-A	2	14
	RPL43B	60S ribosomal protein L43-B	1	20
	RPP1B	60S acidic ribosomal protein P1-beta	1	15
Stress response	*HSC82*	ATP-dependent molecular chaperone HSC82	1	14
	SSE2	Heat shock protein homolog SSE2	1	7
Other proteins	*ADH2*	Alcohol dehydrogenase 2	2	8
	INO1	inositol-3-phosphate synthase	2	5
	GAL83	SNF1 protein kinase subunit beta-3	1	8
	PRS3	Ribose-phosphate pyrophosphokinase 3	1	7
	DCR2	phosphatase dcr2	1	5
	SEC17	alpha-soluble nsf attachment protein	1	5
	ADH1	*Alcohol dehydrogenase 1*	*1*	*4*
	IDP2	Isocitrate dehydrogenase [NADP] cytoplasmic	1	4
	MDH2	Malate dehydrogenase, cytoplasmic	1	3

Appendix 12: Comparison of proteins interacting with Cca1 in the *in vivo* assay from whole-cell extract of yeast cells grown on glucose and glycerol to OD_{600} of 1.0 in triplicates tested. Common proteins are in red.

Proteins interacting with Cca1 in the *in vivo* assay on glycerol	**Proteins interacting with Cca1 in the *in vivo* assay on glucose**
ARG1	*AAP1*
AAT2	*ACO1*
ABP1	*AHP1*
ACC1	*AIM10*
ACH1	*APE2*
AGX1	*DED81*
APE2	*DPS1*
ARA1	*FAA1*
ARG4	*GUS1*
ARL1	*HSP82*
ARO10	*IMD4*
ARO9	*KRS1*
ATP4	*MET6*
ATP5	*PMA1*
ATP7	*SAH1*
BAT1	*SEC18*
BAT2	*THS1*
BFR1	*TRM44*
BMH2	*YNL247W*
CAT2	
CDC33	
CDC60	
CIT1	
CIT2	
COF1	
COR1	
COX6	
CPR1	
CYC1	
CYT1	
DED81	
DPS1	
DUG1	

EFB1	
ENO1	
ERG13	
ERG20	
ERG6	
ETR1	
FBP1	
FPR1	
FUM1	
GDH1	
GDH2	
GDH3	
GGC1	
GLK1	
GND1	
GRE3	
GSP2	
GUA1	
GUS1	
GUT1	
GVP36	
HNT1	
HOM2	
HOM6	
HSP10	
HSP82	
HTA1	
HTB1	
HXK1	
HYP2	
HYR1	
ICL1	
IDH1	
IDH2	
IDP1	
ILV3	
IMD4	
INO1	
IPP1	

ISU1	
KAP123	
KGD1	
KGD2	
KRS1	
LAP3	
LEU4	
LPD1	
LSC1	
LSC2	
LSP1	
LYS1	
MBF1	
MCK1	
MDH1	
MDH2	
MDH3	
MDJ1	
MET17	
MET6	
MIC60	
MLS1	
MMF1	
MRP1	
MVD1	
NDE1	
NPL3	
ODC1	
OM14	
PBI2	
PCK1	
PDB1	
PDH1	
PDX1	
PEP4	
PGM2	
PIL1	
PMA1	
PNC1	

POL30	
POR1	
PRB1	
PRX1	
PSA1	
PYC1	
RGI1	
RIB4	
RNA1	
RNR4	
RPL33A	
RPL33B	
RPL38	
RPL43B	
RPP1B	
SAH1	
SDH2	
SDH3	
SEC53	
SES1	
SGT2	
SHM2	
SOD1	
SOD2	
SPE3	
STI1	
SUB2	
TAL1	
TEF4	
THR4	
TKL1	
TMA19	
TOM40	
TRP2	
TRP5	
TRR1	
TRX1	
TUF1	
UBC1	

URA5	
VAS1	
VPS1	
WTM1	
YAT1	
YDL124W	
YDR341C	
YHM2	
YMR099C	
YMR226C	
YNK1	
YNL134C	
ZEO1	

Appendix 13: Comparison of proteins interacting with Cca1 in the *in vivo* assay from mitochondrial fraction of yeast cells grown on glucose and glycerol to OD_{600} of 1.0 in one biological replicate tested. Common proteins are in red.

Proteins interacting with Cca1 in mitochondrial fraction in glycerol	Proteins interacting with Cca1 in mitochondrial fraction in glucose
AIM45	*ACO1*
AFG3	*AI2*
AIM17	*ALD4*
BAT1	*ALD5*
Cat2	*ATP1*
CBP3	*ATP2*
CBP6	*BAT1*
CIR1	*DUG1*
CIR2	*FAA1*
CIT1	*GGC1*
CIT3	*GND1*
COR1	*ILV3*
COX1	*ILV6*
COX13	*LYS4*
COX2	*MDJ1*
COX4	*MDM38*
COX6	*MIR1*
CRC1	*MSS116*
CYC1	*PUF3*
CYT1	*SUP35*
DLD1	*SYG1*
DLD2	*VAS1*
DSS1	*YLR283W*
ERG6	
ETR1	
FAA2	
FIS1	
FMP45	
FUM1	
GCV3	
GGC1	

HSP78	
ICL2	
IDH1	
IDH2	
IDP1	
IDP3	
KGD2	
LPD1	
LSC1	
LSC2	
LSP1	
LYS12	
LYS4	
MAS2	
MDH1	
MDJ1	
MDM38	
MGM101	
MGR1	
MGR3	
MIC10	
MIC26	
MIC60	
MMF1	
MSS51	
MSY1	
NCE102	
NDE1	
NDE2	
NDI1	
OAC1	
ODC1	
ODC2	
OPI3	
PAM16	
PDB1	
PDH1	

PDX1	
PHB2	
PHO88	
POR1	
PRX1	
PSD1	
QCR10	
QCR7	
RCF2	
RIP1	
RRF1	
RSM22	
SDH2	
SDH4	
SHH4	
SHM1	
SHY1	
SOD2	
SSQ1	
TIM44	
TIM50	
TOM20	
TOM40	
TUF1	
VAR1	
YHM2	
YLH47	
YMC1	
YME2	

Appendix 14: Comparison of proteins interacting with Cca1 in the *in vivo* assay from nuclear fraction of yeast cells grown on glucose and glycerol to OD_{600} of 1.0 in one biological replicate tested. Common proteins are in red.

Proteins interacting with Cca1 in nuclear fraction in glycerol	Proteins interacting with Cca1 in nuclear fraction in glucose
ARO9	*ARO4*
ASM4	*BFR1*
BDF1	*BFR2*
BFR2	*CBF5*
BMH2	*CRM1*
BRX1	*CSE1*
CDC14	*DBP2*
CDC33	*DBP3*
CIC1	*FPR3*
CKA2	*FRA1*
CKB2	*HRP1*
COF1	*KAP123*
CPR1	*KAP95*
CTR9	*KRI1*
DBP2	*MAK21*
ENO1	*MAK5*
ERB1	*MKT1*
ERG13	*MPP10*
FPR4	*MSN4*
GAR1	*NCL1*
GBP2	*NIC96*
GID7	*NOC2*
GLC3	*NOC3*
GLC7	*NOP1*
GRE3	*NOP4*
GSP2	*NOP56*
HMG1	*NOP58*
HRB1	*NOP9*
HTA1	*NPL3*
HTB1	*NSP1*
IES2	*NUG1*
IPP1	*PPZ1*
JEN1	*RSC8*

KAP123	*SAN1*
KAP95	*SCP160*
KRE33	*SEC63*
MAK16	*SET2*
MOT2	*SUI3*
NAP1	*TAF12*
NHP6B	*TAF5*
NIC96	*TFG1*
NOC3	*TKL1*
NOP1	*UBP14*
NOP58	*WTM1*
NPL3	*ZUO1*
NQM1	
NSP1	
NUP157	
NUP170	
NUP192	
NUP49	
NUP53	
NUP57	
PHO23	
PNC1	
POB3	
POL30	
POM33	
PRE1	
PRP43	
PWP1	
REP1	
RFC1	
RFC2	
RFC3	
RFC4	
RFC5	
RIX1	
RPD3	
RPN11	
RPN3	
RPN7	

RRB1	
RRP5	
RSC8	
RVB2	
RXT3	
SBP1	
SDS23	
SEC63	
SIN3	
SNU13	
SPT16	
SUB2	
SUI3	
TAF12	
TAF5	
TAL1	
TEF4	
TKL1	
TRX1	
UBP15	
UBP6	
UME1	
UTP11	
UTP15	
UTP22	
UTP4	
UTP6	
UTP8	
UTP9	
WTM1	
XRN1	
YDL124W	
YGR250C	
YRA1	
YTM1	
ZUO1	

Appendix 15: Comparison of proteins interacting with Cca1 in the *in vivo* assay from cytosolic fraction of yeast cells grown on glucose and glycerol to OD_{600} of 1.0 in one biological replicate tested. Common proteins are in red.

Proteins interacting with Cca1 in cytosolic fraction in glucose	Proteins interacting with Cca1 in cytosolic fraction in glycerol
AAT2	*ADH1*
ADE5,7	*ADH2*
ADE3	*DCR2*
ADE6	*EFT2*
ARC1	*GAL83*
ARG1	*GUS1*
ARG4	*HSC82*
ARO4	*HYP2*
ASC1	*IDP2*
ASN1	*INO1*
ASN2	*MDH2*
BPL1	*PDC1*
CDC60	*PRS3*
CPR6	*RPL43B*
DED81	*RPL8A*
DLD3	*RPP1B*
DPS1	*SEC17*
ENO1	*SSE2*
ERG20	
FRS2	
GDH1	
GLY1	
GND1	
GUA1	
GUS1	
HSP82	
IMD2	
INO1	
KRS1	
LYS2	
MET17	
MVD1	
NCL1	
PAN5	

PGI1	
PGM1	
PRO3	
PYC1	
RNA1	
RNR1	
RPL27A	
RPS16B	
RPS1A	
SES1	
SHM2	
STI1	
THS1	
TKL1	
TRM44	
TRP2	
TRP3	
TYS1	
YDR341C	
YNL247W	